

Ab initio calculations on nuclear matter properties including the effects of three-nucleons interaction

Alessandro Lovato

In collaboration with:

Omar Benhar, Stefano Fantoni, Cristina Losa and Kevin E. Schmidt.



Nuclear matter

Equation of state for dense nucleon matter

R. B. Wiringa and V. Fiks*

Physics Division, Argonne National Laboratory, Argonne, Illinois 60439

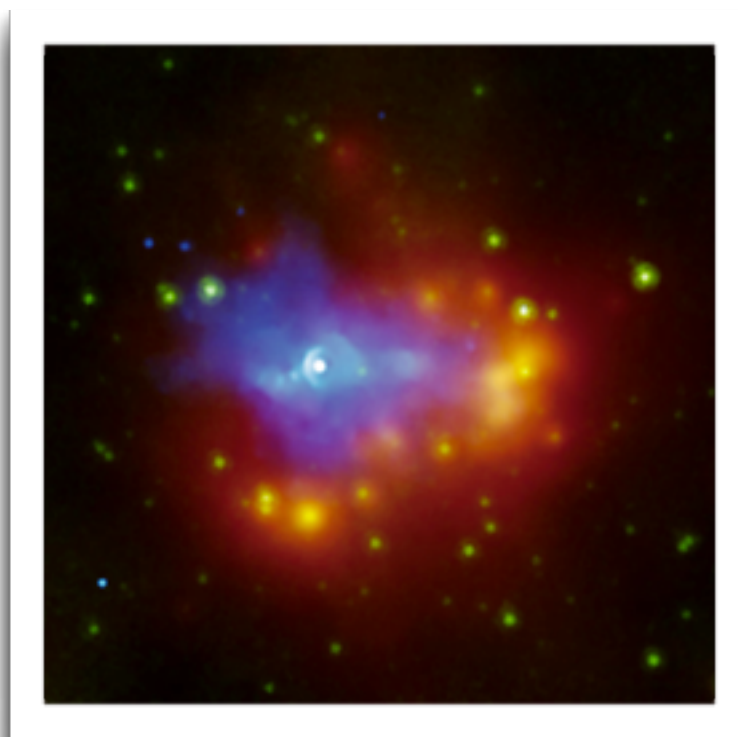
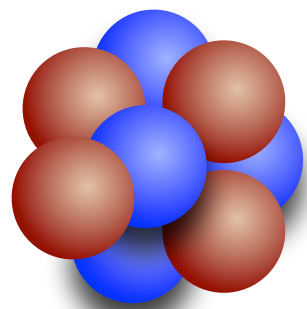
A. Fabrocini

*Department of Physics, University of Illinois at Urbana-Champaign, Urbana, Illinois 61801
and Dipartimento di Fisica, Università di Pisa, I-56100 Pisa, Italy*

(Received 17 March 1988)

Bulk properties of nuclear matter

- Infinite uniform system of nucleons interacting through strong interactions only
- Extremely useful model to investigate the properties of atomic nuclei and neutron star matter.



Thermal energies
negligible compared
to Fermi energies

$$T = 0$$

Cold nuclear matter

- Characterized by

density
proton fraction

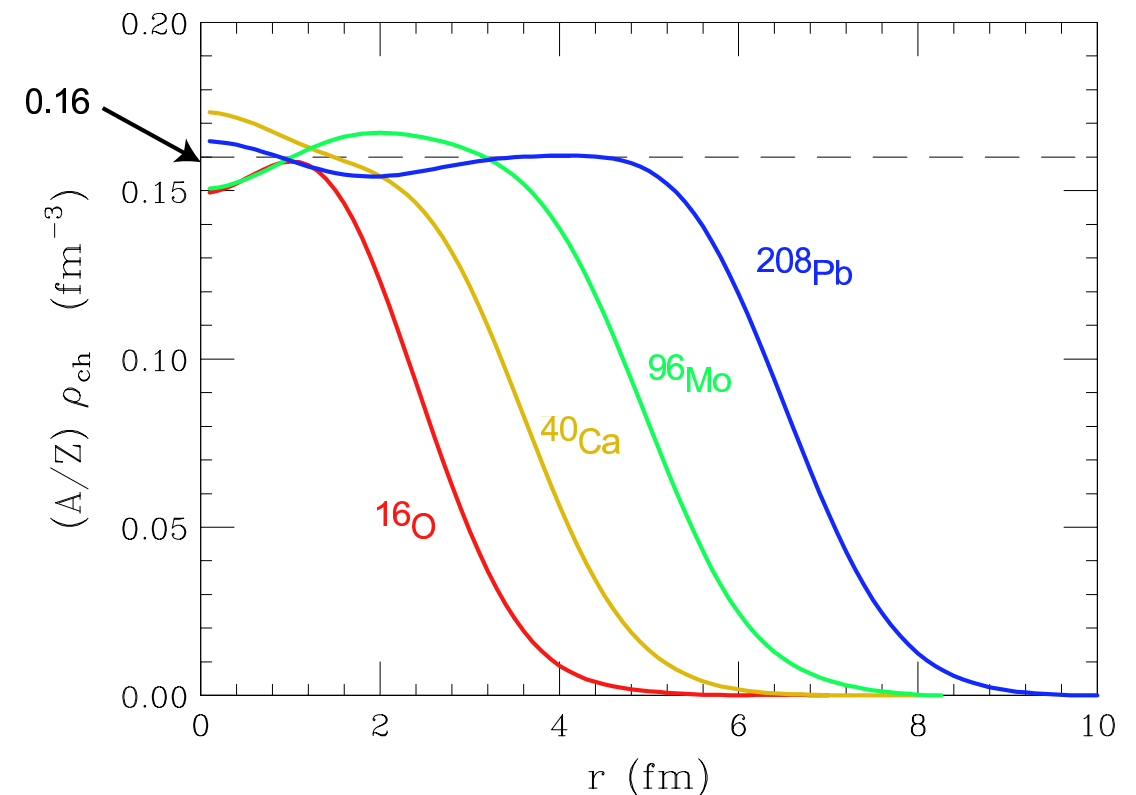
$$\left\{ \begin{array}{l} \rho = \rho_p + \rho_n \\ x_p = \frac{\rho_p}{\rho} \end{array} \right.$$

SNM	$x_p = 0.5$
PNM	$x_p = 0$

Bulk properties of nuclear matter

The nuclear charge distribution is almost constant within the nuclear volume and its central value is basically the same for all stable nuclei

$$\rho_0 = \frac{3}{4\pi r_0^3} \simeq 0.16 \pm 0.02 \text{ fm}^{-3}$$



The binding energy can be parametrized according to the semiempirical mass formula

$$B(Z, A) = \frac{1}{A} \left[a_V A - a_S A^{2/3} - a_C Z(Z-1) A^{1/3} - a_A \frac{(A-2Z)^2}{4A} + a_P \lambda A^{1/2} \right]$$

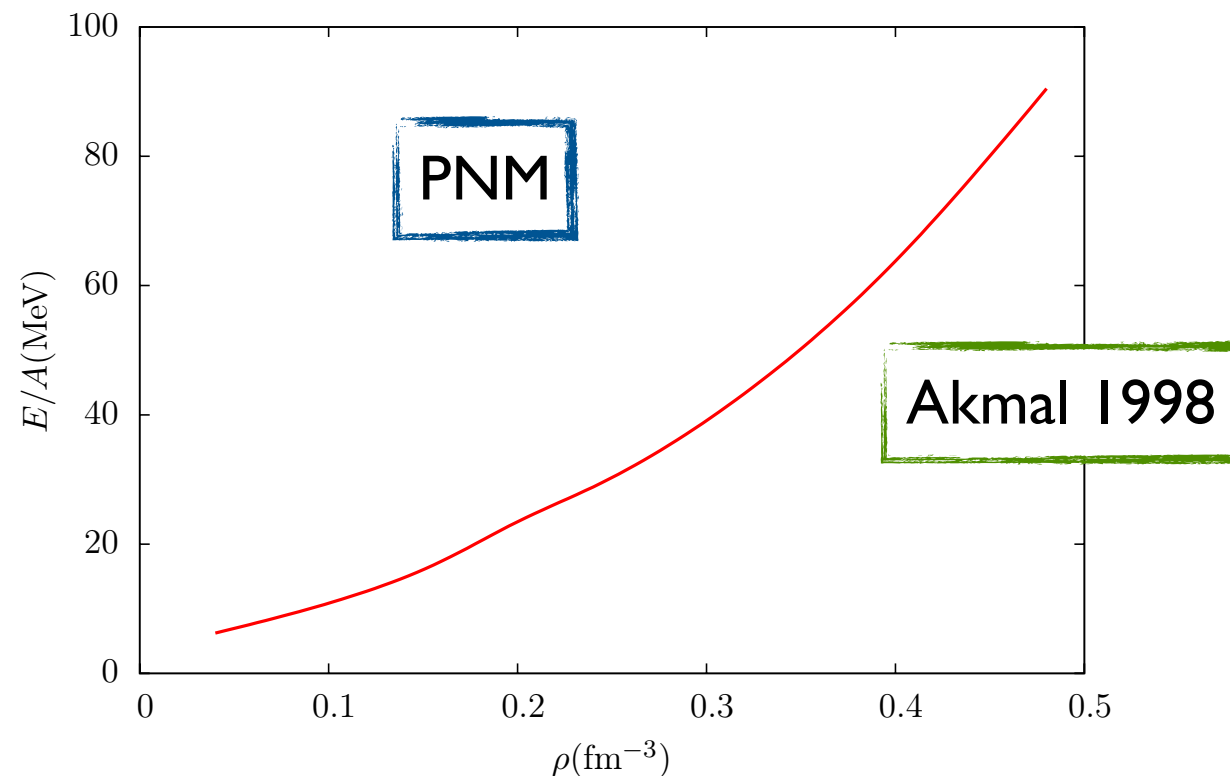
SNM limit: $Z = A/2$, $A \rightarrow \infty$

$$E_0 \equiv E(\rho_0) = a_V = -15.6 \pm 0.2 \text{ MeV}$$

In the vicinity of equilibrium density

$$K_0 = \frac{9\rho_0^2}{A} \left(\frac{\partial^2 E_{\text{SNM}}(\rho)}{\partial \rho^2} \right) = 220 \pm 30 \text{ MeV}$$

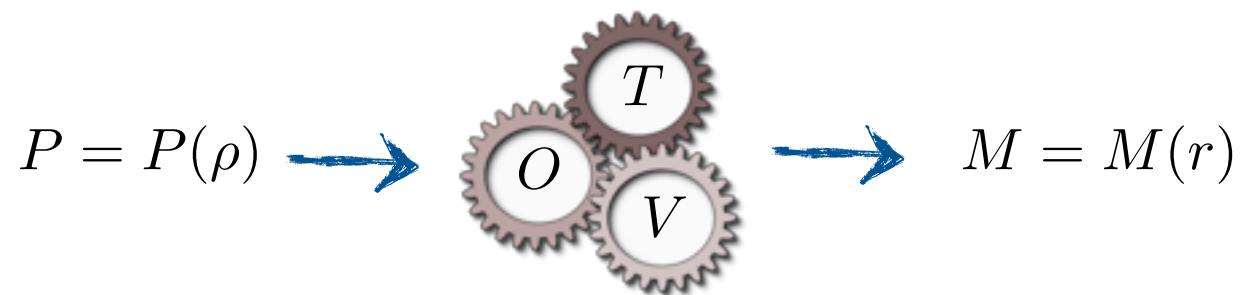
Nuclear matter equation of state



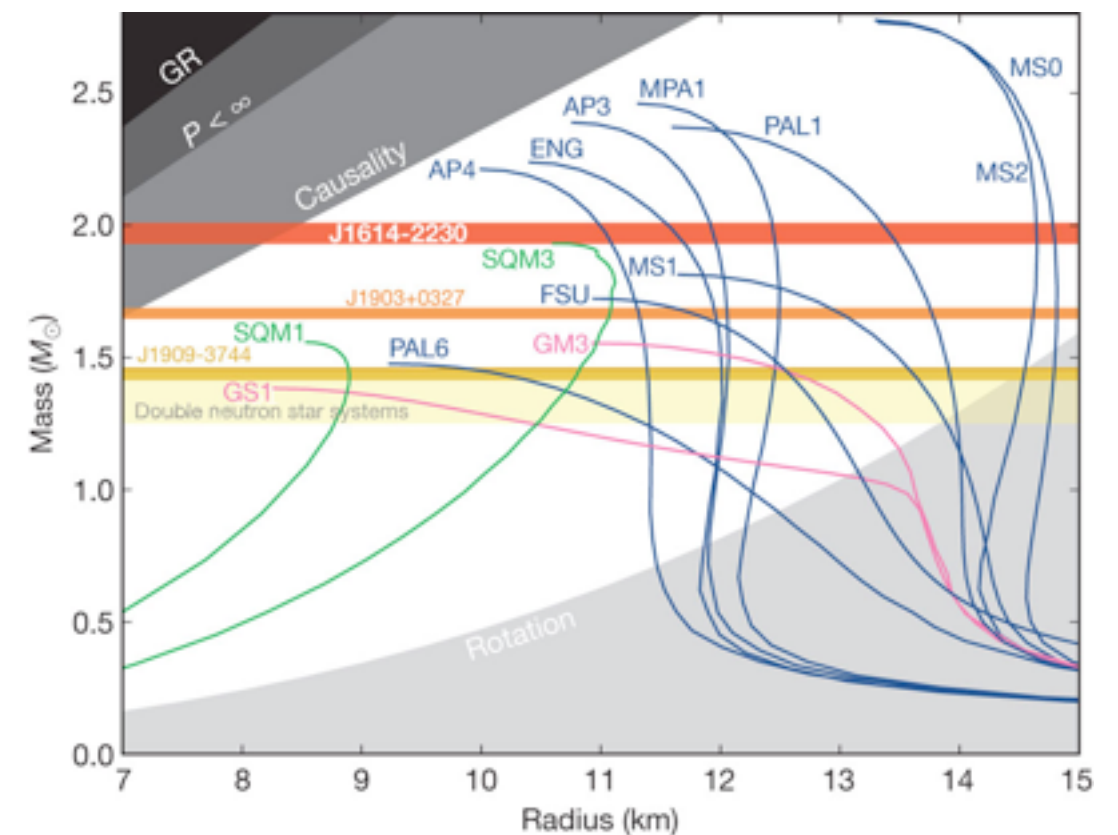
EoS links the thermodynamical variables specifying the state of a macroscopic physical system.

$$E = E(\rho) \quad \longrightarrow \quad P(\rho) = - \left(\frac{\partial E}{\partial V} \right)_A$$

EOS determines the structure of neutron stars



Astrophysical data constraint nuclear interactions.



Nuclear hamiltonian

Nuclear hamiltonian

Non relativistic pointlike protons and neutrons interacting through the hamiltonian

$$\hat{H} = \sum_i -\frac{\nabla_i^2}{2m} + \sum_{j>i} \hat{v}_{ij} + \sum_{k>j>i} \hat{V}_{ijk}$$

Our aim is to perform “**ab initio**” many-body calculation of nuclear matter properties.

The interaction must not to be affected by uncertainties involved in many body techniques.



The potential is determined on few-body observables that, for a given interaction model, can be exactly computed.

Ab initio many body calculations

- Fully predictive
- Their approximations can be estimated
- Provide a test for the interaction

Argonne NN potential

Phenomenological NN potential are generally written as

$$\hat{v} = \hat{v}_{\pi}(r_{12}) + \hat{v}_I(r_{12}) + \hat{v}_S(r_{12})$$

OPE

TPE

Heavier mesons, Nucleons' overlap

Argonne NN potential

Phenomenological NN potential are generally written as

$$\hat{v} = \hat{v}_{\pi}(r_{12}) + \hat{v}_I(r_{12}) + \hat{v}_S(r_{12})$$

OPE

TPE

Heavier mesons, Nucleons' overlap

Highly realistic Argonne v_{18} potential is written in the form

$$v_{18}(r_{12}) = \sum_{p=1}^{18} v^p(r_{12}) \hat{O}_{12}^p$$

Radial functions shaped to fit ~ 4300 np and pp scattering data below 350 MeV of Nijmegen database.

- Static part $\hat{O}_{ij}^{p=1-6} = (1, \sigma_{ij}, S_{ij}) \otimes (1, \tau_{ij})$ Deuteron and S and D wave phase shifts
- Spin-orbit $\hat{O}_{ij}^{p=7-8} = \mathbf{L}_{ij} \cdot \mathbf{S}_{ij} \otimes (1, \tau_{ij})$ P wave phase shifts

The remaining operators are needed to achieve the description of the Nijmegen scattering data with $\chi^2 \simeq 1$. They accounts for quadratic spin-orbit interaction and charge symmetry breaking effects.

Three-body force

- Originates from the fact that nucleons are not elementary particles.
- It is not an iteration of the NN force

Three-body force

- Originates from the fact that nucleons are not elementary particles.
- It is not an iteration of the NN force



NN force

Three-body force

- Originates from the fact that nucleons are not elementary particles.
- It is not an iteration of the NN force



NN force



NNN force

UIX three-body force

The three-body potential has to be symmetric under the exchange of particles 1, 2 and 3

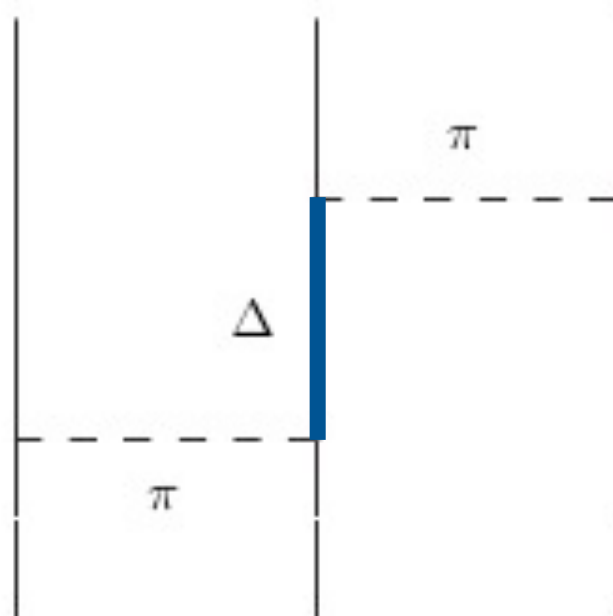
$$\hat{V}_{123} = \hat{V}(1 : 23) + \hat{V}(2 : 13) + \hat{V}(3 : 12)$$

All the NNN potential we will be considering satisfy the symmetry

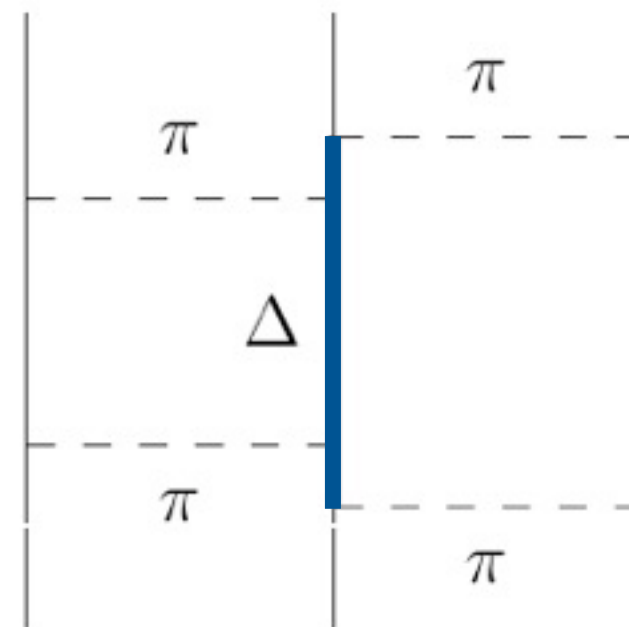
$$\hat{V}(i : jk) = \hat{V}(i : kj)$$

UIX potential consists of two contributions:

- Fujita Myiazawa



- Scalar repulsive term



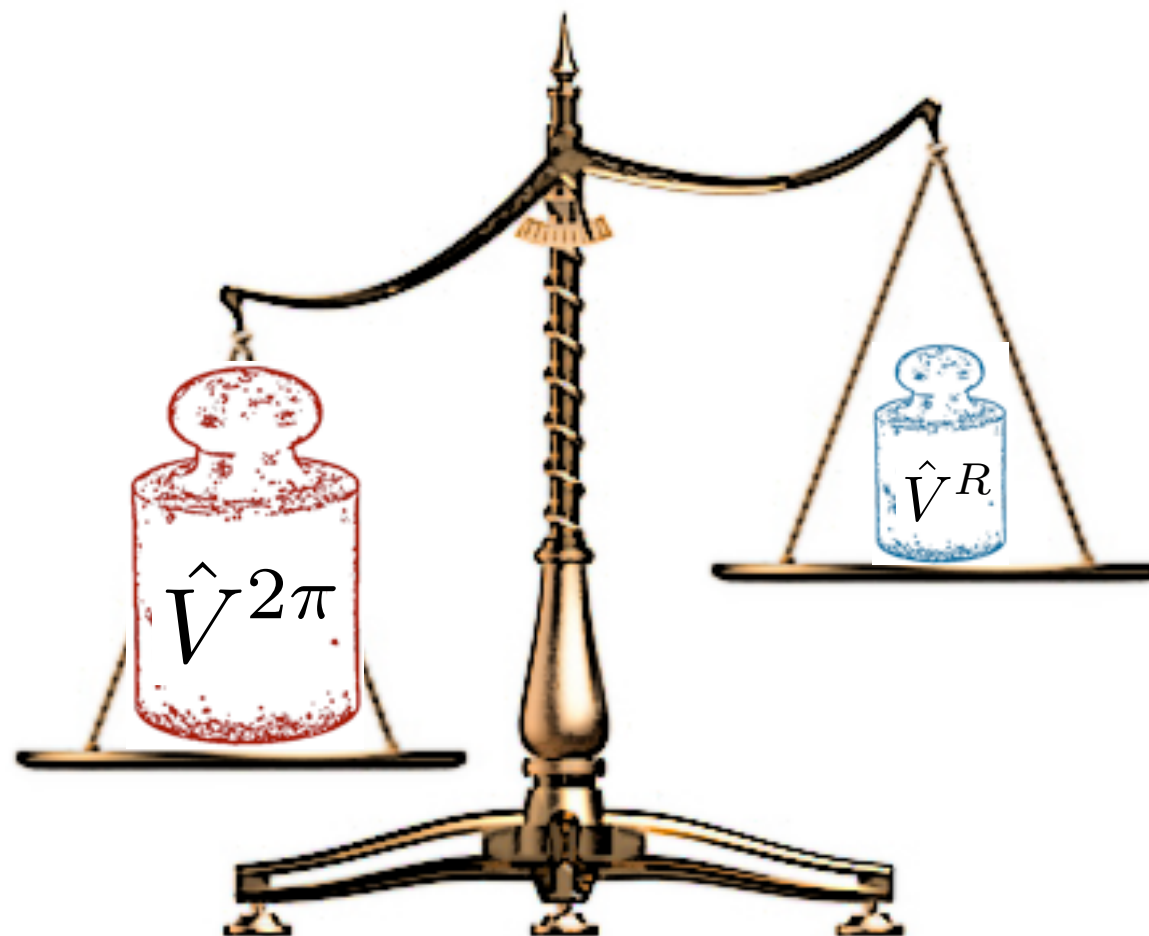
UIX three-body force

UIX potential has two parameters

- $A_{2\pi}$ adjusted to reproduce the binding energy of 3H
- U_0 tuned for FHNC/SOC calculation to reproduce the saturation density of SNM

Lagaris and Pandharipande argued that, because of correlations, the relative weight of the contribution depends upon the density of the system.

Low density



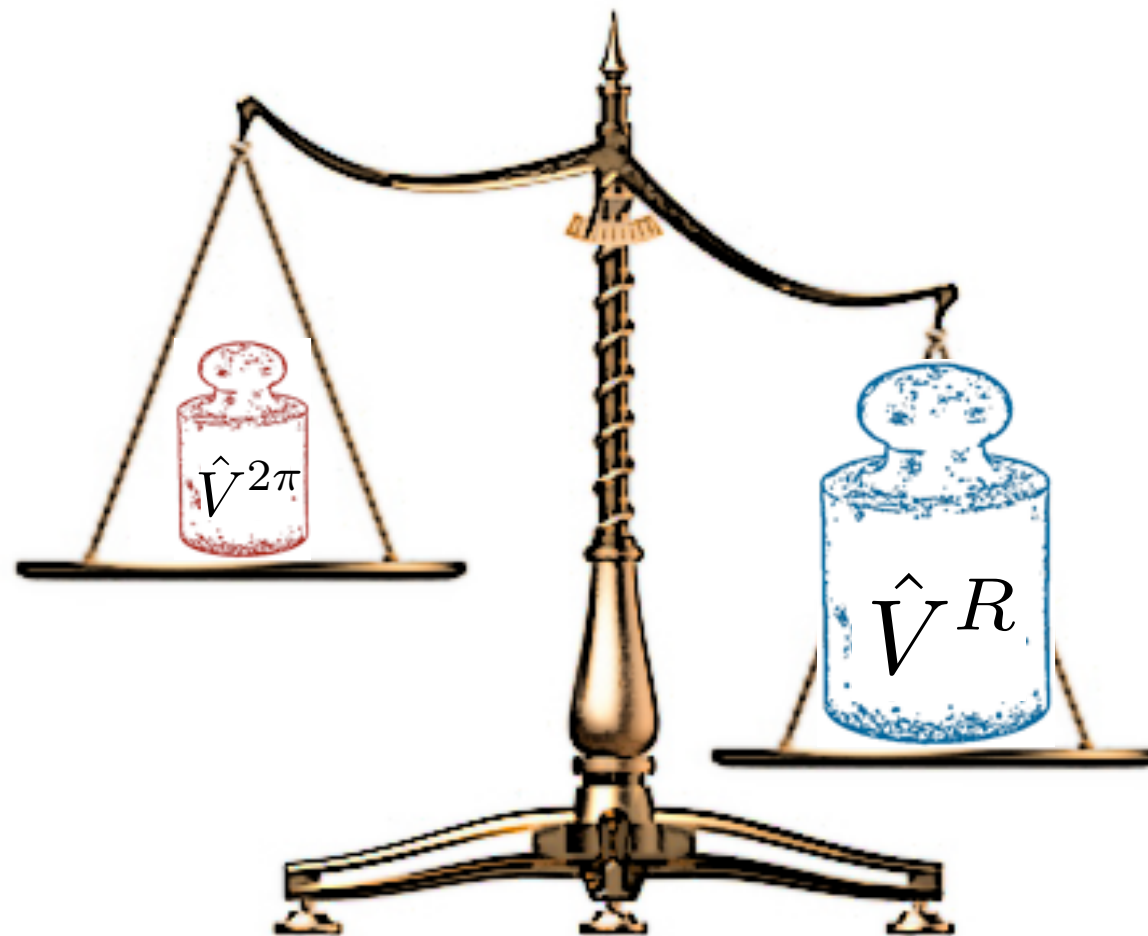
UIX three-body force

UIX potential has two parameters

- $A_{2\pi}$ adjusted to reproduce the binding energy of 3H
- U_0 tuned for FHNC/SOC calculation to reproduce the saturation density of SNM

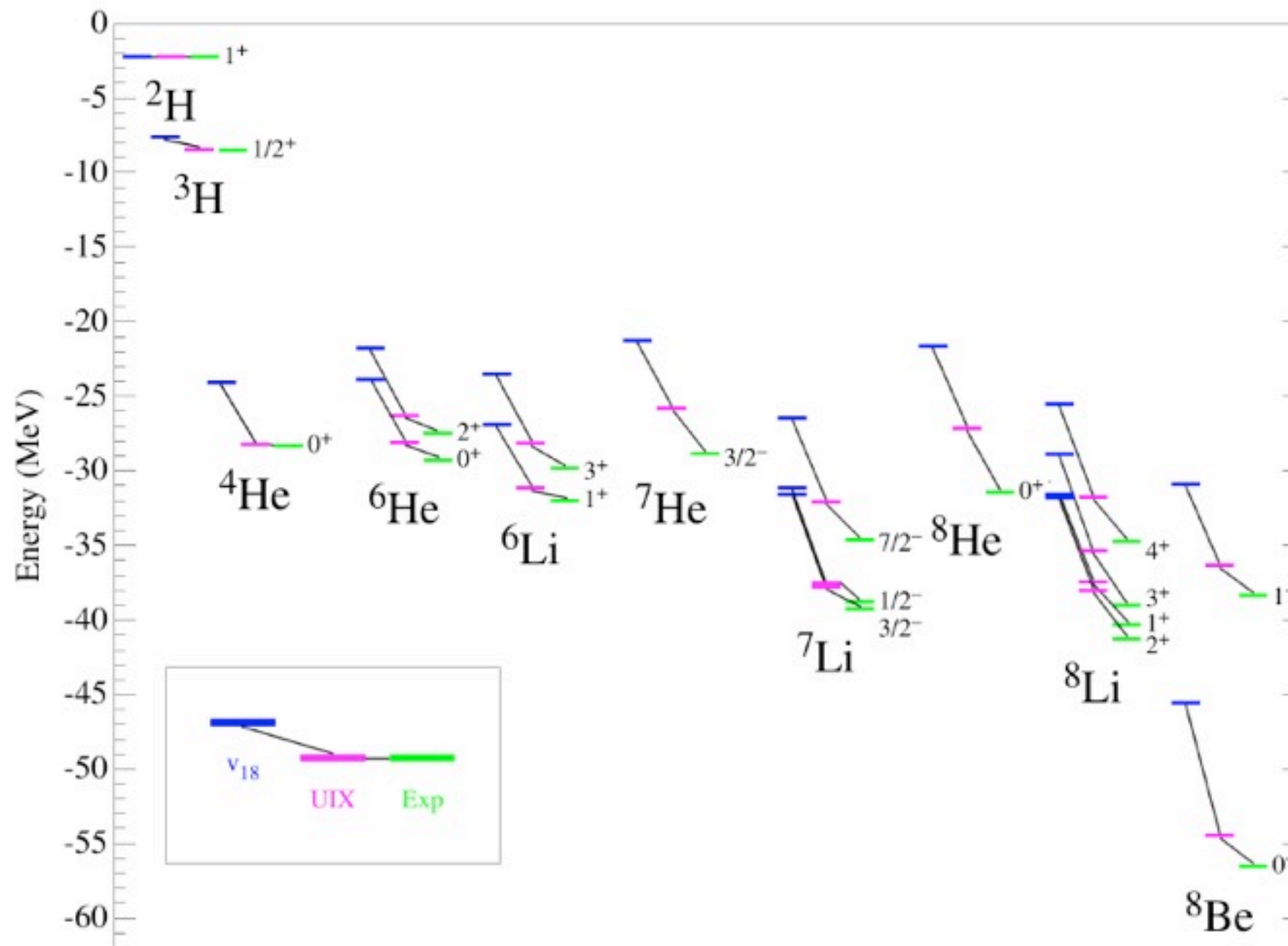
Lagaris and Pandharipande argued that, because of correlations, the relative weight of the contribution depends upon the density of the system.

High density



UIX three-body force

- Improved description of three and more nuclei bound and scattering states.

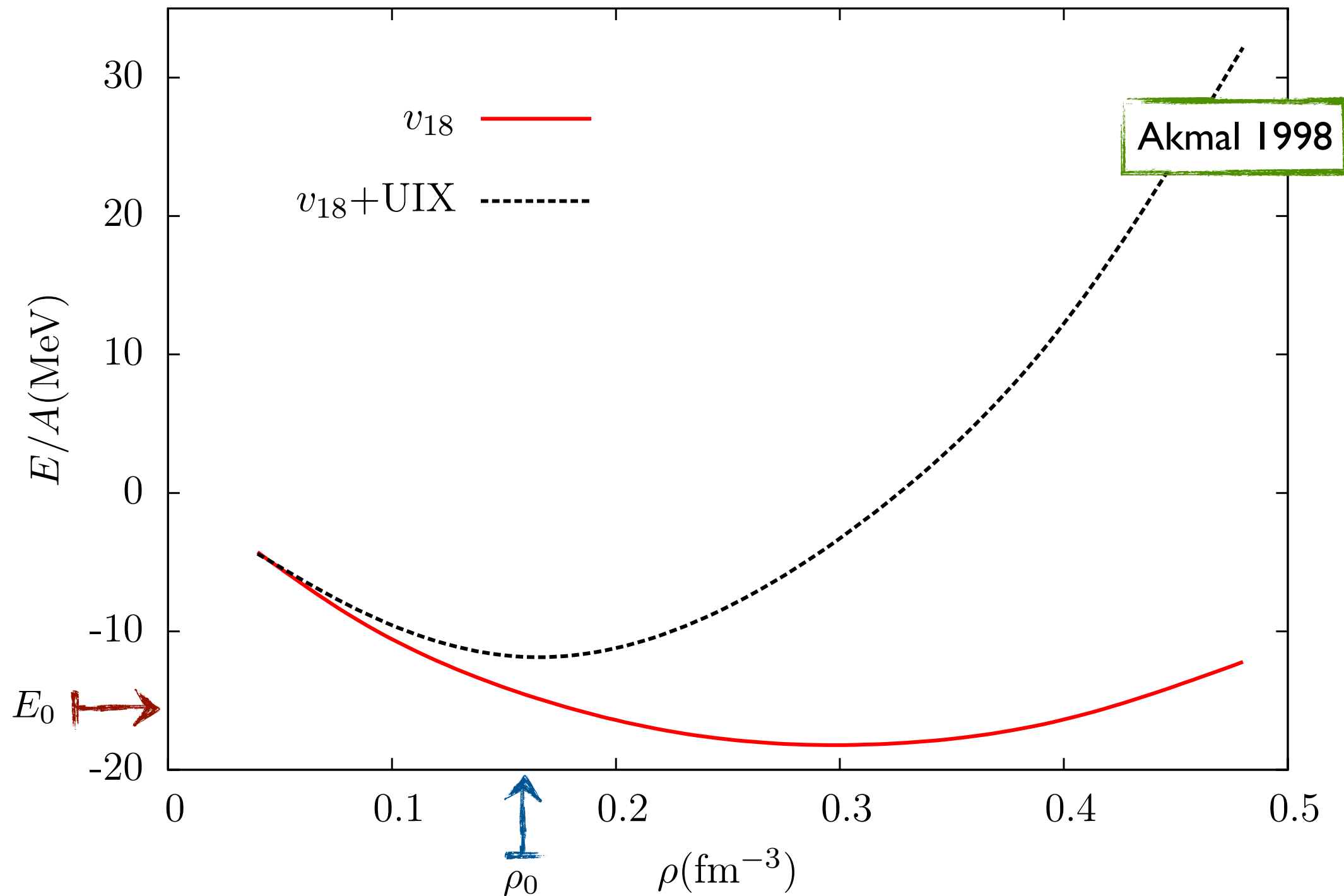


- Improved description of the neutron-deuteron scattering length

	v_{18}	$v_{18} + \text{UIX}$	Exp.
$^2a_{nd}(\text{fm})$	1.258	0.578	$0.645 \pm 0.003 \pm 0.007$

UIX three-body force

- Equilibrium density of symmetric nuclear matter reproduced, but SNM is underbound.



UIX three-body force

In addition to the discrepancies with experimental data, there are theoretical “issues” concerning the UIX potential

- $\hat{V}^{2\pi}$: no a priori reasons to stop at the first order in the perturbative expansion in terms of the coupling constant $g^2/(4\pi) \simeq 14$.
- \hat{V}^R : adjusting U_0 to reproduce ρ_0 makes the potential affected by the approximations of the many-body technique. Is still “**ab initio**”?



Chiral perturbation theory

If u and d quarks were massless, QCD would be invariant under the **chiral symmetry group**.

$$G = SU(2)_R \times SU(2)_L$$

For the hadronic spectrum to be reproduced, G is **spontaneously broken**

$$G = SU(2)_R \times SU(2)_L \quad \rightarrow \quad H = SU(2)_I$$

Goldstone theorem

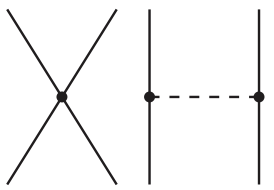
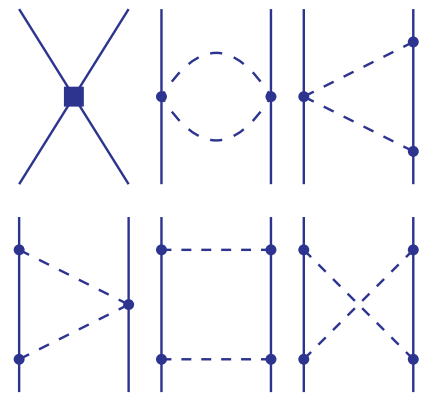
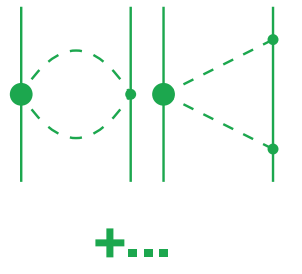
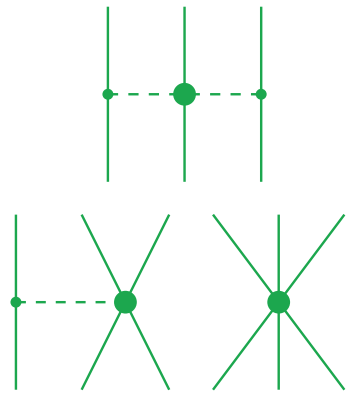
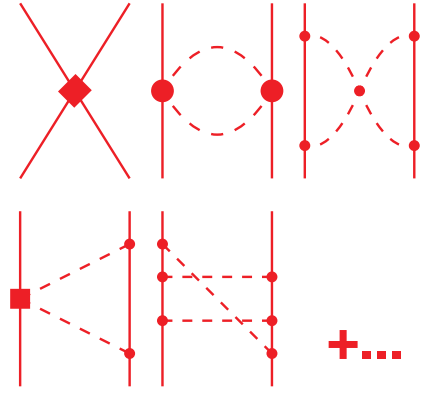
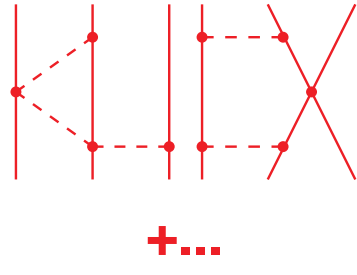
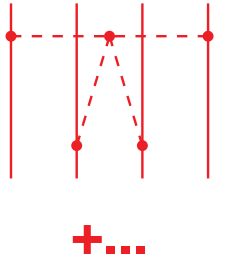
- Three massless pseudoscalar bosons appear
- Goldstone bosons decouple in small momentum limit

Expansion in
powers of
 $\frac{q}{\Lambda_\chi}$!!!

Pions !!!



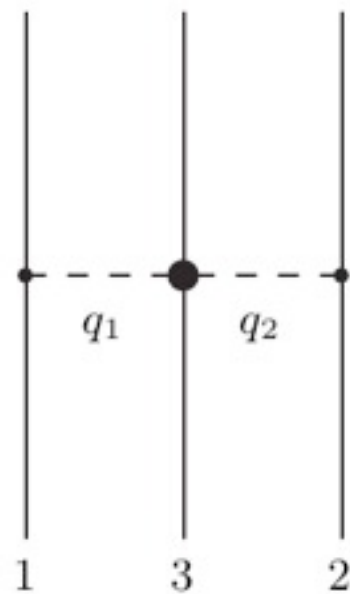
Chiral perturbation theory

			2b force	3b force	4b force
LO	\leftrightarrow	$\left(\frac{q}{\Lambda_\chi}\right)^0$			
NLO	\leftrightarrow	$\left(\frac{q}{\Lambda_\chi}\right)^2$			
N ² LO	\leftrightarrow	$\left(\frac{q}{\Lambda_\chi}\right)^3$			
N ³ LO	\leftrightarrow	$\left(\frac{q}{\Lambda_\chi}\right)^4$			

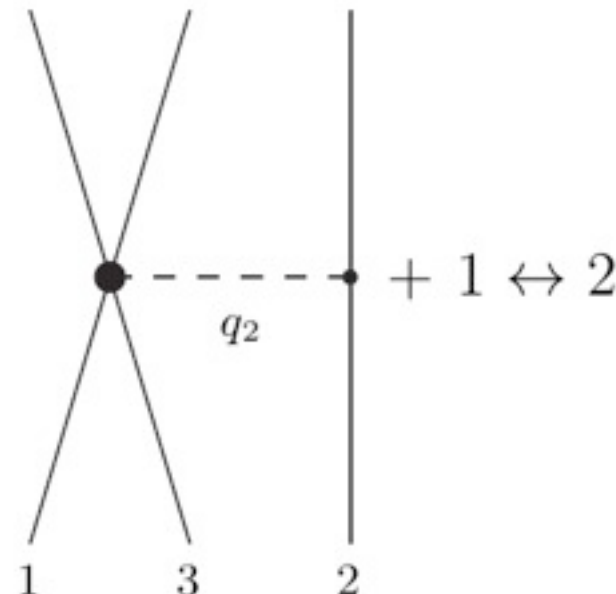
Chiral NNN potential

In a theory without explicit Δ degrees of freedom, the first contribution to the chiral 3NF appears at N²LO in the Weinberg counting scheme.

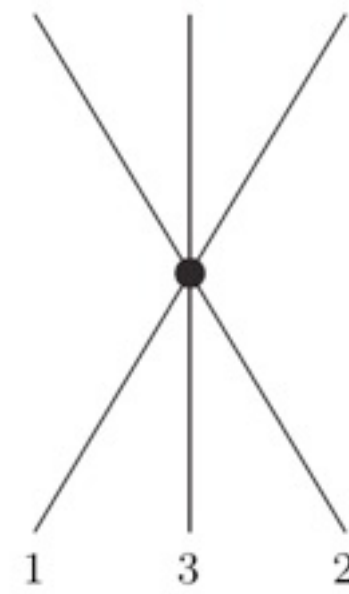
Two-pion exchange (TPE)



One-pion exchange (OPE)



Contact term



Fourier transforming the Chiral NNLO 3-body potential, originally derived in momentum space, yields a local expression in coordinate space

$$\hat{V}^{\chi}(3 : 12) = \int \frac{d^3 q_1}{(2\pi)^3} \frac{d^3 q_2}{(2\pi)^3} \tilde{V}^{\chi}(3 : 12) F_{\Lambda}(q_1^2) F_{\Lambda}(q_2^2) e^{i\mathbf{q}_1 \cdot \mathbf{r}_{13}} e^{i\mathbf{q}_2 \cdot \mathbf{r}_{23}}$$

Cutoff function $F_{\Lambda}(q_i^2) = \exp\left(-\frac{q_i^4}{\Lambda^4}\right)$

- Depends on momentum transfer
- Generates power of q/Λ_{χ} beyond NNLO

Many-body methods

Many body wave function

Non relativistic many body theory is aimed at solving the equation

$$\hat{H}\Psi_n(x_1, \dots, x_A) = E_n \Psi_n(x_1, \dots, x_A)$$

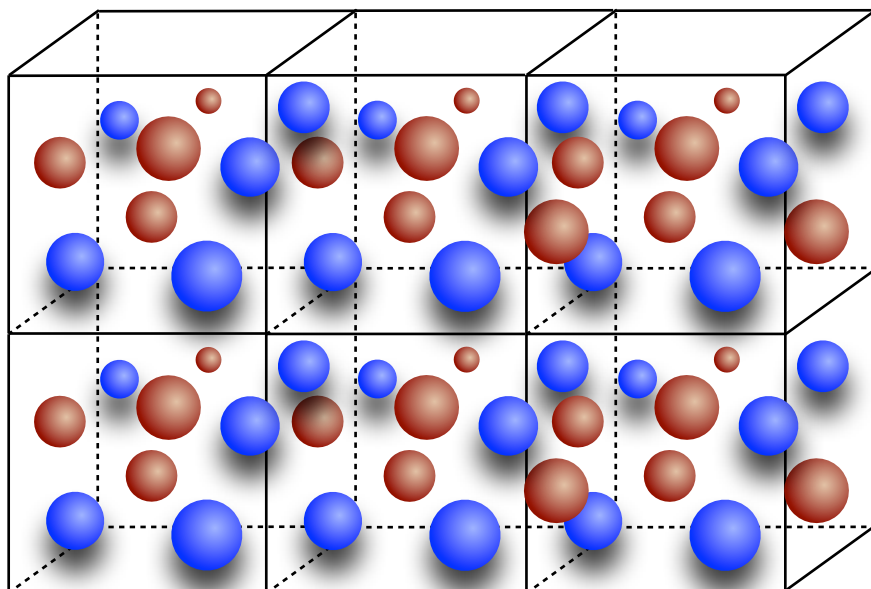
The independent particle model wave function is a Slater determinant of single particle wave functions

$$\longleftrightarrow \Phi_0 = \mathcal{A}[\phi_{n_1}(x_1) \dots \phi_{n_a}(x_a)] .$$

The antisymmetrization operator is conveniently written in terms of two-particles exchange

$$\mathcal{A} = 1 - \sum_{i < j} \hat{P}_{ij} + \sum_{i < j < k} (\hat{P}_{ij} \hat{P}_{jk} + \hat{P}_{ik} \hat{P}_{kj}) + \dots$$

- Translation invariance implies that single particle wave functions be plane waves
- The infinite system can be conveniently described within a box of volume V with periodic boundary conditions



$$\left\{ \begin{array}{l} \phi_{n_i}(x_i) = \frac{e^{i\mathbf{k}_i \cdot \mathbf{r}_i}}{\sqrt{V}} \eta_{\alpha_i} \\ \eta_{\alpha_i} \equiv \chi_{\sigma_i} \chi_{\tau_i} \longleftrightarrow \text{Pauli spinors} \\ k_i = \frac{2\pi}{L} n_i \quad i = x, y, z \quad n_i = 0, \pm 1, \dots \end{array} \right.$$

Many body wave function

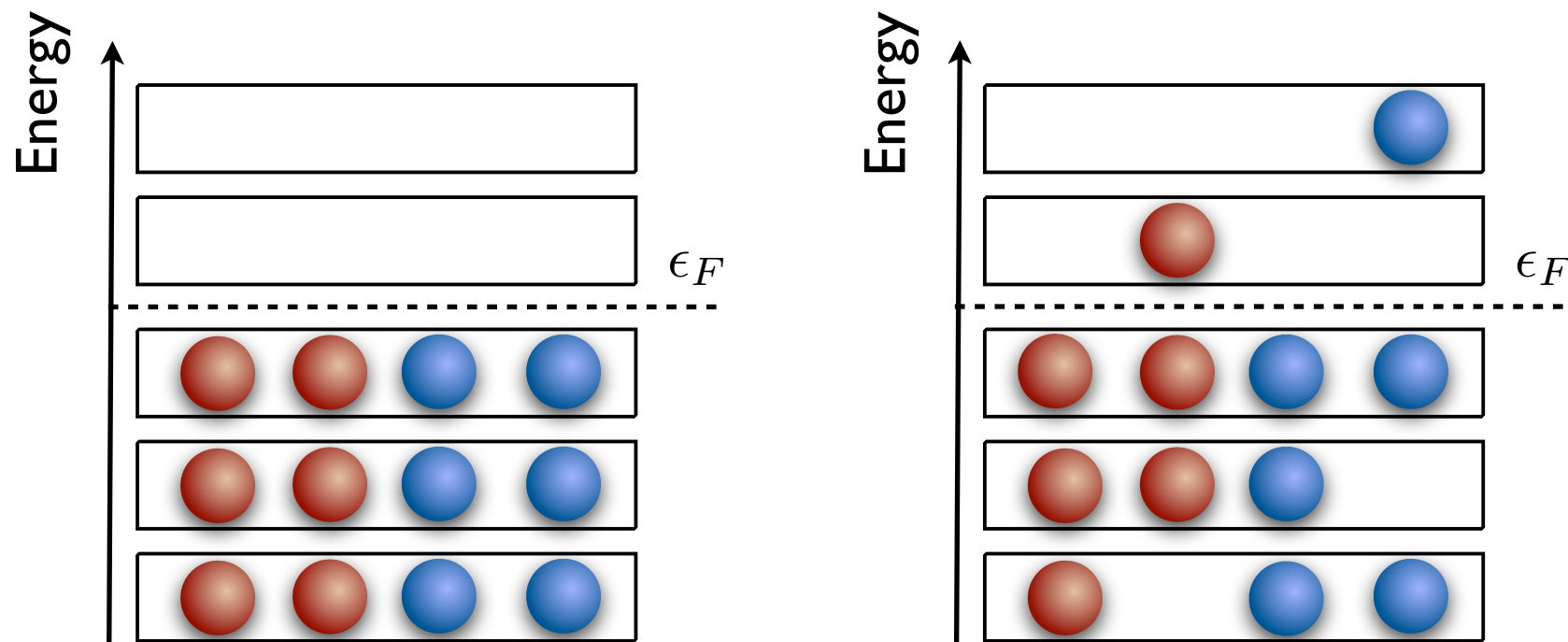
Excited states are constructed removing n occupied states from the Slater determinant and replacing them with n virtual states

n-particle n-hole states

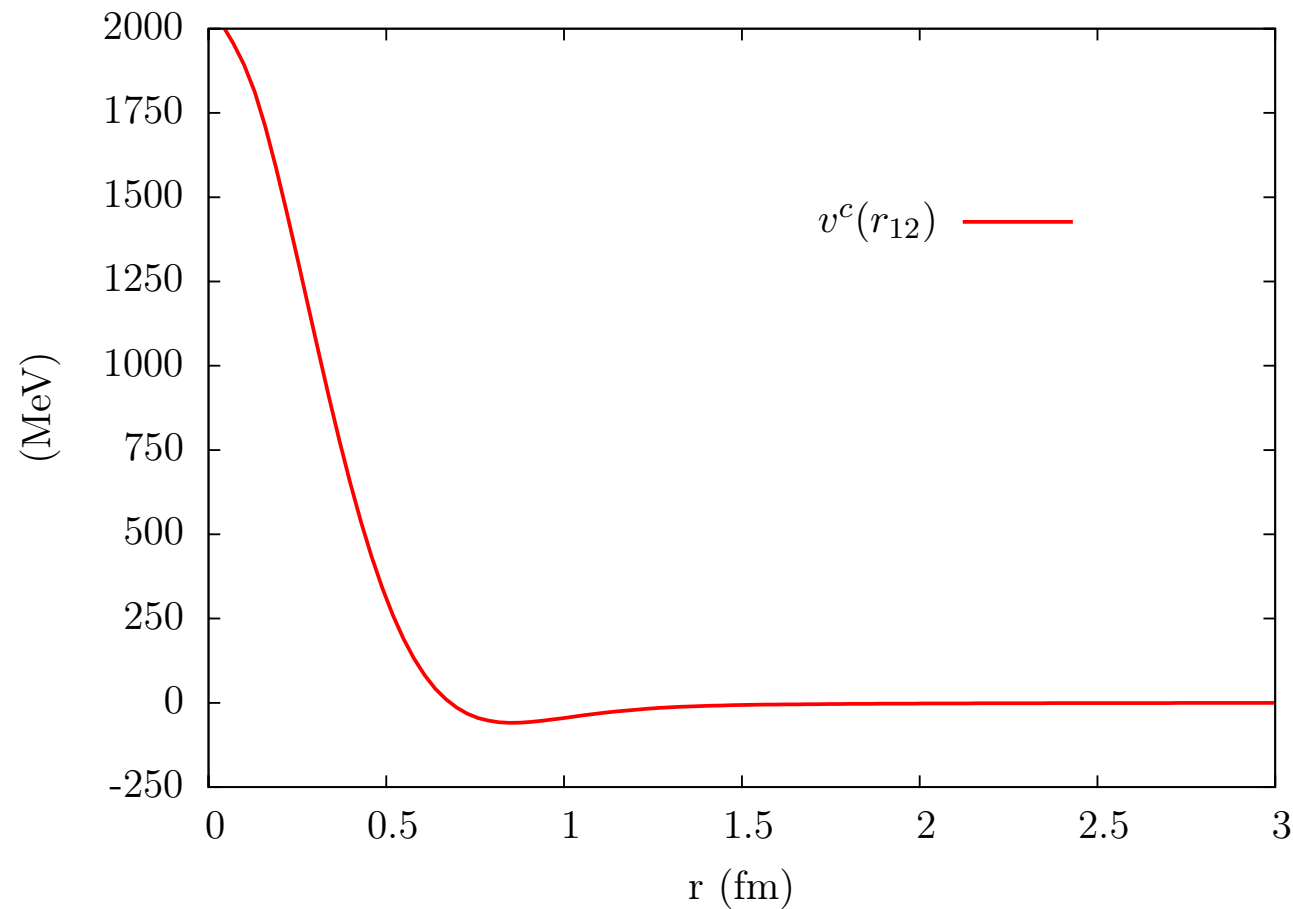


$$\Phi_n(x) \equiv \Phi_{h_1, \dots, h_n; p_1, \dots, p_n}(x)$$

In the following one among the possible 2p 2h state is represented.



Need for correlations



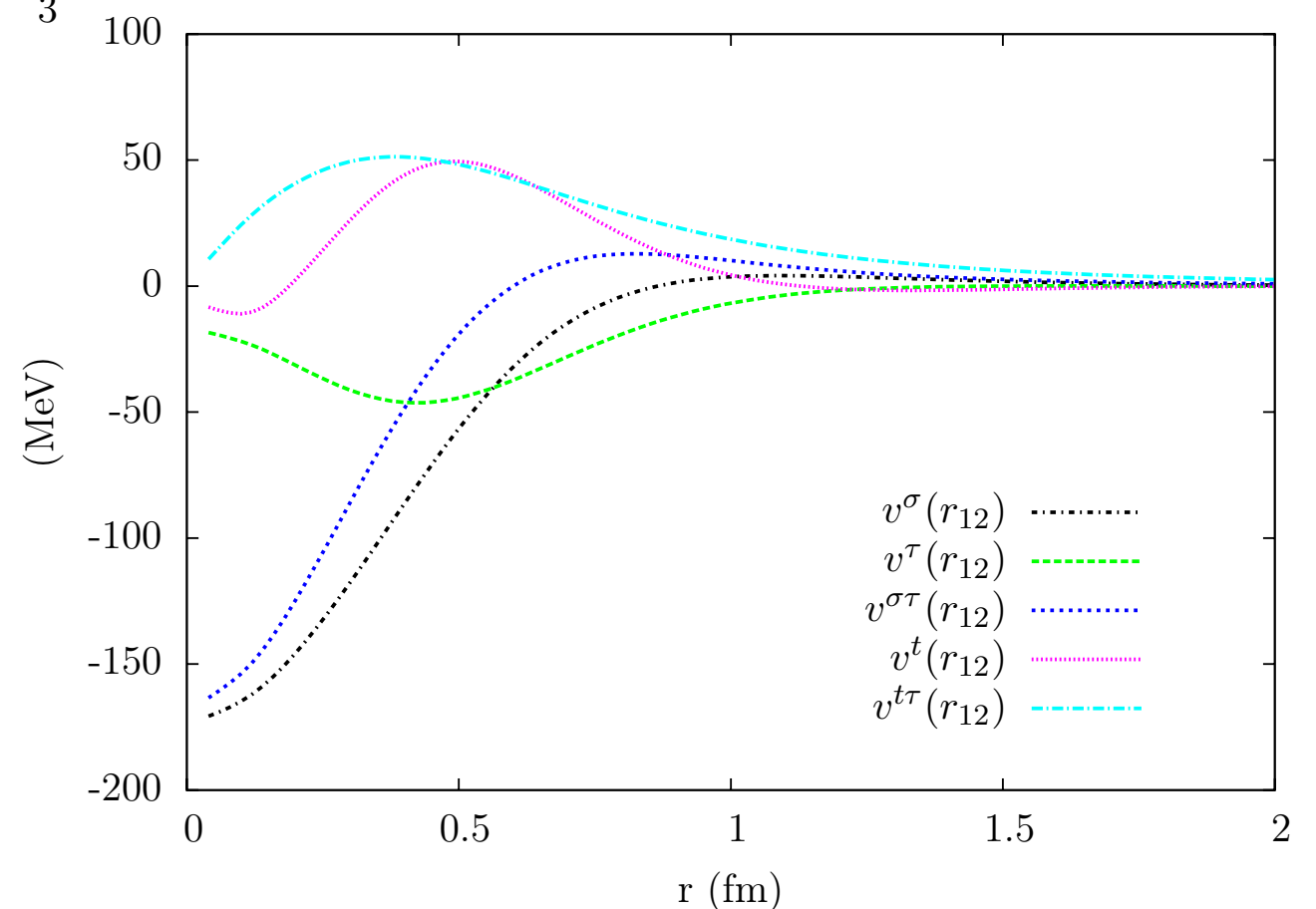
Repulsive core in the central channel of the Argonne potential



Standard perturbation theory in FG basis is not converging

Small probability of finding any couple of nucleons at short distances.

The NN interaction is highly state dependent



Correlated basis function theory

The correlated states are defined as

$$|\Psi_n\rangle \equiv \frac{\hat{\mathcal{F}}|\Phi_n\rangle}{\langle\Phi_n|\hat{\mathcal{F}}^\dagger\hat{\mathcal{F}}|\Phi_n\rangle}$$

The correlation operator reflects the complexity of the NN interaction

$$\hat{\mathcal{F}} = \left(\mathcal{S} \prod_{j>i=1}^A \hat{F}_{ij} \right) \quad \longleftrightarrow \quad \hat{F}_{ij} = \sum_{p=1}^6 f^p(r_{ij}) \hat{O}_{ij}^p$$

The radial functions $f^p(r_{ij})$ are determined by minimizing the energy expectation value

$$E_V \equiv \langle\Psi_0|\hat{H}|\Psi_0\rangle \equiv \frac{\langle\Phi_0|\hat{\mathcal{F}}^\dagger\hat{H}\hat{\mathcal{F}}|\Psi_0\rangle}{\langle\Phi_0|\hat{\mathcal{F}}^\dagger\hat{\mathcal{F}}|\Psi_0\rangle} \geq E_0$$

→ The expectation value of the two-body potential per particle is given by

$$\frac{\langle\hat{v}\rangle}{A} = \frac{1}{A} \sum_{i<j} \langle\Psi_0|\hat{v}_{ij}|\Psi_0\rangle = \frac{\rho}{2} \sum_p \int d\mathbf{r}_{12} g^p(r_{12}) v^p(r_{12})$$

→ The expectation values of the three body potential and of the kinetic energy can be expressed in terms of the two-body distribution functions and their derivatives.

CBF and cluster expansion

We are aimed at computing $g^p(\mathbf{r}_1, \mathbf{r}_2) = \frac{A(A-1)}{\rho^2} \frac{\text{Tr}_{12} \int dx_{3,\dots,A} \Phi_0^* \hat{\mathcal{F}}^\dagger \hat{O}_{12}^p \hat{\mathcal{F}} \Phi_0}{\int dx_{1,\dots,A} \Phi_0^* \hat{\mathcal{F}}^\dagger \hat{\mathcal{F}} \Psi_0}.$



Integration over the coordinates of a huge number of particles !!!

Cluster expansion method!

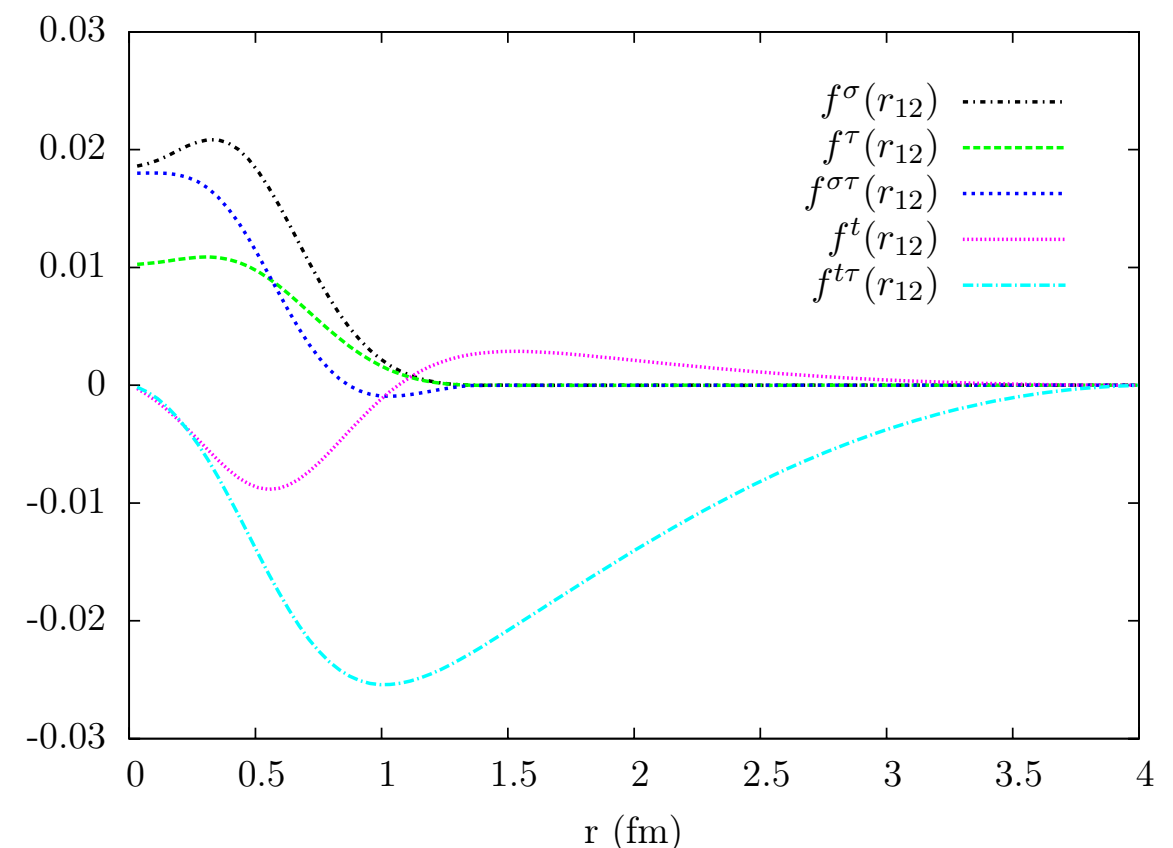
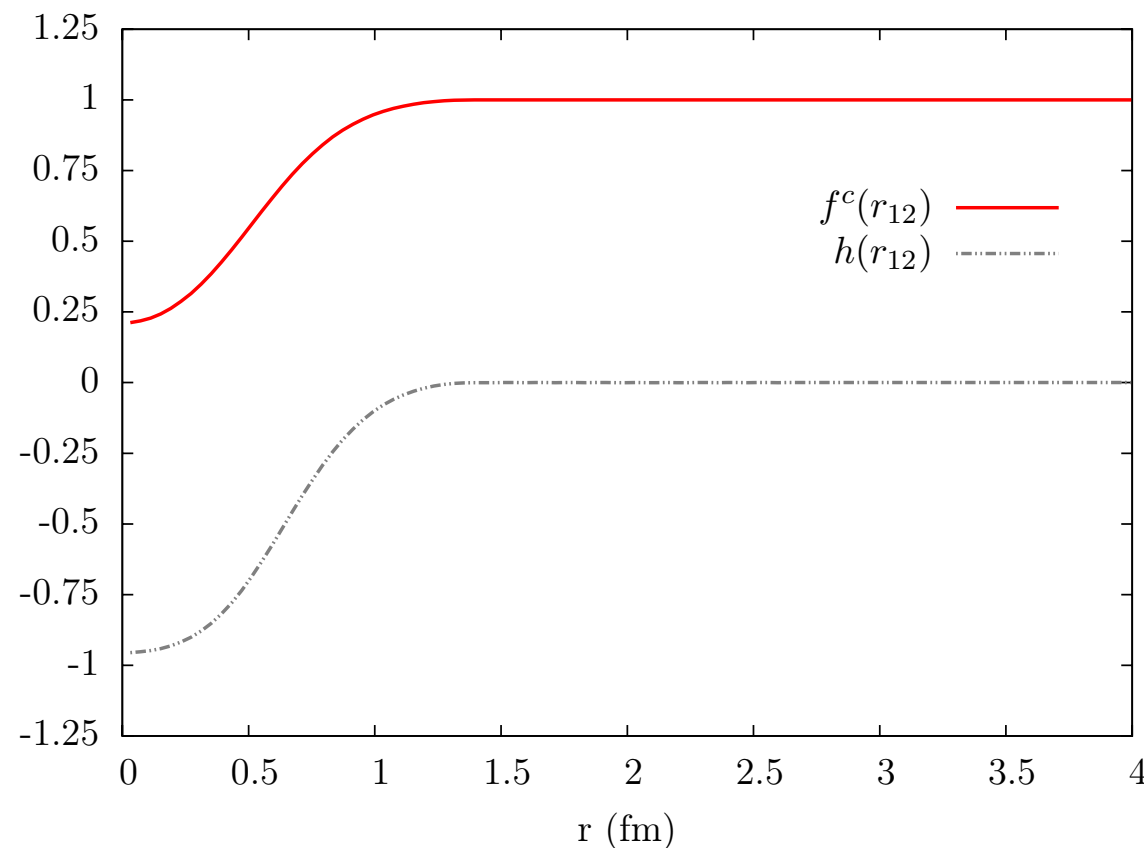


The two-body distribution function is expanded in terms of the following quantities

$$h_{ij} = f_{ij}^c - 1$$

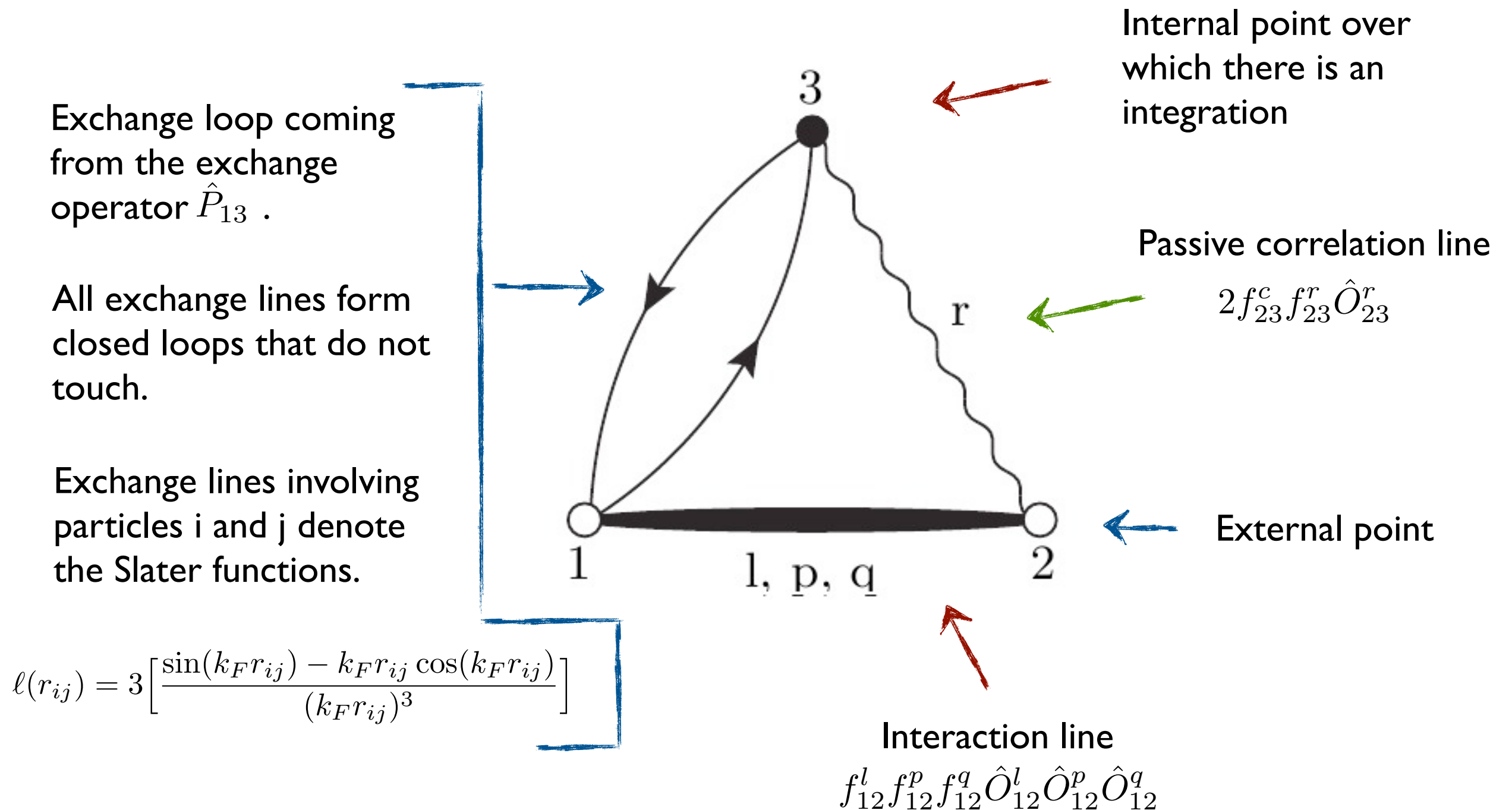
$$2f_{ij}^c f_{ij}^{p>1}$$

$$f_{ij}^{p>1} f_{ij}^{q>1}$$



CBF and cluster expansion

The cluster terms of the expansion can be represented by cluster diagrams



CBF and cluster expansion

A diagram is **linked** if each couple of points is connected by a sequence of lines.

The unlinked diagram coming from the expansion of the numerator cancel with those of the denominator.



Only linked diagrams have to be summed in the calculation of $g^p(r_{12})$.

SUMMATION SCHEMES

- Scalar diagrams are massively summed by means of the FHNC/SOC equations.



They form a self-consistent scheme that allows for summing all the scalar diagrams



but the so-called “elementary diagrams”

- Operator diagrams: SOC approximation.

Only diagrams with at most two operators arriving at a given point are considered.



Possible violations of the variational principle!

Energy minimization: simulated annealing

Variational energy depends on a set of parameters

$$E_V = E_V(d_c, d_t, \beta_p, \alpha_p)$$

To minimize the energy we have employed a “**simulated annealing**” procedure.

Metropolis algorithm

$$s \equiv \{d_c, d_t, \beta_p, \alpha_p\} \xrightarrow{\text{red arrow}} s' \equiv \{d'_c, d'_t, \beta'_p, \alpha'_p\} \quad \text{acceptance} \quad P_{ss'} = \exp \left[-\frac{E_V(s') - E_V(s)}{T} \right]$$

As the temperature is lowered, the parameters stay closer to the minimum of E_V .



Diffusion Monte Carlo

The results of the FHNC/SOC calculations depend on the accuracy of the trial wave function

$$\Psi_T(X) = \frac{\hat{\mathcal{F}}\Phi_0(X)}{\int dx_{1\dots A} \Phi_0^*(X) \hat{\mathcal{F}}^\dagger \hat{\mathcal{F}} \Phi_0(X)}$$

The trial wave function can be expanded on the complete set of eigenstates of the hamiltonian

$$|\Psi_T\rangle = \sum_n c_n |\Psi_n\rangle \quad \leftarrow \triangle ! \text{ not CBF states !!!}$$

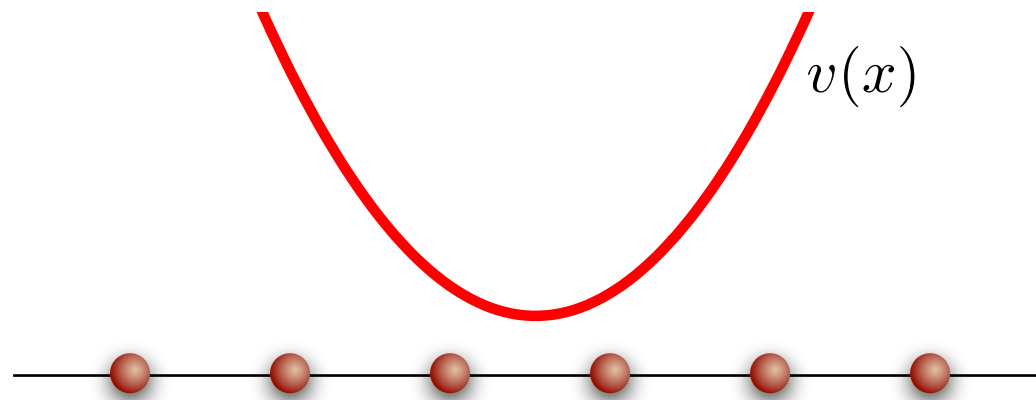
The evolution in imaginary time $\tau = it/\hbar$ projects out the true ground state

$$\lim_{\tau \rightarrow \infty} e^{-(H-E_T)\tau} |\Psi_T\rangle = \lim_{\tau \rightarrow \infty} c_0 e^{-(E_0-E_T)\tau} |\Psi_0\rangle$$

DMC is a stochastic method for solving the imaginary-time many-body Schrödinger equation

$$\left\{ \begin{array}{l} -\frac{\partial}{\partial \tau} |\Psi(\tau)\rangle = (\hat{H} - E_T) |\Psi(\tau)\rangle \\ |\Psi(\tau=0)\rangle = |\Psi_T\rangle \end{array} \right. \longrightarrow |\Psi(\tau + \Delta\tau)\rangle = e^{-(\hat{H}-E_T)\Delta\tau} |\Psi(\tau)\rangle$$

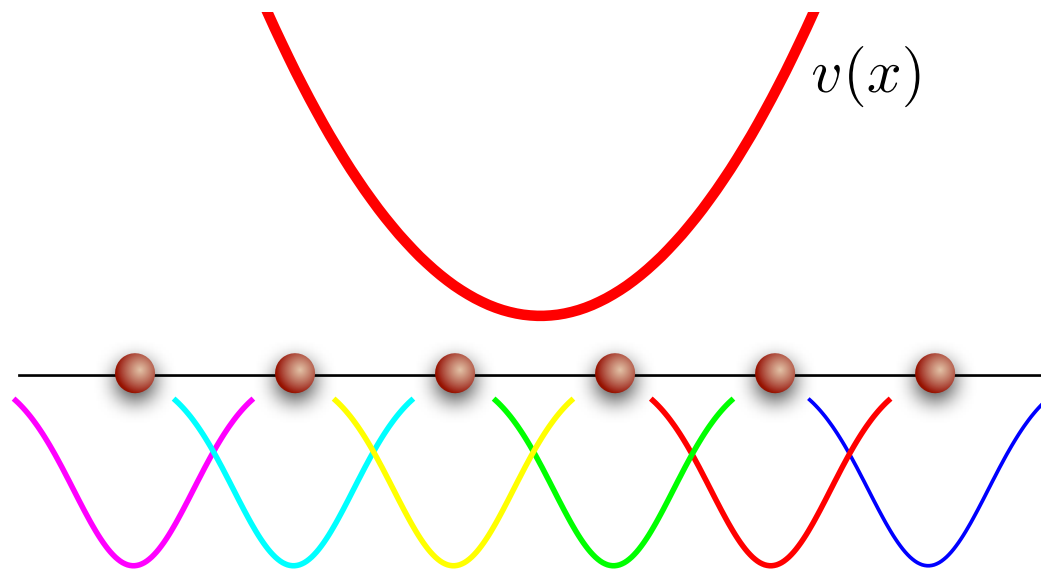
Diffusion Monte Carlo



- A set of walkers is sampled from the trial wave function

$$\Psi(R, \tau) = \sum_k \delta(R - R_k)$$

Diffusion Monte Carlo



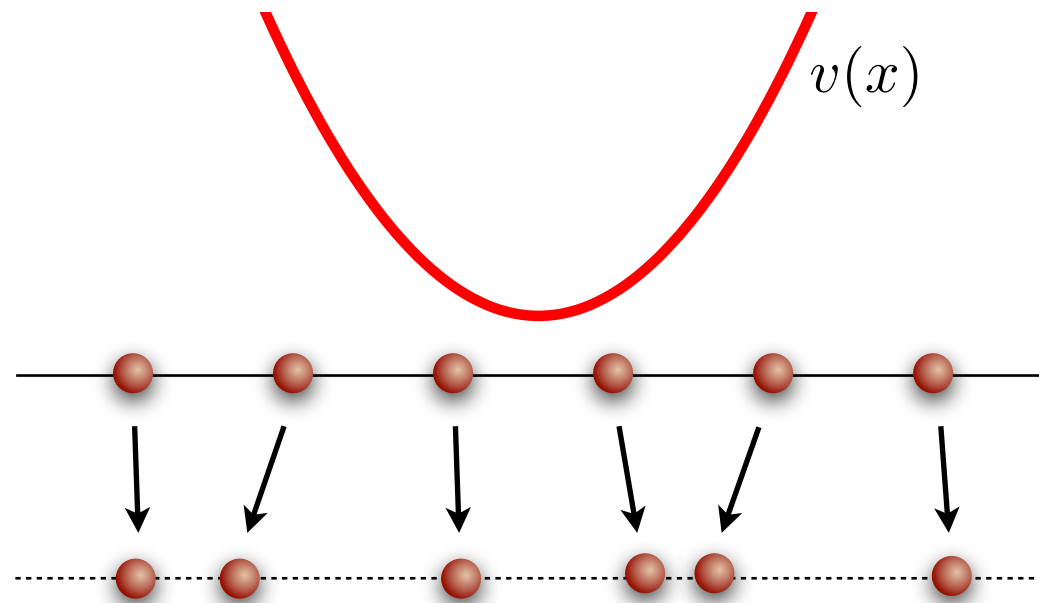
- A set of walkers is sampled from the trial wave function

$$\Psi(R, \tau) = \sum_k \delta(R - R_k)$$

- Gaussian drift according to

$$\Psi(R, \tau + d\tau) = \sum_k G_d(R, R_k, d\tau)$$

Diffusion Monte Carlo



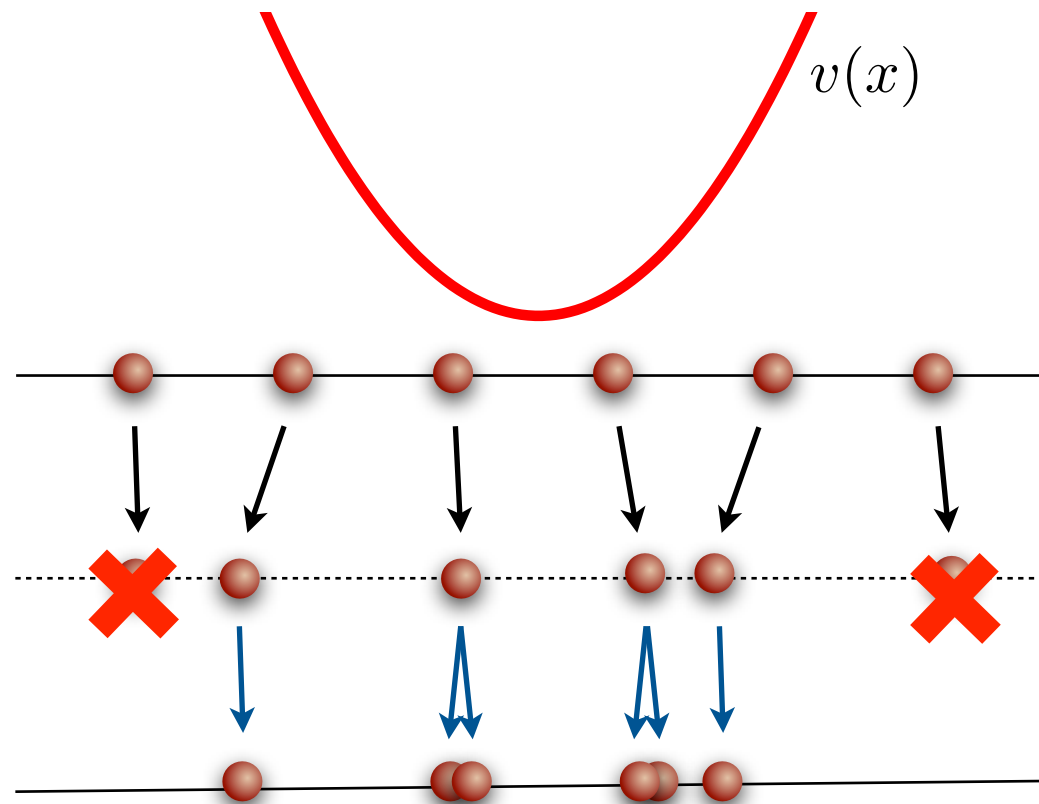
- A set of walkers is sampled from the trial wave function

$$\Psi(R, \tau) = \sum_k \delta(R - R_k)$$

- Gaussian drift according to

$$\Psi(R, \tau + d\tau) = \sum_k G_d(R, R_k, d\tau)$$

Diffusion Monte Carlo



- A set of walkers is sampled from the trial wave function

$$\Psi(R, \tau) = \sum_k \delta(R - R_k)$$

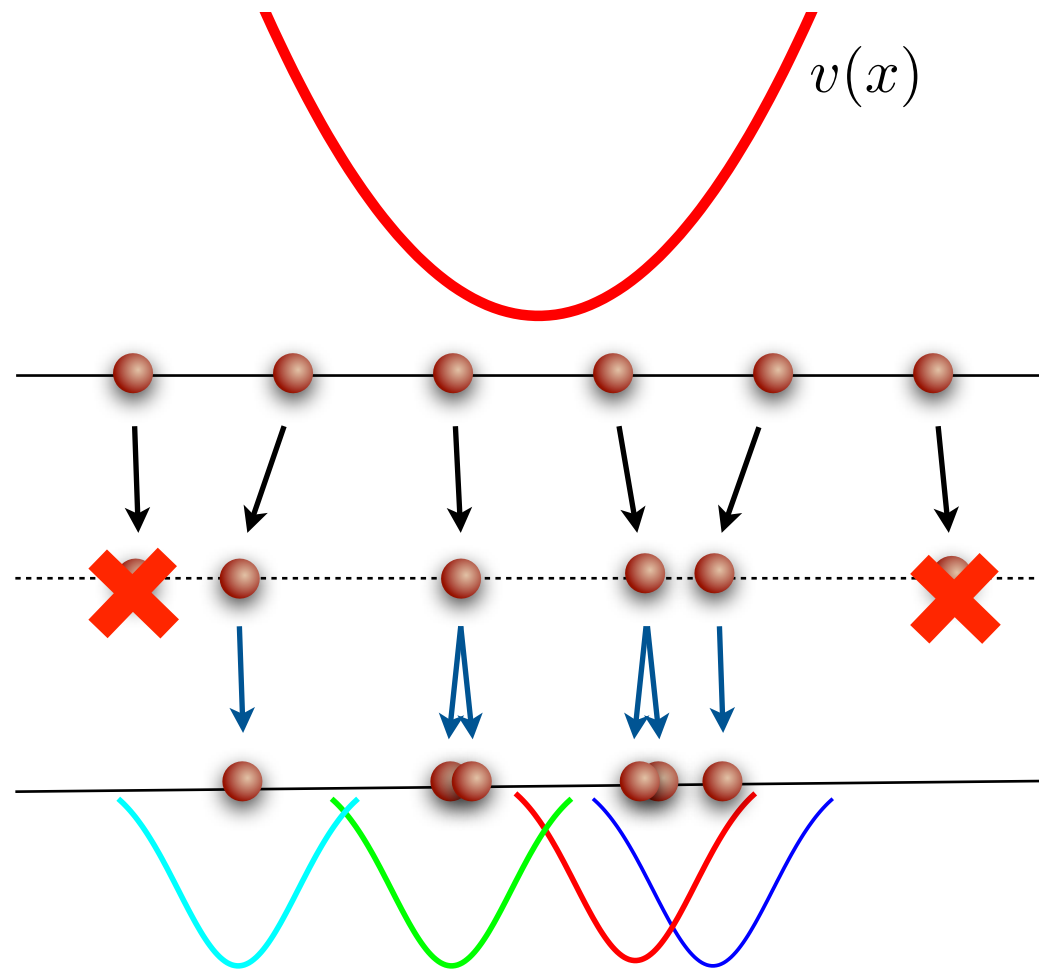
- Gaussian drift according to

$$\Psi(R, \tau + d\tau) = \sum_k G_d(R, R_k, d\tau)$$

- Branching: integer number of copies of the walker

$$\text{INT}[G_b(R, R', d\tau) + \eta]$$

Diffusion Monte Carlo



- A set of walkers is sampled from the trial wave function

$$\Psi(R, \tau) = \sum_k \delta(R - R_k)$$

- Gaussian drift according to

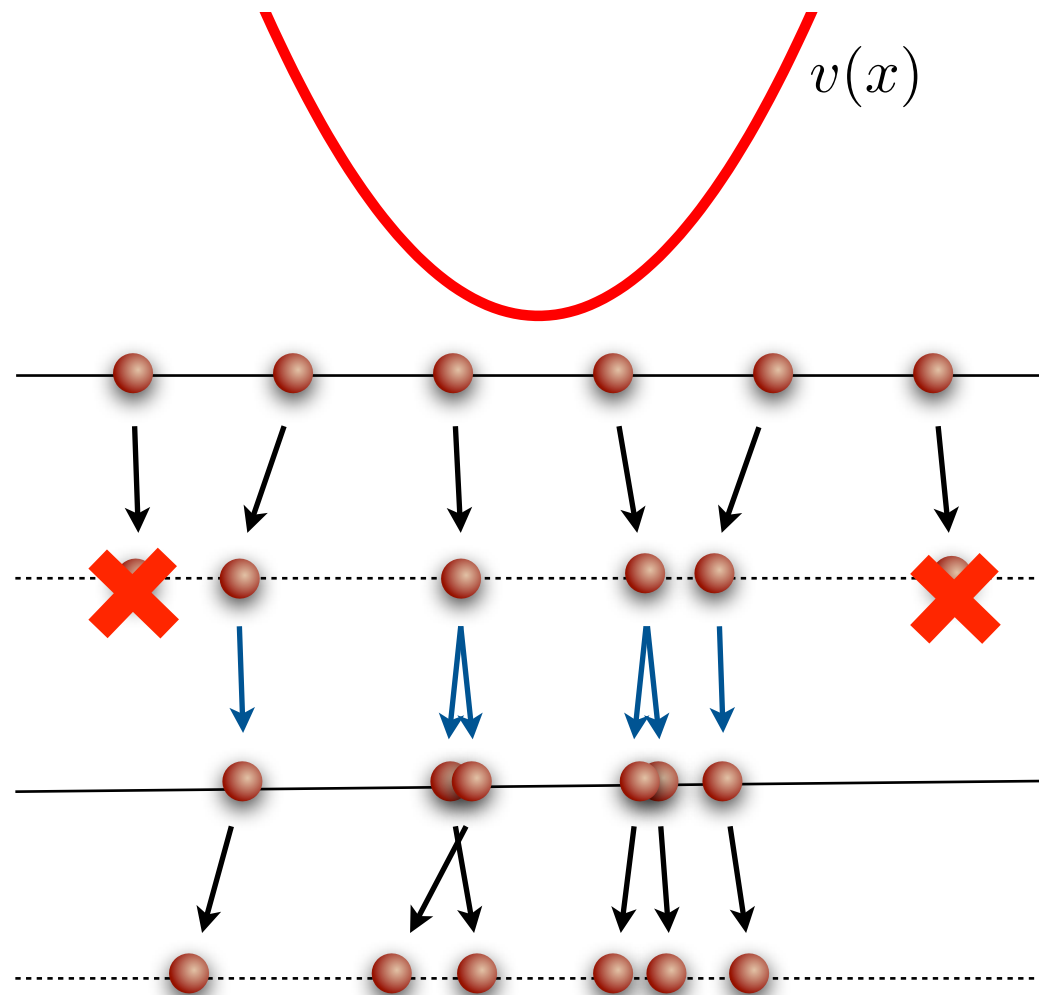
$$\Psi(R, \tau + d\tau) = \sum_k G_d(R, R_k, d\tau)$$

- Branching: integer number of copies of the walker

$$\text{INT}[G_b(R, R', d\tau) + \eta]$$

- Iterate adjusting E_T to keep the population under control

Diffusion Monte Carlo



- A set of walkers is sampled from the trial wave function

$$\Psi(R, \tau) = \sum_k \delta(R - R_k)$$

- Gaussian drift according to

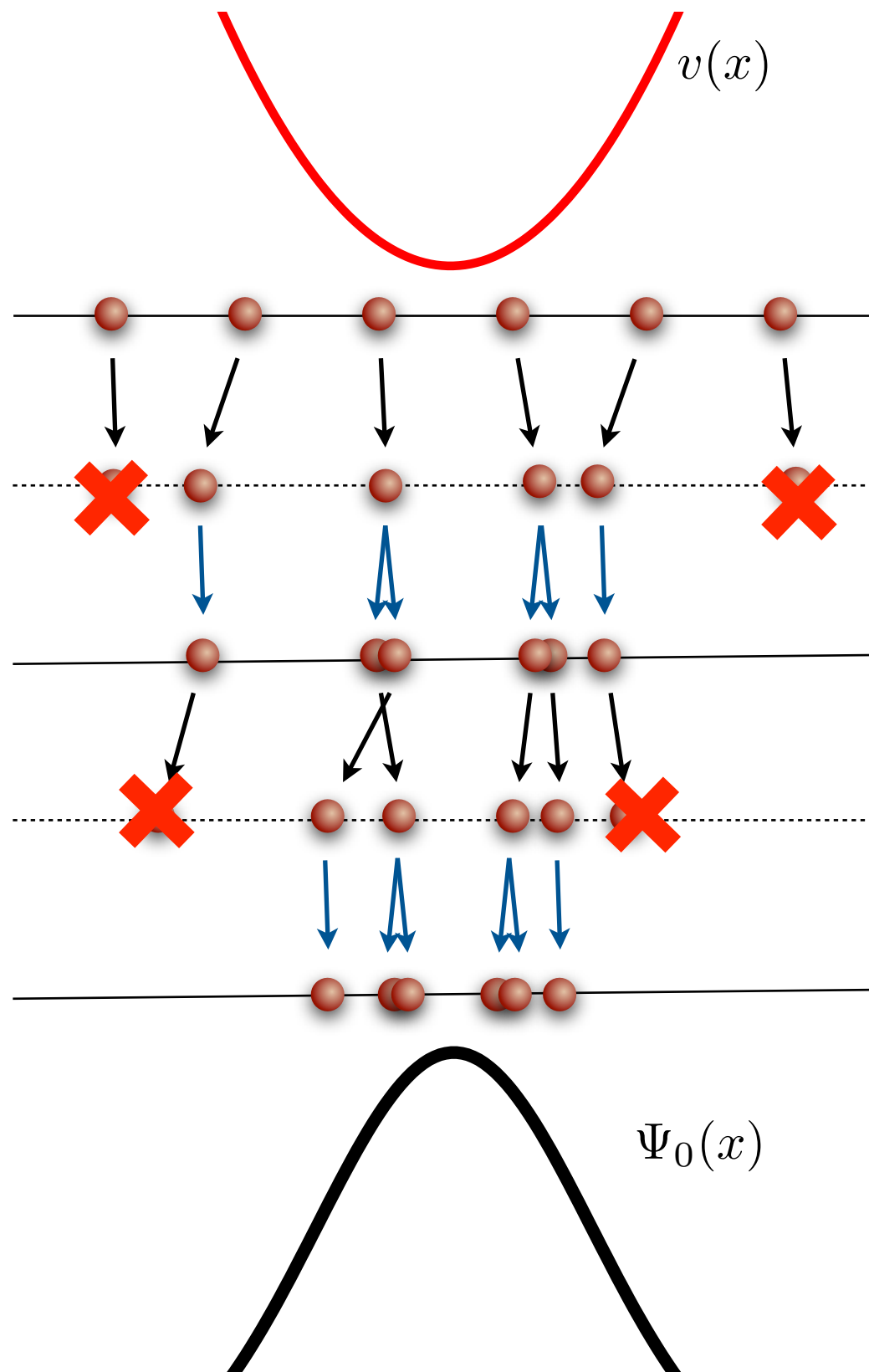
$$\Psi(R, \tau + d\tau) = \sum_k G_d(R, R_k, d\tau)$$

- Branching: integer number of copies of the walker

$$\text{INT}[G_b(R, R', d\tau) + \eta]$$

- Iterate adjusting E_T to keep the population under control

Diffusion Monte Carlo



- A set of walkers is sampled from the trial wave function

$$\Psi(R, \tau) = \sum_k \delta(R - R_k)$$

- Gaussian drift according to

$$\Psi(R, \tau + d\tau) = \sum_k G_d(R, R_k, d\tau)$$

- Branching: integer number of copies of the walker

$$\text{INT}[G_b(R, R', d\tau) + \eta]$$

- Iterate adjusting E_T to keep the population under control

The ground-state expectation values of observables that commute with \hat{H} can be estimated by

$$\langle \hat{O} \rangle = \frac{\sum_{\{R\}} \langle R | \hat{O} | \Psi_T \rangle}{\sum_{\{R\}} \langle R | \Psi_T \rangle} = \frac{\sum_{\{R\}} [O \Psi_T](R)}{\sum_{\{R\}} \Psi_T(R)}$$

Spin-isospin: GFMC and AFDMC

GFMC

Imaginary time evolution algorithm applied for each many-body spin-isospin configuration

$$|^3H\rangle = \begin{pmatrix} a_{\uparrow\uparrow\uparrow}(R) \\ a_{\uparrow\uparrow\downarrow}(R) \\ a_{\uparrow\downarrow\uparrow}(R) \\ a_{\uparrow\downarrow\downarrow}(R) \\ a_{\downarrow\uparrow\uparrow}(R) \\ a_{\downarrow\uparrow\downarrow}(R) \\ a_{\downarrow\downarrow\uparrow}(R) \\ a_{\downarrow\downarrow\downarrow}(R) \end{pmatrix} \longrightarrow 2^A \frac{A!}{Z!(A-Z)!}$$



Can deal with v_{18} + UIX



Limited to $A=12$ nucleons:
not feasible for nuclear
matter calculation

AFDMC

Single particle spin configuration $|^3H\rangle = [c_1^\uparrow |\uparrow\rangle_1 + c_1^\downarrow |\downarrow\rangle_1] \otimes [c_2^\uparrow |\uparrow\rangle_2 + c_2^\downarrow |\downarrow\rangle_2] \otimes [c_3^\uparrow |\uparrow\rangle_3 + c_3^\downarrow |\downarrow\rangle_3] \longrightarrow \nu A$

Hubbard Stratonovich transformation to reduce
spin-isospin dependence from quadratic to linear

$$e^{-\frac{1}{2}\lambda\hat{O}^2} = \frac{1}{\sqrt{2\pi}} \int dx e^{-\frac{x^2}{2} + \sqrt{-\lambda}x\hat{O}}.$$



Can deal with larger systems (114 nucleons)



Spin-orbit term and UIX included in the pure neutron case only.

Density dependent nucleon-nucleon interaction from UIX

Motivations

The widely used Argonne v_{18} + UIX interaction model fails to reproduce the empirical equilibrium properties of nuclear matter.

Can this fact be ascribed to deficiencies of the variational wave function?

Tenet

n-body potentials ($n \geq 3$) can be replaced by an effective two-nucleon potential, obtained through an average over the degrees of freedom of $n - 2$ particles.

This effective potential $\hat{v}_{12}(\rho) = \sum_p v^p(\rho, r_{12}) \hat{O}_{12}^p$

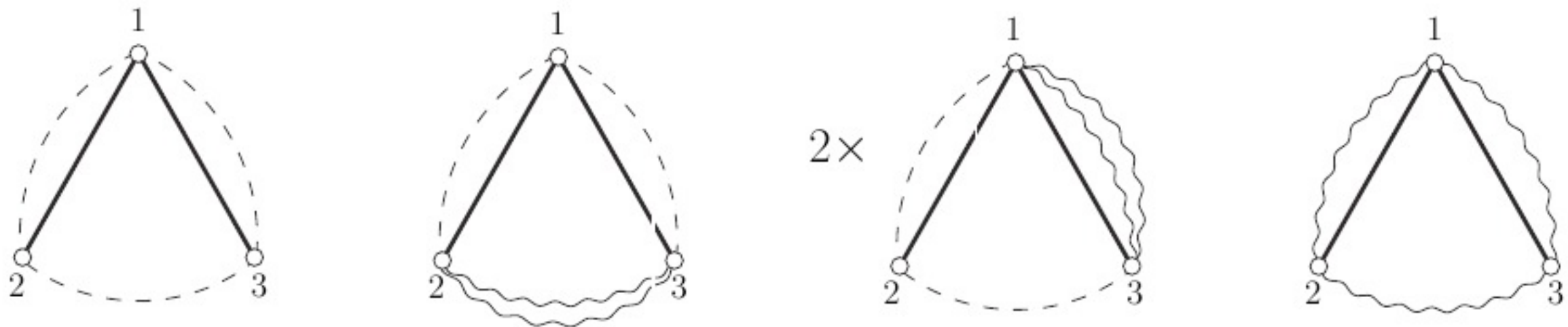
- Has to be obtained from a microscopic model of the three-nucleon force providing a fairly accurate description of the properties of light nuclei.
- Could be easily implemented in AFDMC.
- Could be used to include the effects of three nucleon interactions in the calculation of the nucleon-nucleon scattering cross section in the nuclear medium.

Three-body potential in CBF

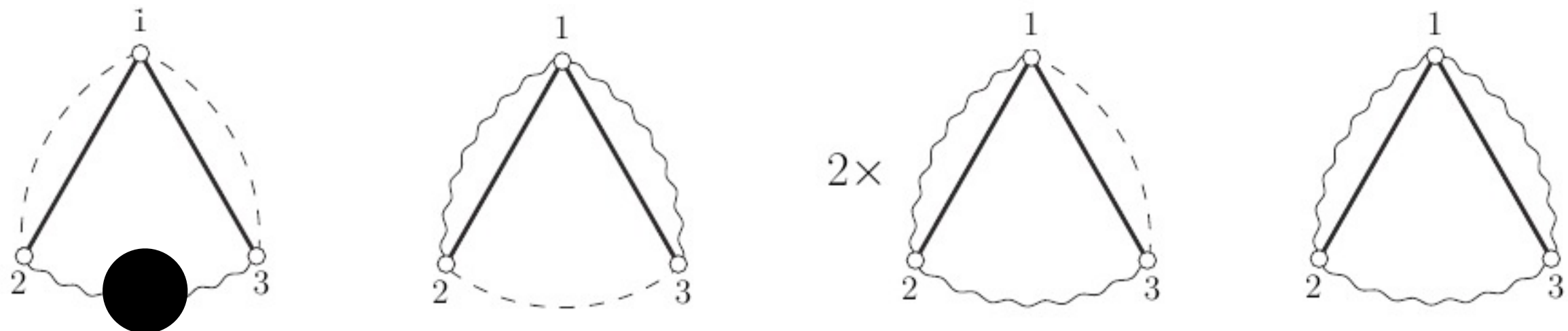
Expectation value of the three body potential

$$\langle \hat{V}_{123} \rangle = \frac{\int dx_{1\dots A} \Phi_0^* \hat{\mathcal{F}}^\dagger \hat{V}_{123} \hat{\mathcal{F}} \Phi_0}{\int dx_{1\dots A} \Phi_0^* \hat{\mathcal{F}}^\dagger \hat{\mathcal{F}} \Phi_0}$$

Diagrams involved in the calculation of the scalar repulsive term.



Diagrams involved in the calculation of TPE and OPE terms.



Density dependent potential

As for the two-body potential we can write

$$\hat{V}_{123} \equiv \sum_P V_{123}^P \hat{O}_{123}^P \quad \frac{\langle V_{123} \rangle}{A} = \frac{\rho^2}{3!} \sum_P \int d\mathbf{r}_{12} d\mathbf{r}_{13} V_{123}^P g_{123}^P .$$

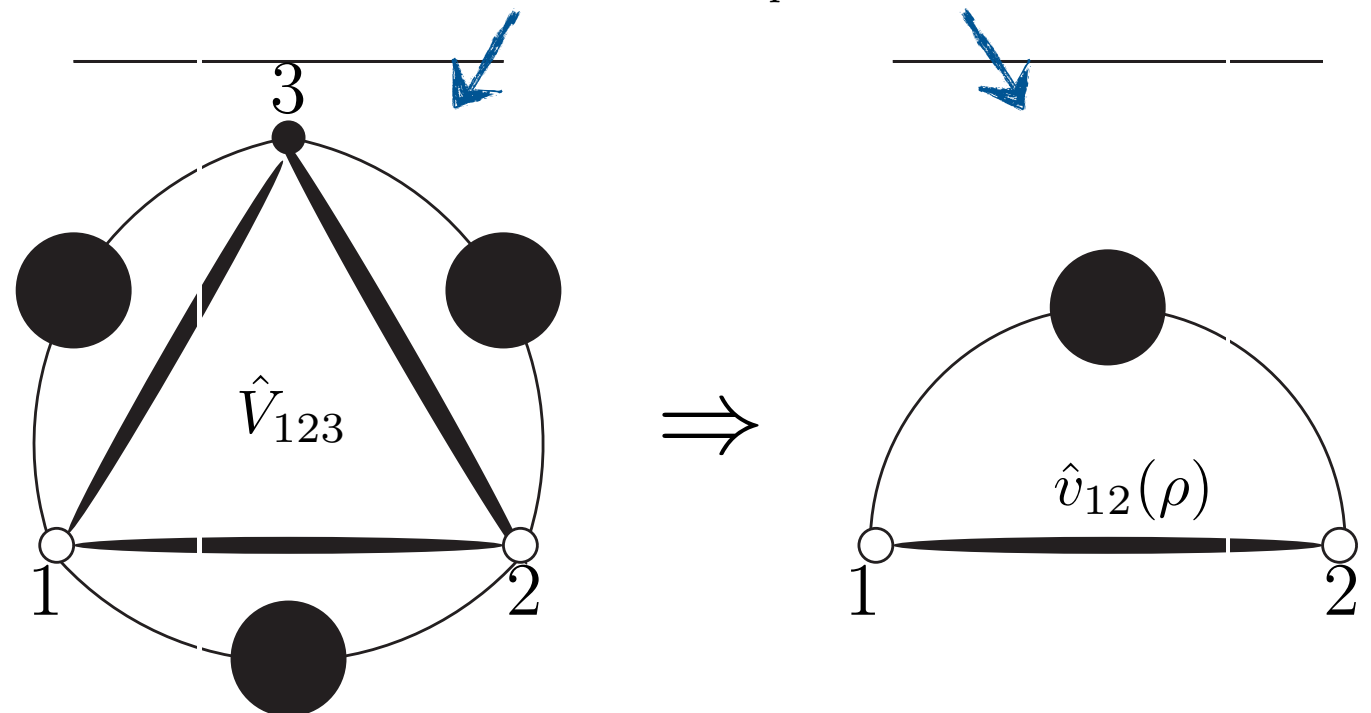
The three-body operatorial distribution function is defined by

$$g_{123}^P = \frac{A!}{(A-3)!} \frac{\text{CTr}_{123} \int dx_4 \dots dx_A \Phi_0^\dagger \mathcal{F}^\dagger \hat{O}_{123}^P \mathcal{F} \Phi_0}{\rho^3 \int dX \Phi_0^\dagger \mathcal{F}^\dagger \mathcal{F} \Phi_0}$$

The expectation values of the effective potential and of \hat{V}_{123} should be equal

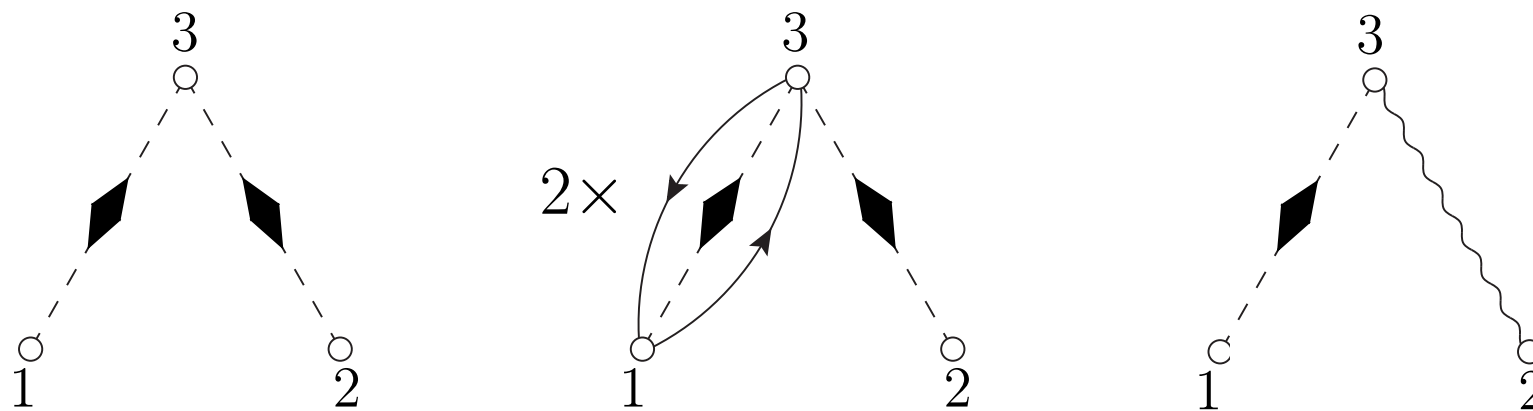
$$\frac{\langle \hat{V}_{123} \rangle}{A} = \frac{\langle \hat{v}_{12}(\rho) \rangle}{A} \quad \sum_P \frac{\rho}{3} \int d\mathbf{r}_3 V_{123}^P g_{123}^P = \sum_p v_{12}^p(\rho) g_{12}^p$$

$\hat{v}_{12}(\rho)$ needs to include the effect of correlation and exchange lines.



Selection of diagrams

- We have selected the leading diagrams contributing to the density dependent potential



- The scalar correlation line has been dressed at first order in perturbation theory in ρ .

$$g_{bose}^{NLO}(r_{12}) \longrightarrow \text{Diagram 1} = 1 + \text{Diagram 2} + \text{Diagram 3} + \text{Diagram 4}$$

Neither exchange lines, nor correlation lines appear between particles 1 and 2

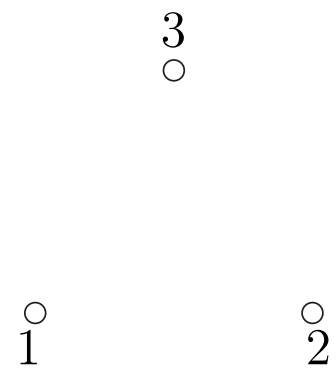


The effective potential has to be multiplied by g_{12}^p that connects particles 1 and 2 in all the possible allowed ways

Statistical and dynamical correlations

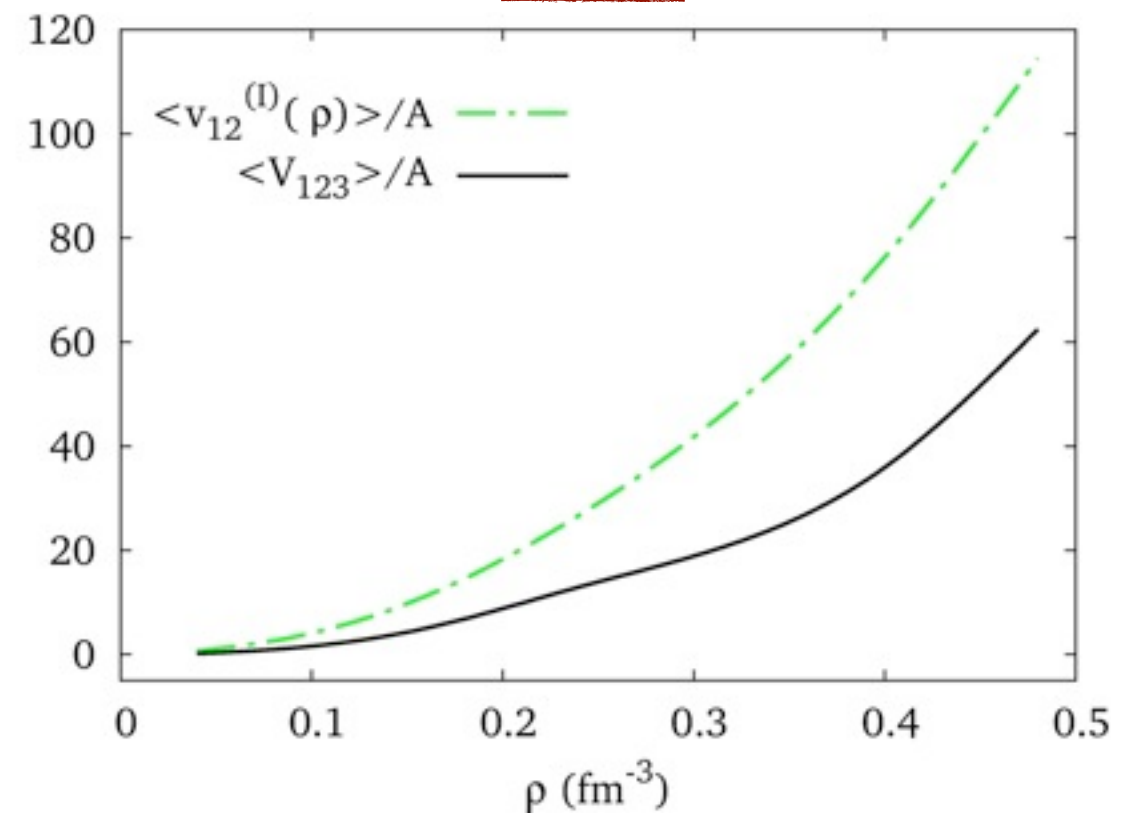
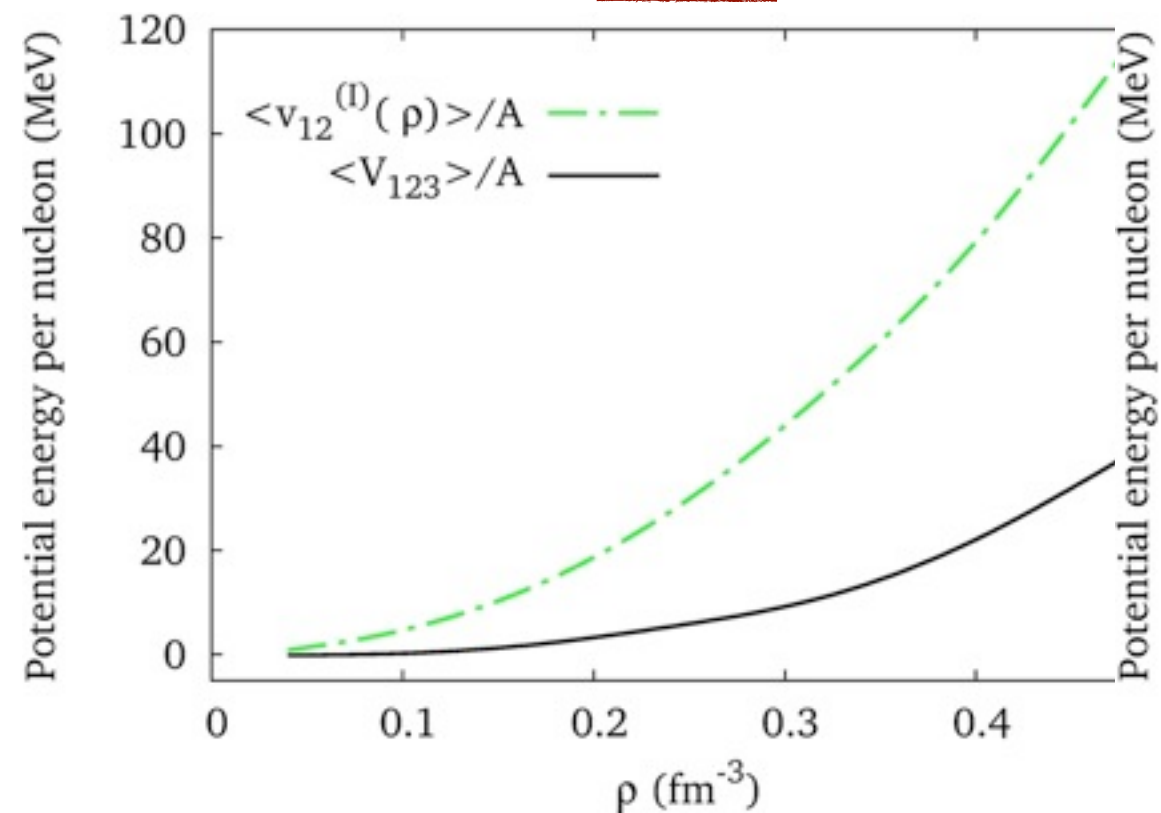
I - Bare approximation

$$\frac{\rho}{3} \int dx_3 \hat{V}_{123}$$



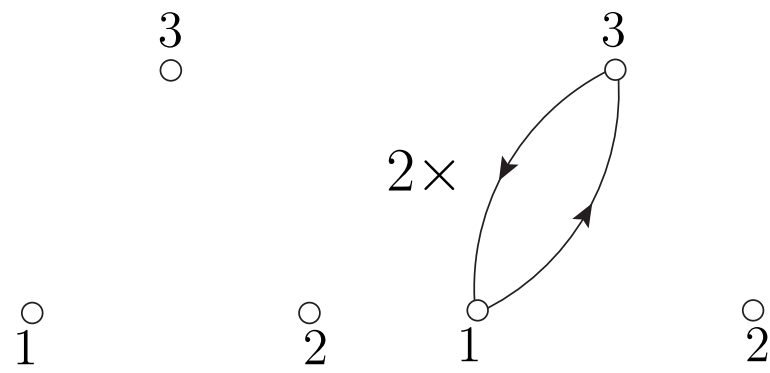
SNM

PNM



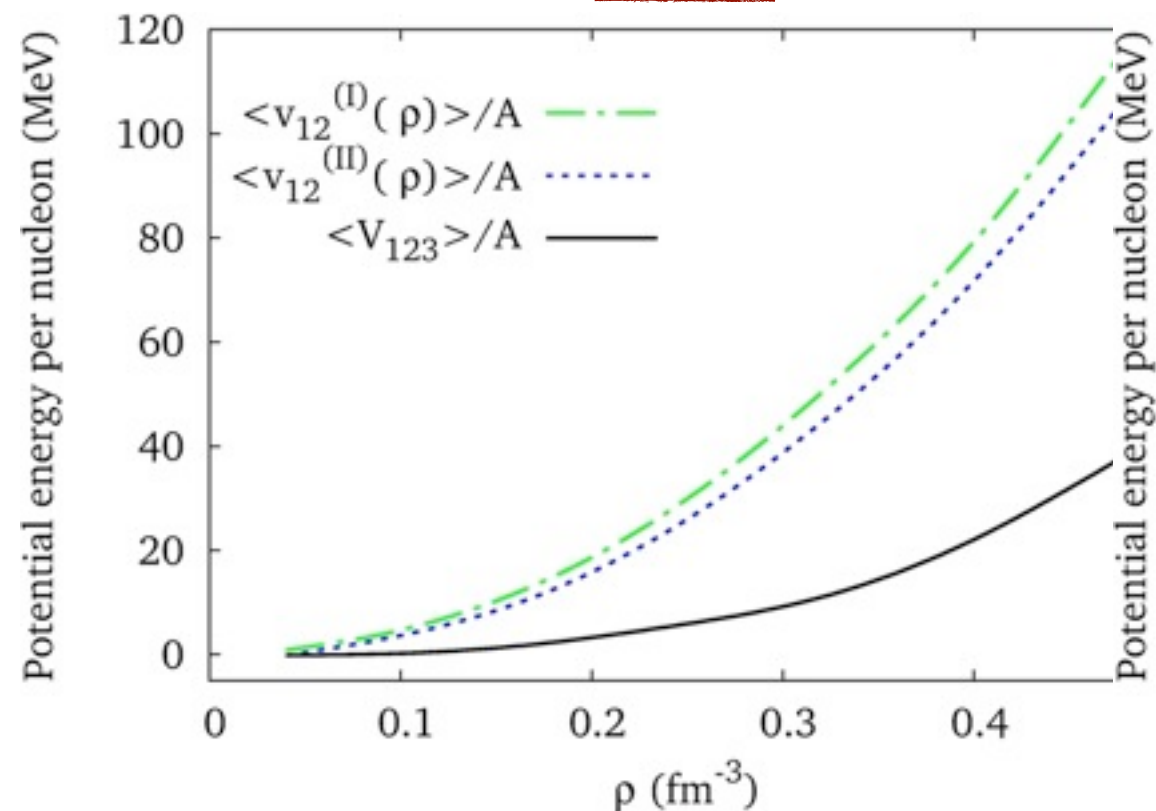
Statistical and dynamical correlations

II - Statistical correlations

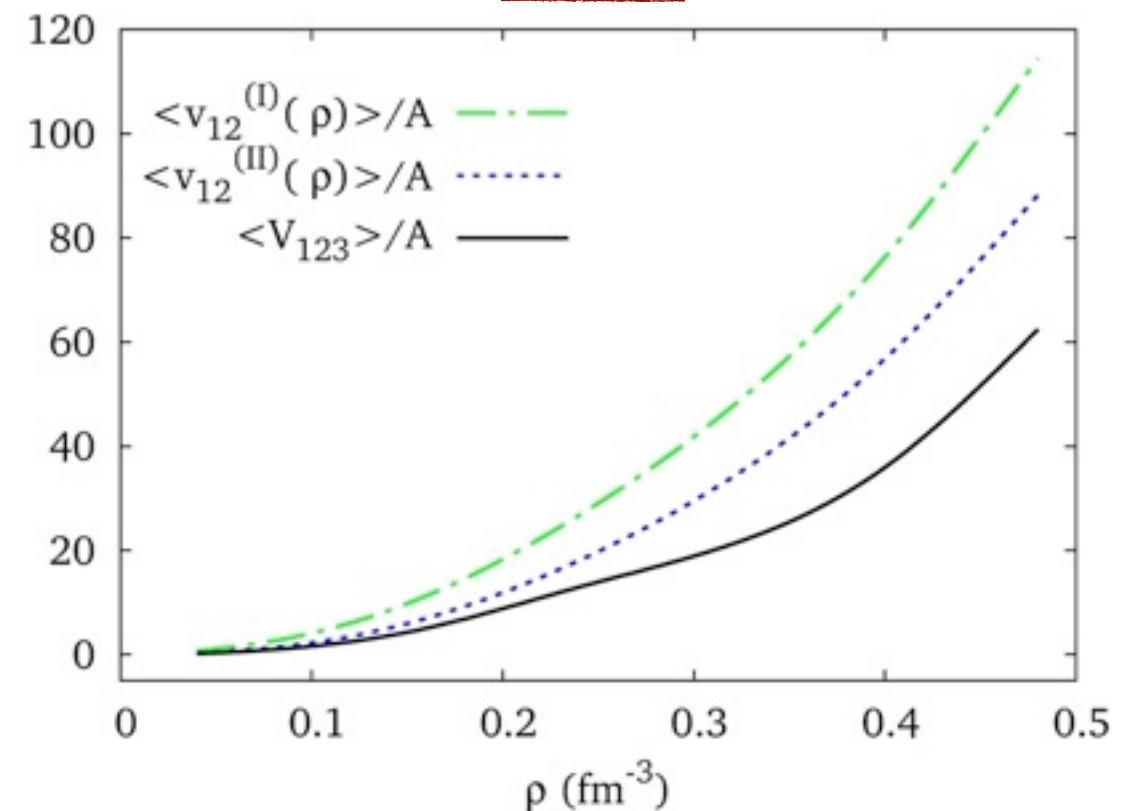


$$\frac{\rho}{3} \int dx_3 \hat{V}_{123} (1 - \hat{P}_{13}^{\sigma\tau} \ell_{13}^3 - \hat{P}_{23}^{\sigma\tau} \ell_{23}^2)$$

SNM

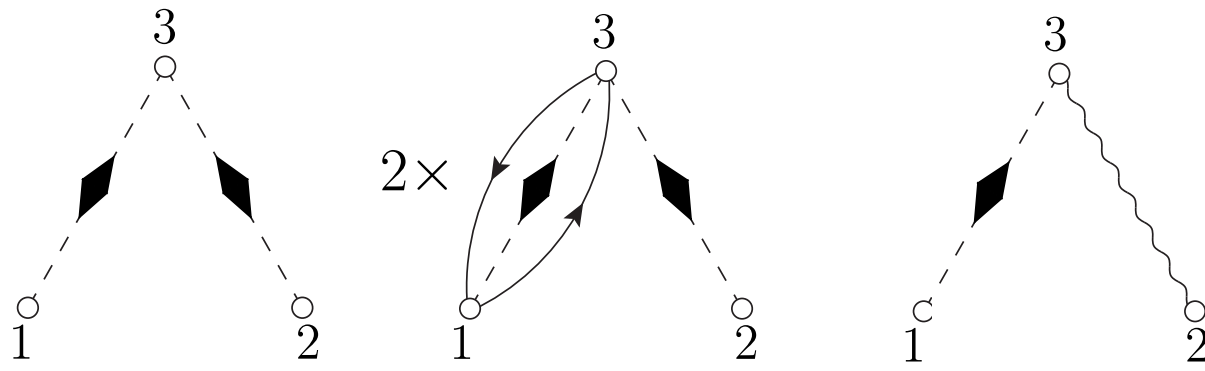


PNM



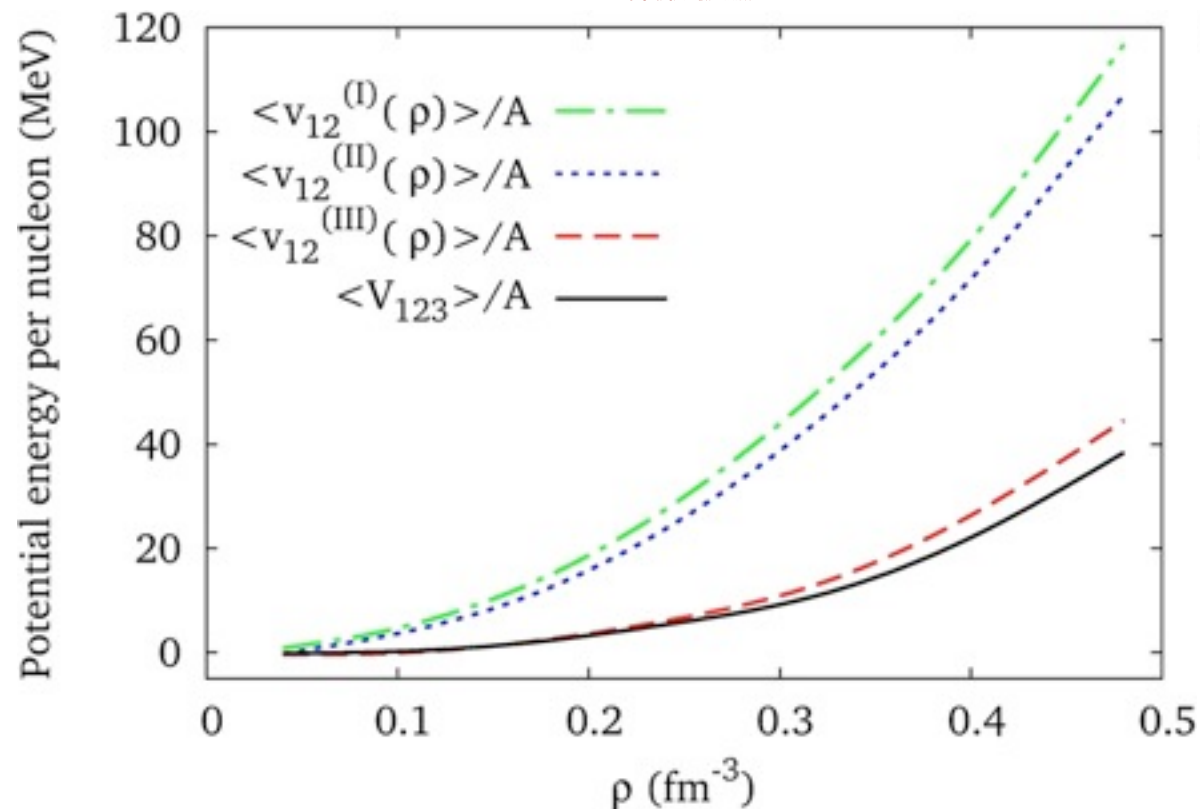
Statistical and dynamical correlations

III - Statistical and dynamical correlations

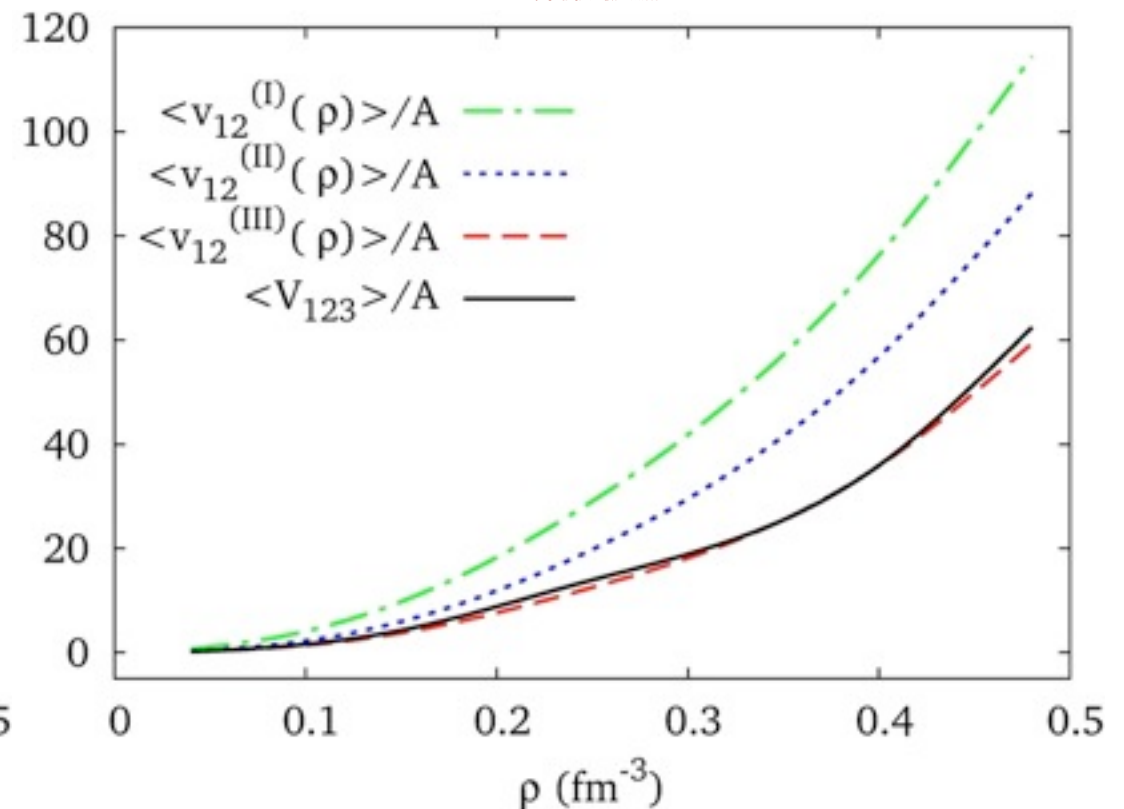


$$\frac{\rho}{3} \int dx_3 \hat{V}_{123} \left[g_{bose}^{NLO}(r_{13}) g_{bose}^{NLO}(r_{23}) \right. \\ \left. \times (1 - 2\hat{P}_{13}^{\sigma\tau} \ell_{13}^2) + 4g_{bose}^{NLO}(r_{13}) f_c(r_{23}) \hat{f}(r_{23}) \right]$$

SNM

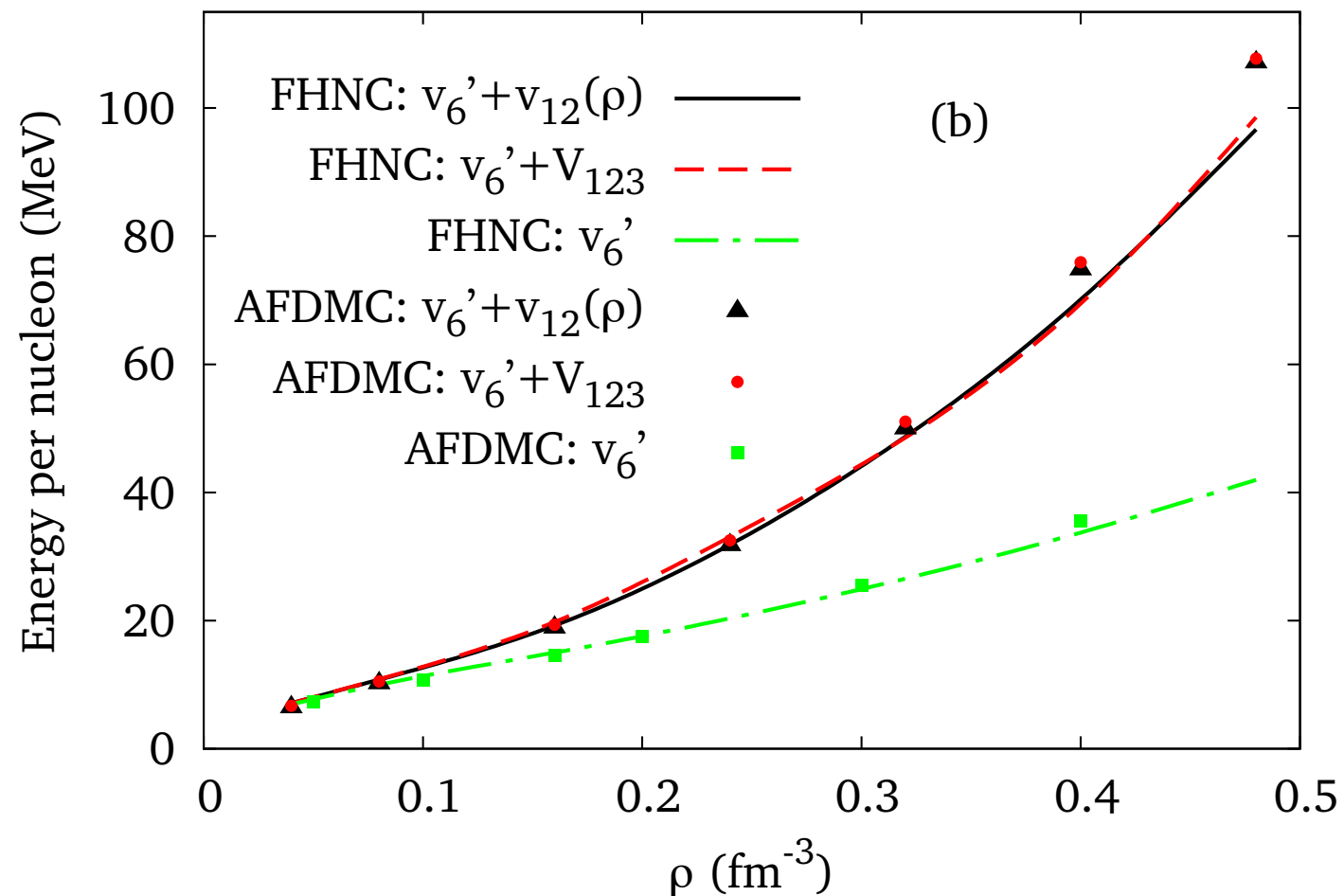
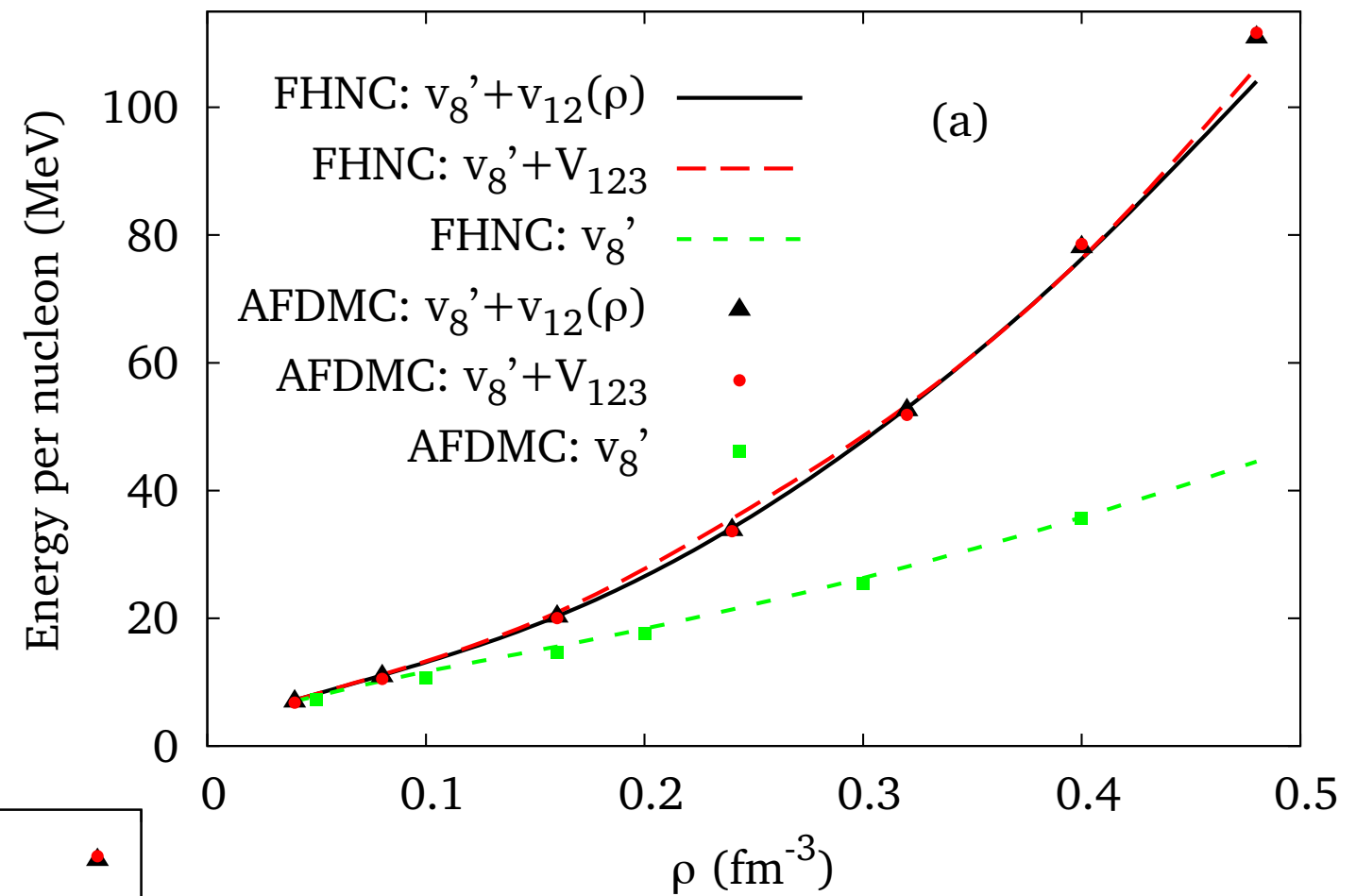


PNM



PNM results

Argonne v'_8 as
two-body potential

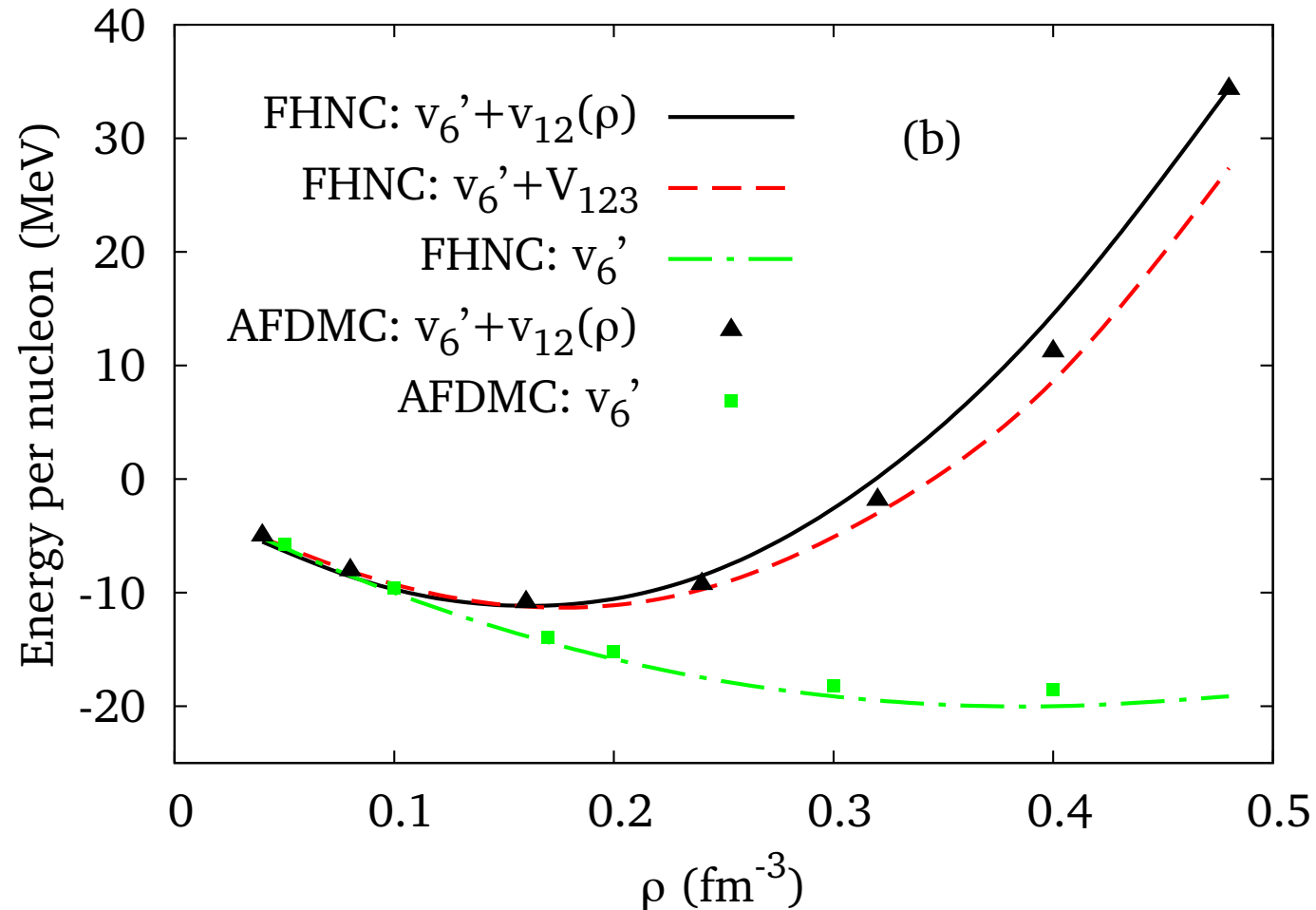
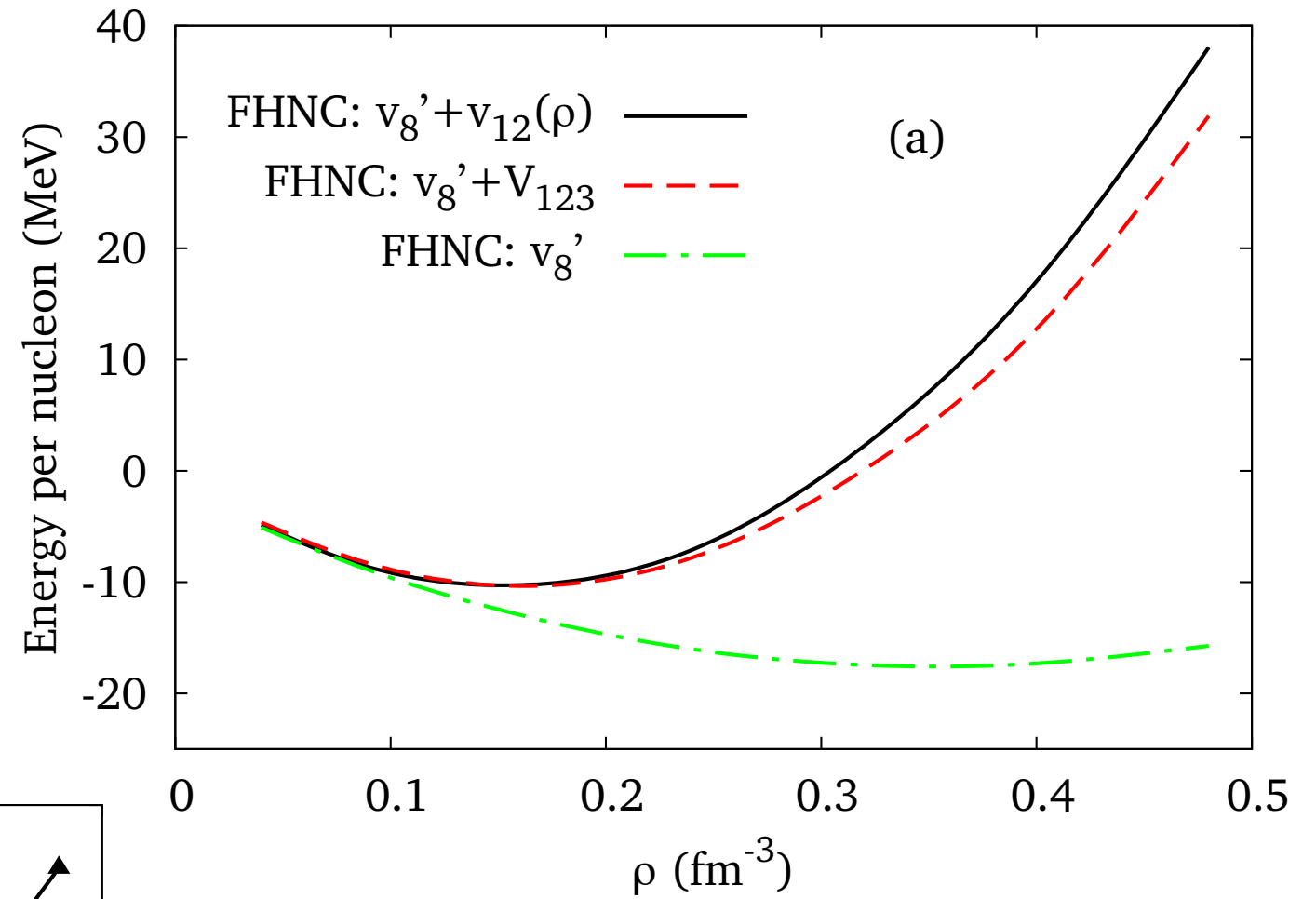


Argonne v'_6 as
two-body potential



SNM results

Argonne v'_8 as
two-body potential



Argonne v'_6 as
two-body potential

SNM results

Saturation densities, binding energy, and compressibility

FHNC/SOC	$v'_6 + V_{123}$	$v'_6 + v(\rho)$	$v'_8 + V_{123}$	$v'_8 + v(\rho)$
ρ_0 (fm ⁻³)	0.17	0.16	0.16	0.15
E_0 (MeV)	-11.3	-11.2	-10.3	-10.3
K (MeV)	205	192	189	198

AFDMC	$v'_6 + v(\rho)$
ρ_0 (fm ⁻³)	0.17
E_0 (MeV)	-10.9
K (MeV)	201

AFDMC calculations do not show an increase of the binding energy of SNM with respect to variational results.

SNM results

Saturation densities, binding energy, and compressibility

FHNC/SOC	$v'_6 + V_{123}$	$v'_6 + v(\rho)$	$v'_8 + V_{123}$	$v'_8 + v(\rho)$
ρ_0 (fm ⁻³)	0.17	0.16	0.16	0.15
E_0 (MeV)	-11.3	-11.2	-10.3	-10.3
K (MeV)	205	192	189	198

AFDMC	$v'_6 + v(\rho)$
ρ_0 (fm ⁻³)	0.17
E_0 (MeV)	-10.9
K (MeV)	201

AFDMC calculations do not show an increase of the binding energy of SNM with respect to variational results.

Discrepancy with experimental data



Exp.	
ρ_0 (fm ⁻³)	0.16
E_0 (MeV)	-16.0
K (MeV)	240

- deficiencies of the UIX model.
- interactions involving more than three nucleons.

A comparative analysis of three-nucleon potentials in nuclear matter

Motivations

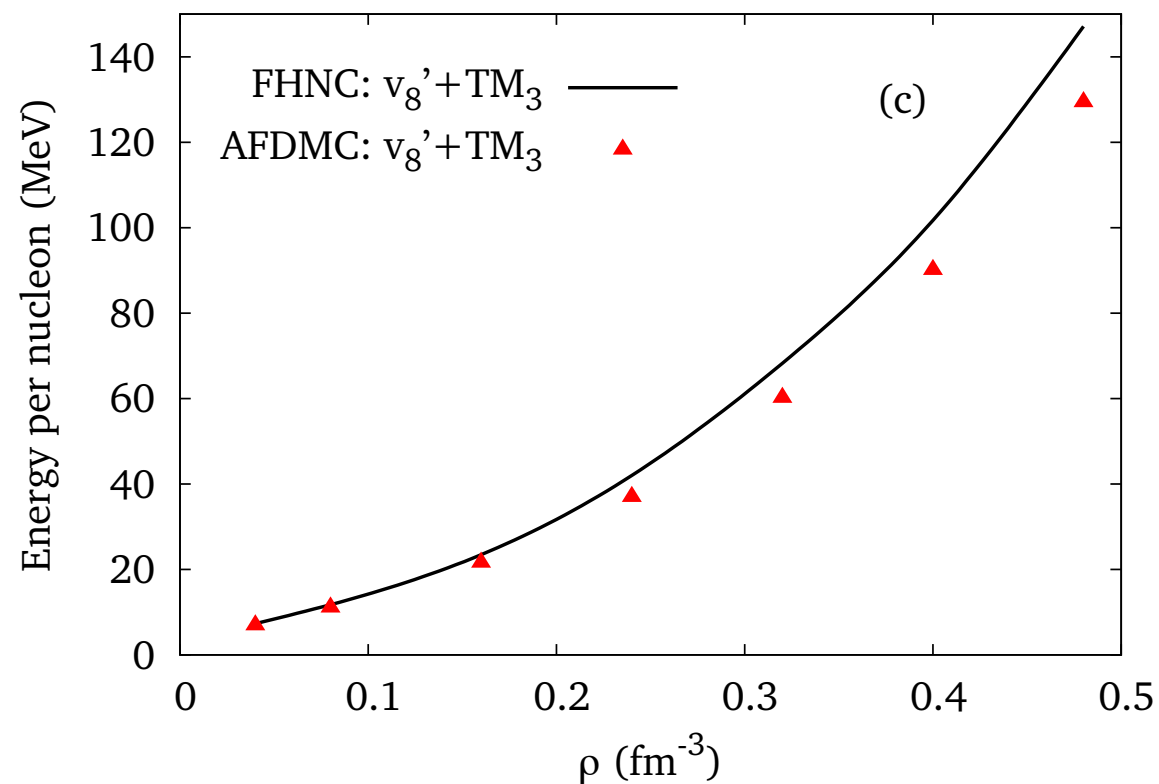
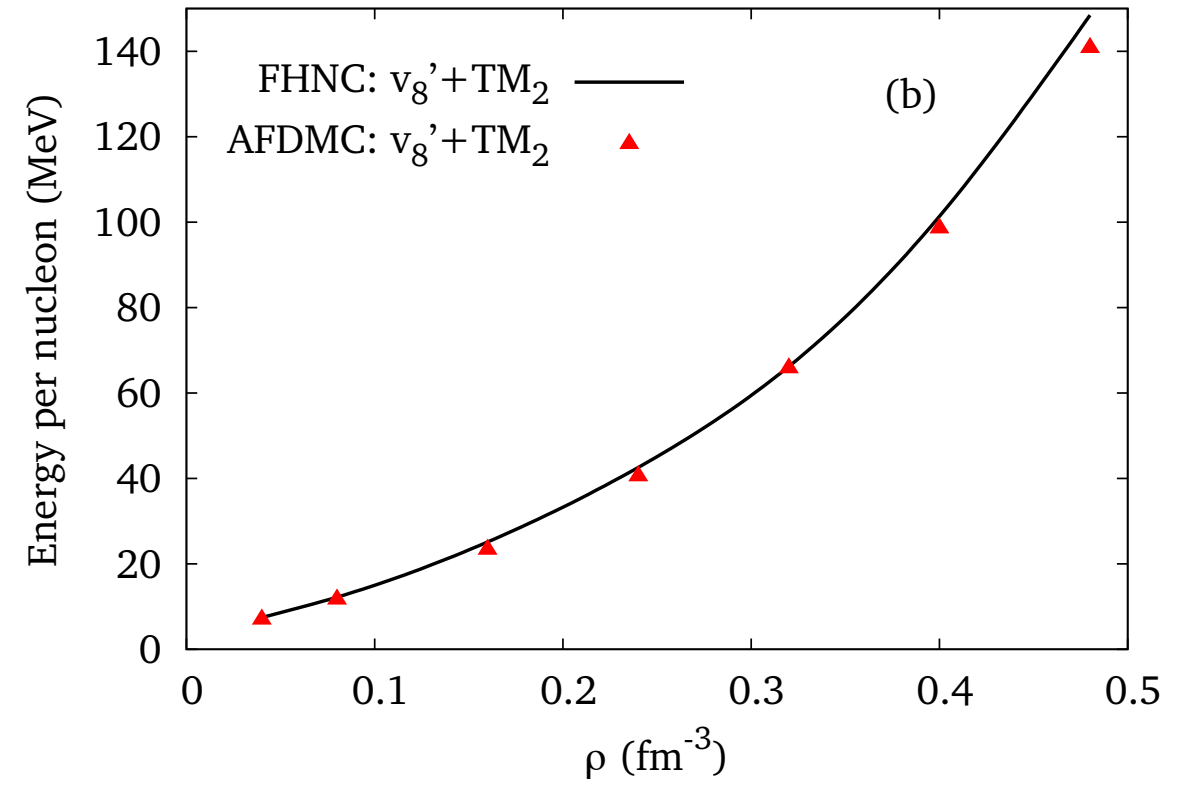
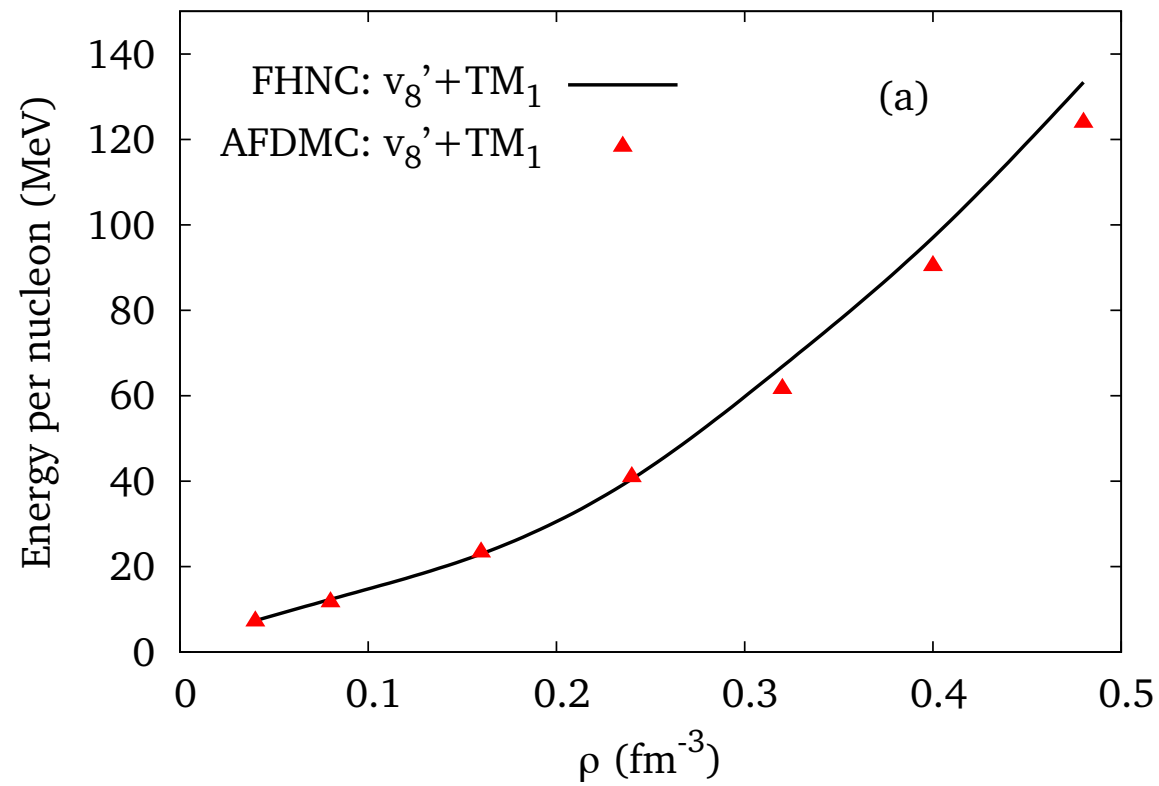
Kievsky et al. in 2010 have found the best-fit values for the TM' and NNLOL 3-body potentials plus Argonne v_{18} NN potential to simultaneously reproduce

$$\left\{ \begin{array}{l} B(^3\text{H}) = -8.482 \text{ MeV} \\ B(^4\text{He}) = -28.30 \text{ MeV} \\ {}^2a_{nd} = 0.645 \pm 0.003 \pm 0.007 \text{ fm} \end{array} \right.$$

We performed a comparative test for such potentials in PNM and SNM

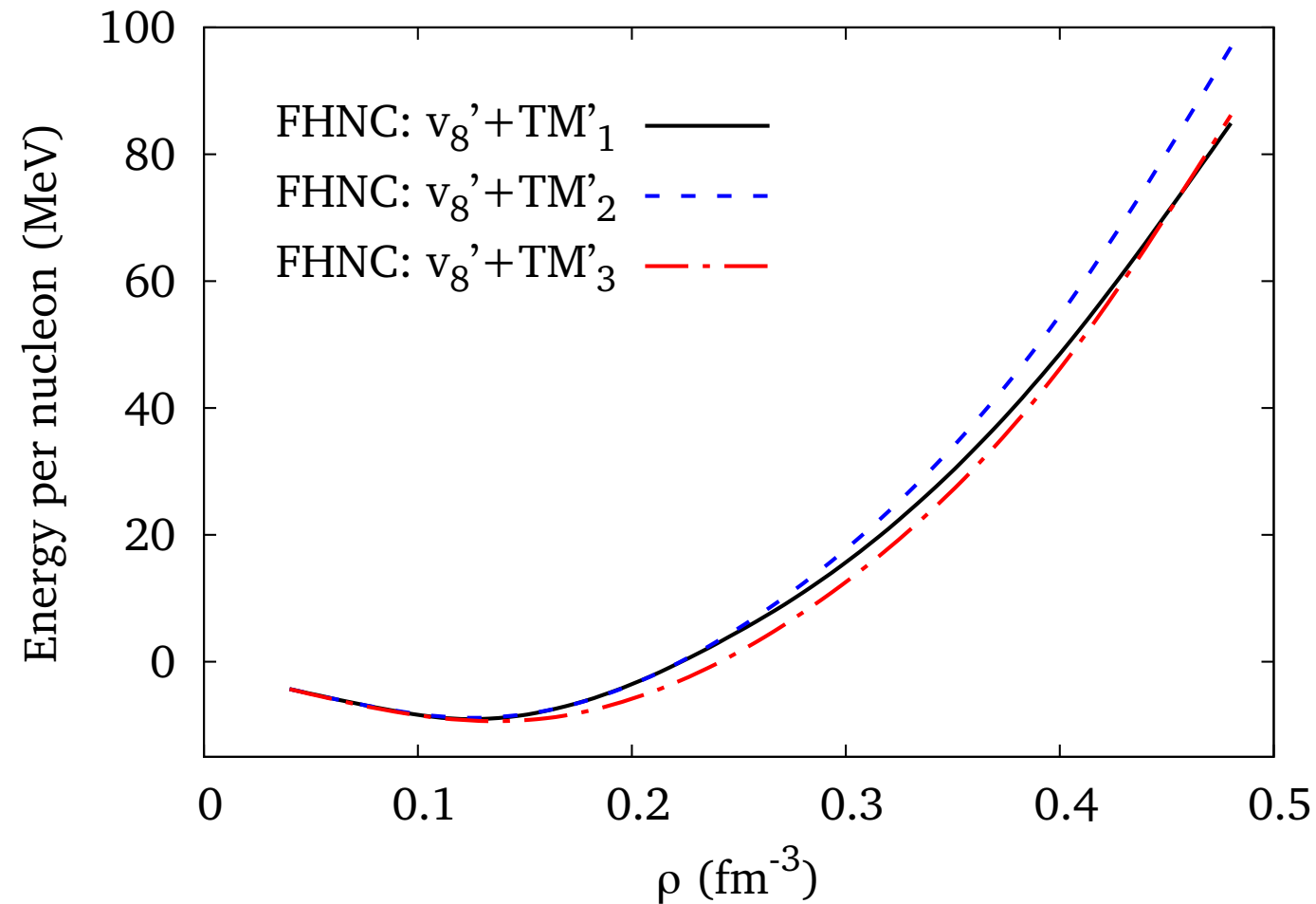
- Would they improve in the descriptions of the binding energy of SNM?
- Would they provide PNM EoS able to account for the $\sim 2M_{\odot}$ neutron star?

TM' results for PNM



Good agreement between
AFDMC and FHNC/SOC results

TM' results for SNM

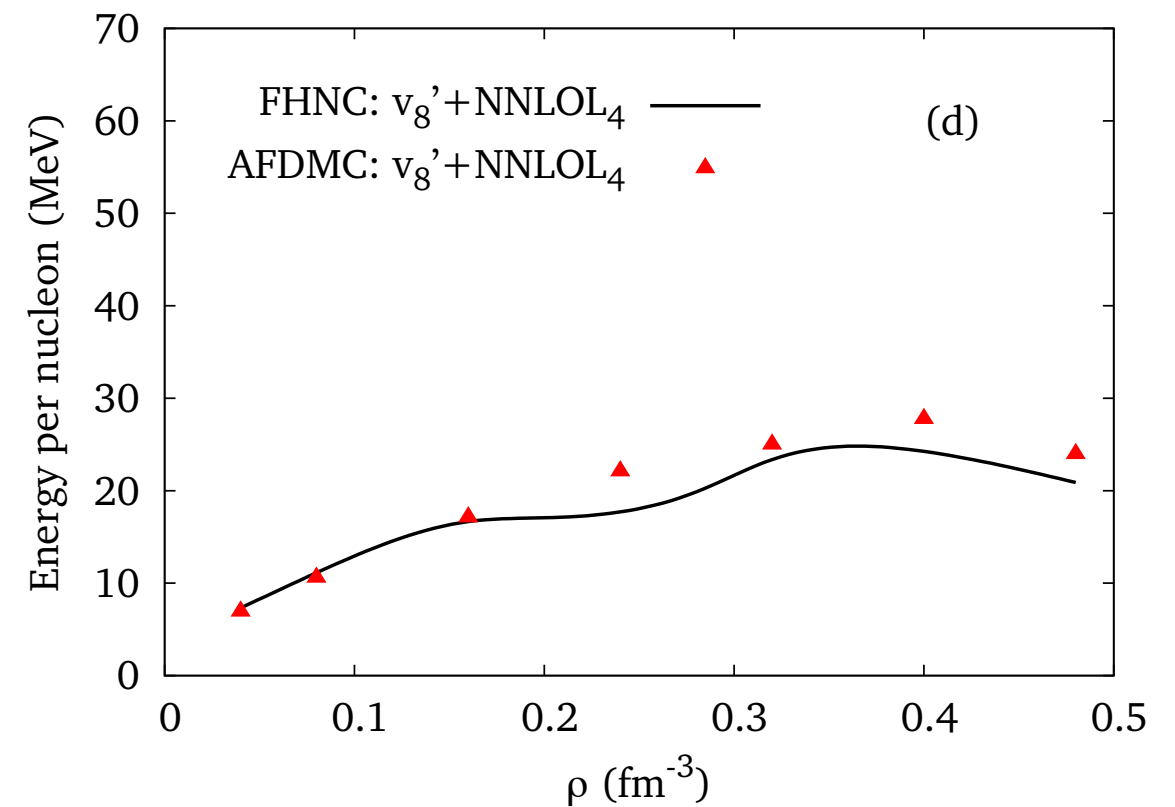
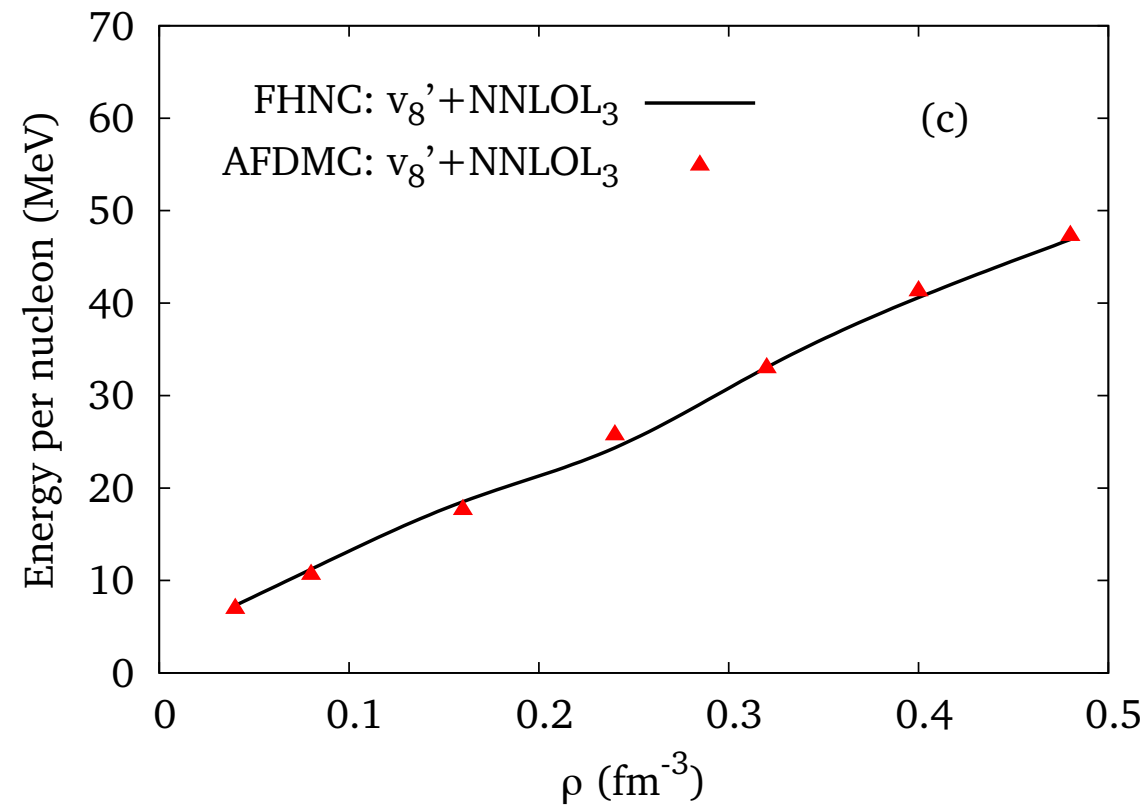
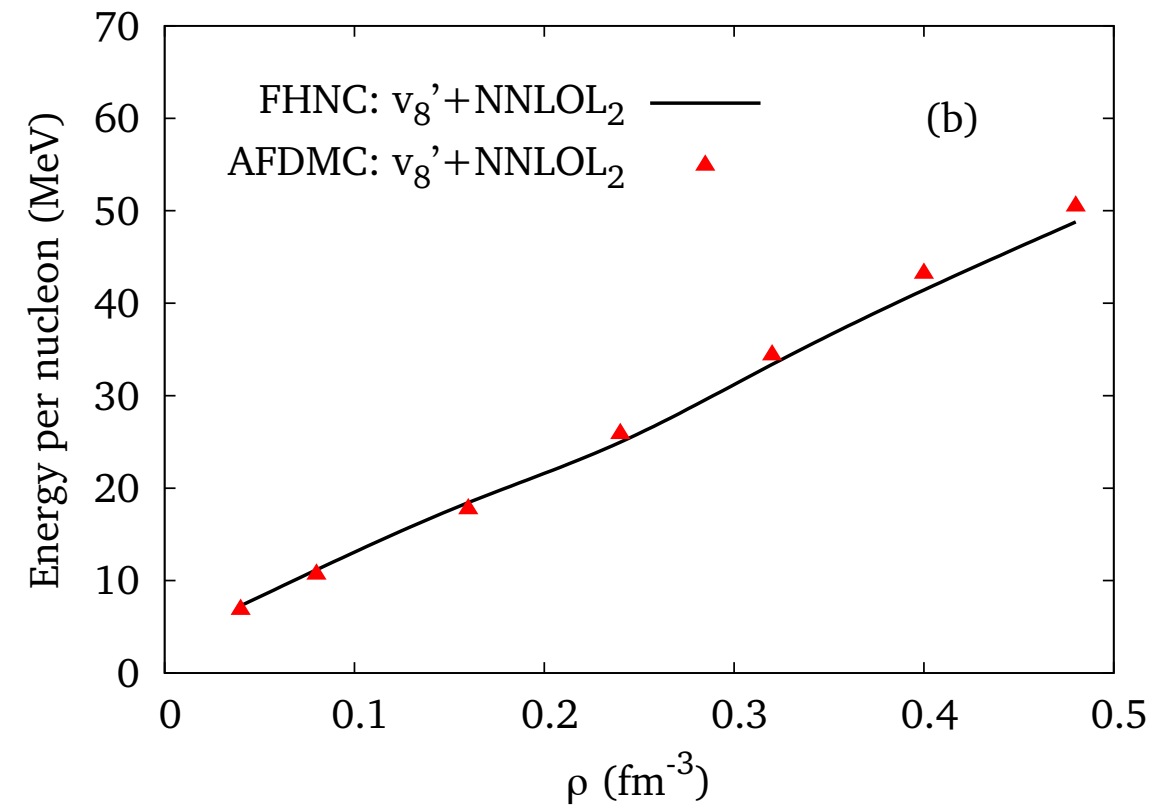
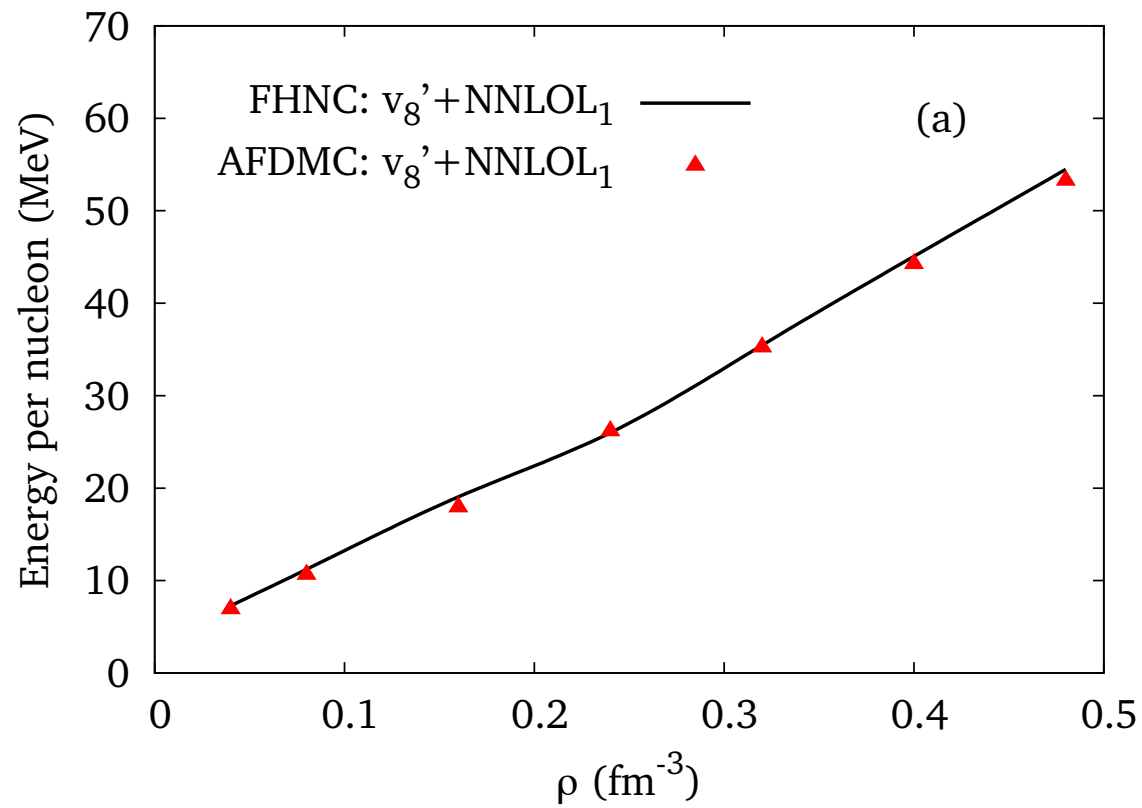


- SNM is underbound
- Reasonable values for the compressibility and saturation density

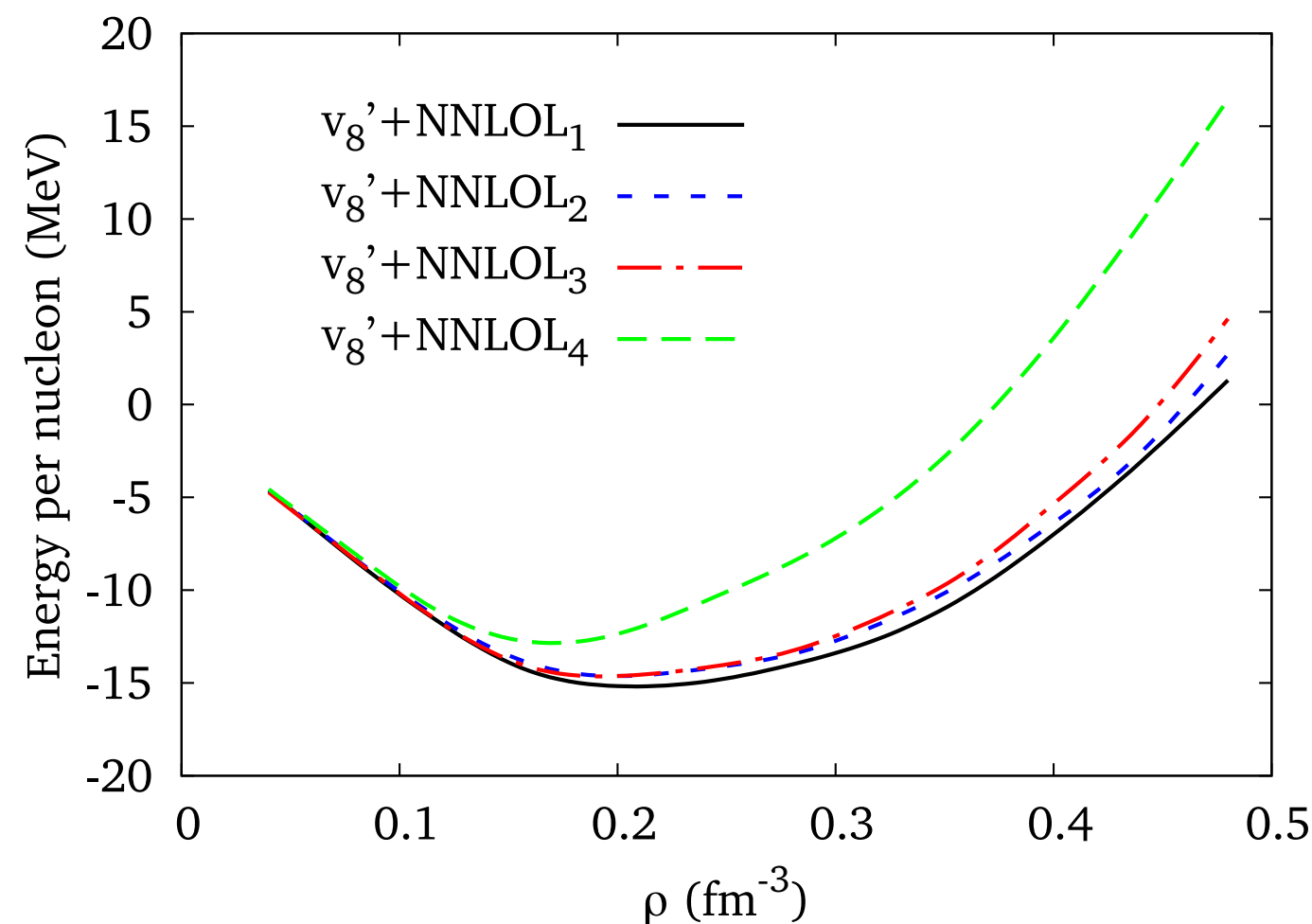
FHNC/SOC	TM' ₁	TM' ₂	TM' ₃
ρ_0 (fm ⁻³)	0.12	0.13	0.14
E_0 (MeV)	-9.0	-8.8	-9.4
K (MeV)	266	243	249

Exp.	
ρ_0 (fm ⁻³)	0.16
E_0 (MeV)	-16.0
K (MeV)	240

NNLOL results for PNM



NNLOL results for SNM



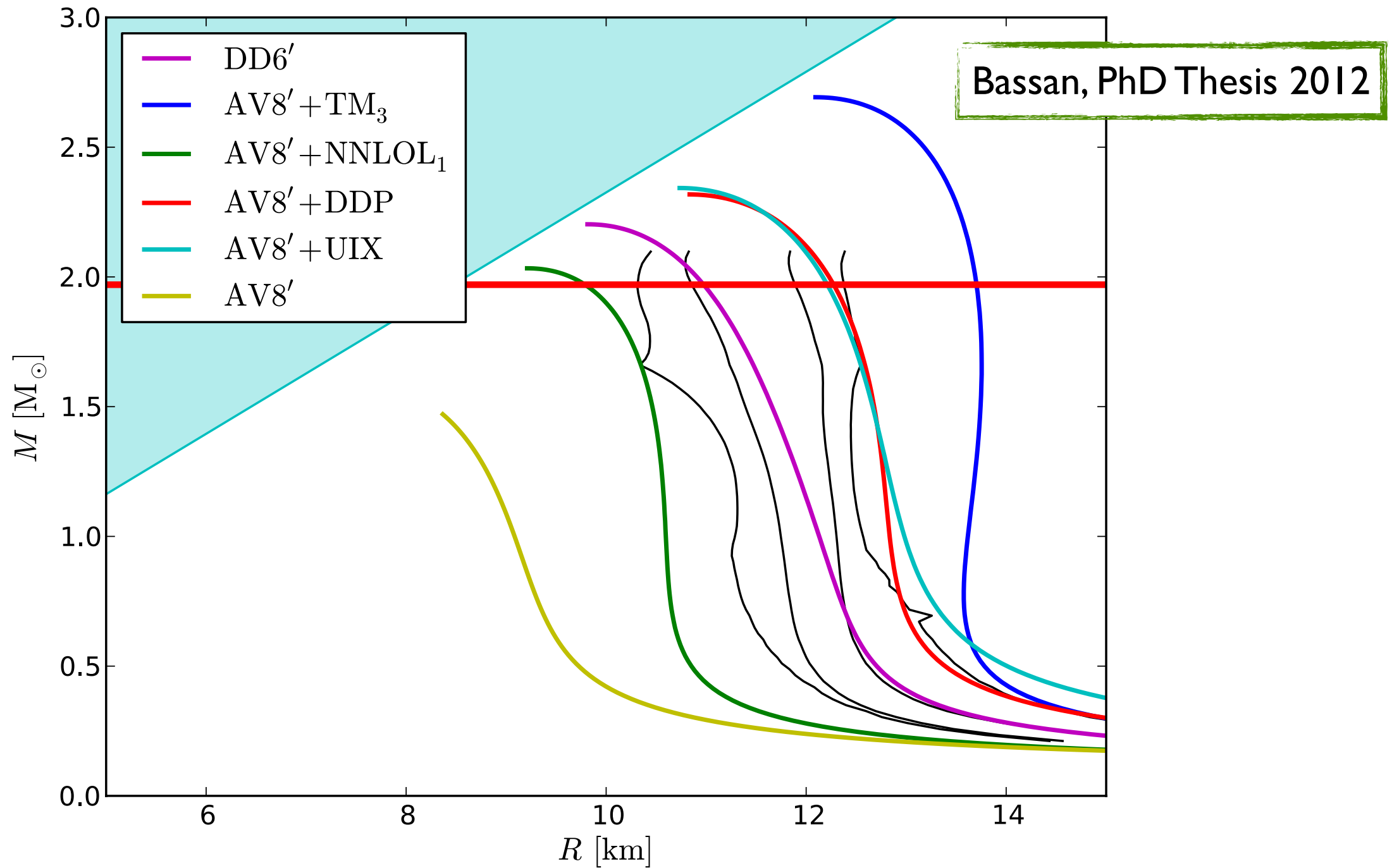
None of the potentials simultaneously explains the binding energy and the saturation density of SNM.



	NNLOL ₁	NNLOL ₂	NNLOL ₃	NNLOL ₄
ρ_0 (fm ⁻³)	0.21	0.20	0.19	0.17
E_0 (MeV)	-15.2	-14.6	-14.6	-12.9
K (MeV)	198	252	220	310

Exp.	
ρ_0 (fm ⁻³)	0.16
E_0 (MeV)	-16.0
K (MeV)	240

Test on neutron stars



Weak response of cold SNM at three-body cluster level

MICROSCOPIC CALCULATION OF THE LONGITUDINAL RESPONSE OF NUCLEAR MATTER

A. FABROCINI

Dept. of Physics and INFN, Sezione di Pisa, University of Pisa, Piazza Torricelli 2, 56100 Pisa, Italy

S. FANTONI

Dept. of Physics and INFN, Sezione di Lecce, University of Lecce, Via Arnesano 73100 Lecce, Italy

Astrophysics

The understanding of the interactions of low-energy neutrinos with nuclear matter is required for the description of a number of properties of compact stars.

Supernovae

Neutrino propagation in nuclear matter, described in terms of the neutrino mean free path, plays a crucial role in the mechanism leading to supernovae explosion.

Neutron stars

Neutrino emission is the main process driving the early stages of neutron stars' cooling.

- The mechanisms for neutrino production, (URCA, Bremsstrahlung ...) depend on the nuclear EoS, which is dictated by strong interactions.
- Neutrino-nucleus scattering is sizably affected by the strong interaction.

A consistent treatment of both processes is advisable

Weak response in non relativistic limit

In the non relativistic limit, nuclear response to weak probes delivering energy ω and momentum \mathbf{q}

$$\begin{aligned} S(\mathbf{q}, \omega) &= \int \frac{dt}{2\pi} \langle \Psi_0 | \hat{O}_{\mathbf{q}}^\dagger(t) \hat{O}_{\mathbf{q}}(0) | \Psi_0 \rangle e^{-i\omega t} \\ &= \frac{1}{A} \sum_f |\langle \Psi_n | \hat{O}_{\mathbf{q}} | \Psi_0 \rangle|^2 \delta(\omega + E_0 - E_n) \end{aligned}$$

Weak response in non relativistic limit

In the non relativistic limit, nuclear response to weak probes delivering energy ω and momentum \mathbf{q}

$$\begin{aligned} S(\mathbf{q}, \omega) &= \int \frac{dt}{2\pi} \langle \Psi_0 | \hat{O}_{\mathbf{q}}^\dagger(t) \hat{O}_{\mathbf{q}}(0) | \Psi_0 \rangle e^{-i\omega t} \\ &= \frac{1}{A} \sum_f |\langle \Psi_n | \hat{O}_{\mathbf{q}} | \Psi_0 \rangle|^2 \delta(\omega + E_0 - E_n) \end{aligned}$$

→ Eigenstates of the Hamiltonian $\hat{H}|\Psi_n\rangle = E_n|\Psi_n\rangle$

Weak response in non relativistic limit

In the non relativistic limit, nuclear response to weak probes delivering energy ω and momentum \mathbf{q}

$$\begin{aligned} S(\mathbf{q}, \omega) &= \int \frac{dt}{2\pi} \langle \Psi_0 | \hat{O}_{\mathbf{q}}^\dagger(t) \hat{O}_{\mathbf{q}}(0) | \Psi_0 \rangle e^{-i\omega t} \\ &= \frac{1}{A} \sum_f |\langle \Psi_n | \hat{O}_{\mathbf{q}} | \Psi_0 \rangle|^2 \delta(\omega + E_0 - E_n) \end{aligned}$$

→ Eigenstates of the Hamiltonian $\hat{H}|\Psi_n\rangle = E_n|\Psi_n\rangle$

→ Energy-conserving delta function

Weak response in non relativistic limit

In the non relativistic limit, nuclear response to weak probes delivering energy ω and momentum \mathbf{q}

$$\begin{aligned} S(\mathbf{q}, \omega) &= \int \frac{dt}{2\pi} \langle \Psi_0 | \hat{O}_{\mathbf{q}}^\dagger(t) \hat{O}_{\mathbf{q}}(0) | \Psi_0 \rangle e^{-i\omega t} \\ &= \frac{1}{A} \sum_f |\langle \Psi_n | \hat{O}_{\mathbf{q}} | \Psi_0 \rangle|^2 \delta(\omega + E_0 - E_n) \end{aligned}$$

→ Eigenstates of the Hamiltonian $\hat{H}|\Psi_n\rangle = E_n|\Psi_n\rangle$

→ Energy-conserving delta function

→ Non relativistic Fermi and Gamow-Teller operators describing low-energy weak interactions

$$\begin{aligned} \hat{O}_{\mathbf{q}}^F &= \sum_i \hat{O}_{\mathbf{q}}^F(i) = g_V \sum_i e^{i\mathbf{q}\cdot\mathbf{r}_i} \tau_i^+, \\ \hat{O}_{\mathbf{q}}^{GT} &= \sum_i \hat{O}_{\mathbf{q}}^{GT}(i) = g_A \sum_i e^{i\mathbf{q}\cdot\mathbf{r}_i} \vec{\sigma}_i \tau_i^+, \end{aligned}$$

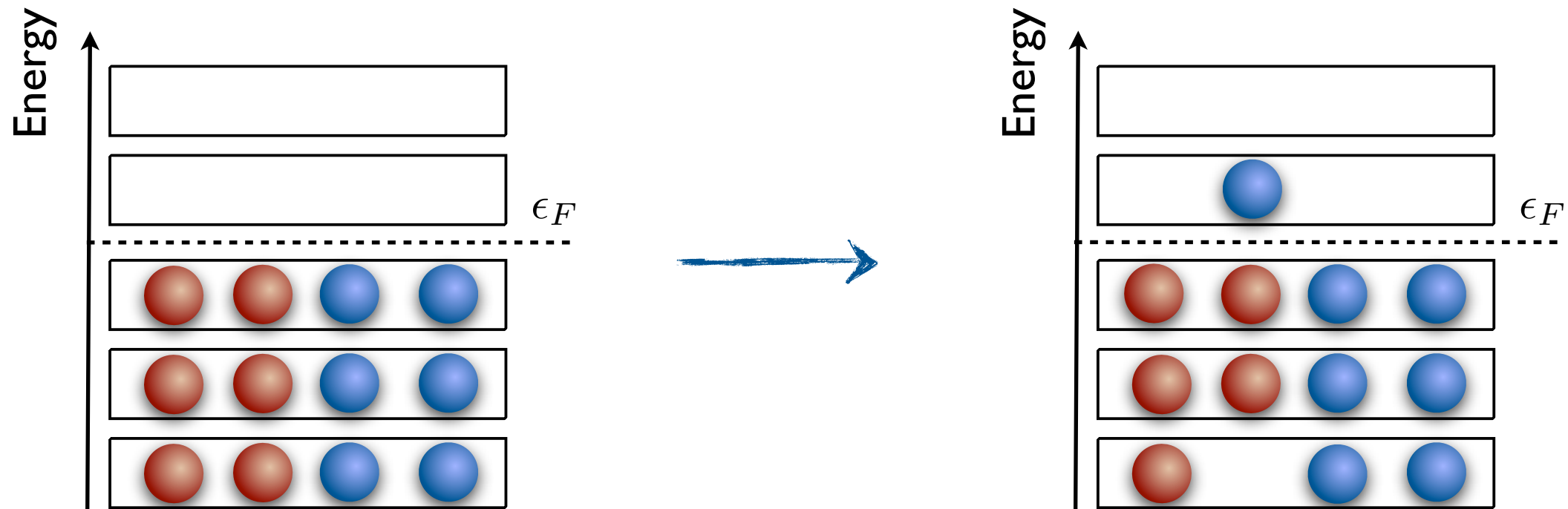
Weak response in CBF

- Within CBF formalism

$$\langle \Psi_n | \hat{O}_{\mathbf{q}} | \Psi_0 \rangle \rightarrow \frac{\langle \Phi_n | \mathcal{F}^\dagger \hat{O}_{\mathbf{q}} \mathcal{F} | \Phi_0 \rangle}{\sqrt{\langle \Phi_0 | \mathcal{F}^\dagger \mathcal{F} | \Phi_0 \rangle \langle \Phi_n | \mathcal{F}^\dagger \mathcal{F} | \Phi_n \rangle}}$$

- We only consider transitions between the correlated ground-state and correlated 1particle-1hole excited states

$$\frac{\langle \Phi_{p_m;h_i} | \mathcal{F}^\dagger \hat{O}_{\mathbf{q}} \mathcal{F} | \Phi_0 \rangle}{\sqrt{\langle \Phi_0 | \mathcal{F}^\dagger \mathcal{F} | \Phi_0 \rangle \langle \Phi_{p_m;h_i} | \mathcal{F}^\dagger \mathcal{F} | \Phi_{p_m;h_i} \rangle}}$$



Effective interaction and weak operators

Instead of working in the full CBF basis, we use the FG basis, defining:

- The effective interaction, defined through the matrix elements of the hamiltonian in the correlated ground state

$$\langle \Psi_0 | \hat{H} | \Psi_0 \rangle \equiv T_F + \langle \Phi_0 | \sum_{j>i} \hat{v}_{ij}^{eff} | \Phi_0 \rangle$$

- The effective weak operators

$$\langle \Phi_{p_m; h_i} | \hat{O}_{\mathbf{q}}^{eff} | \Phi_0 \rangle \equiv \frac{\langle \Phi_{p_m; h_i} | \mathcal{F}^\dagger \hat{O}_{\mathbf{q}} \mathcal{F} | \Phi_0 \rangle}{\sqrt{\langle \Phi_0 | \mathcal{F}^\dagger \mathcal{F} | \Phi_0 \rangle \langle \Phi_{p_m; h_i} | \mathcal{F}^\dagger \mathcal{F} | \Phi_{p_m; h_i} \rangle}}$$

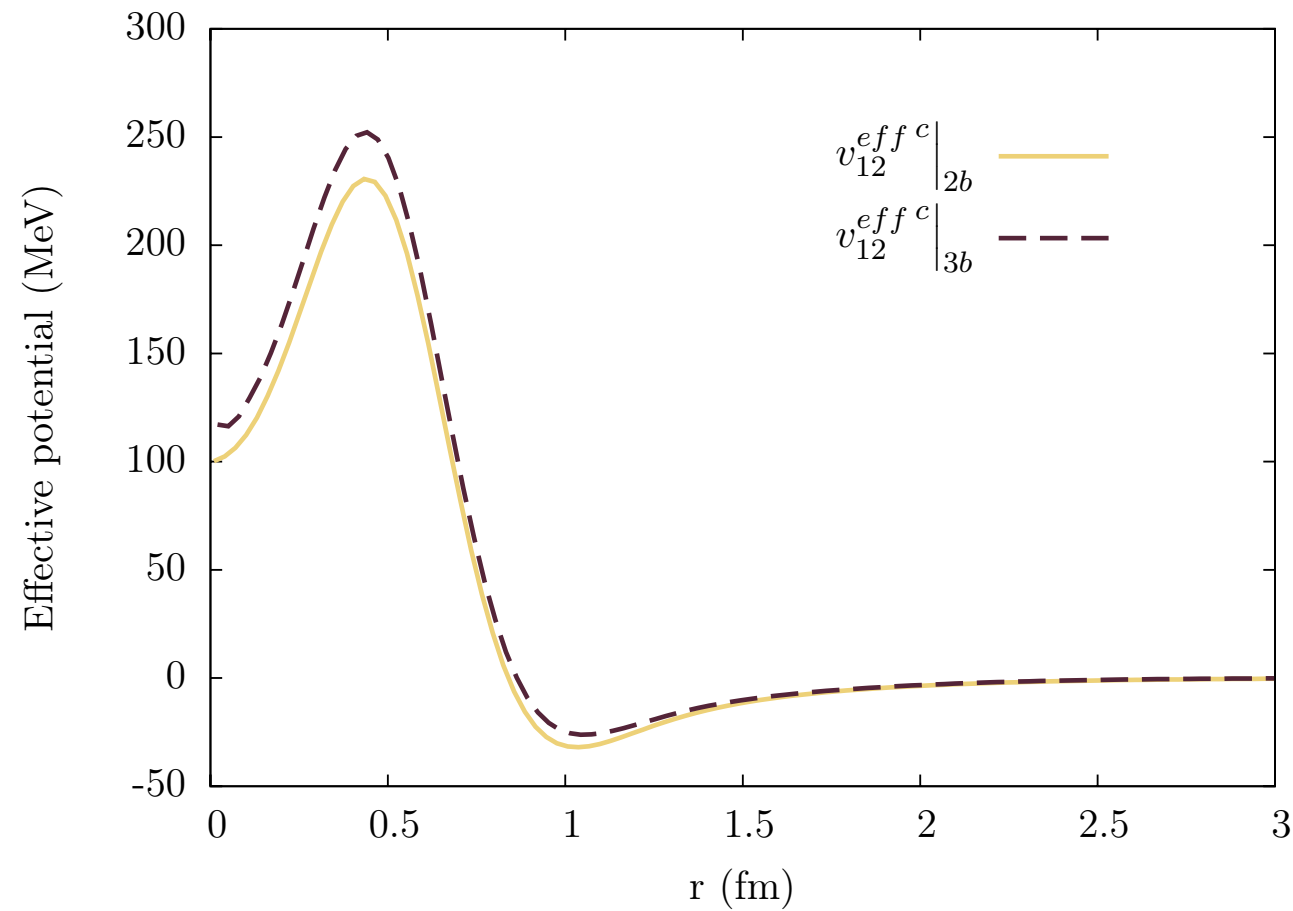
Both effective interaction and effective weak operators incorporates the effects of the short-range correlations.

Cluster expansion of the
CBF matrix elements



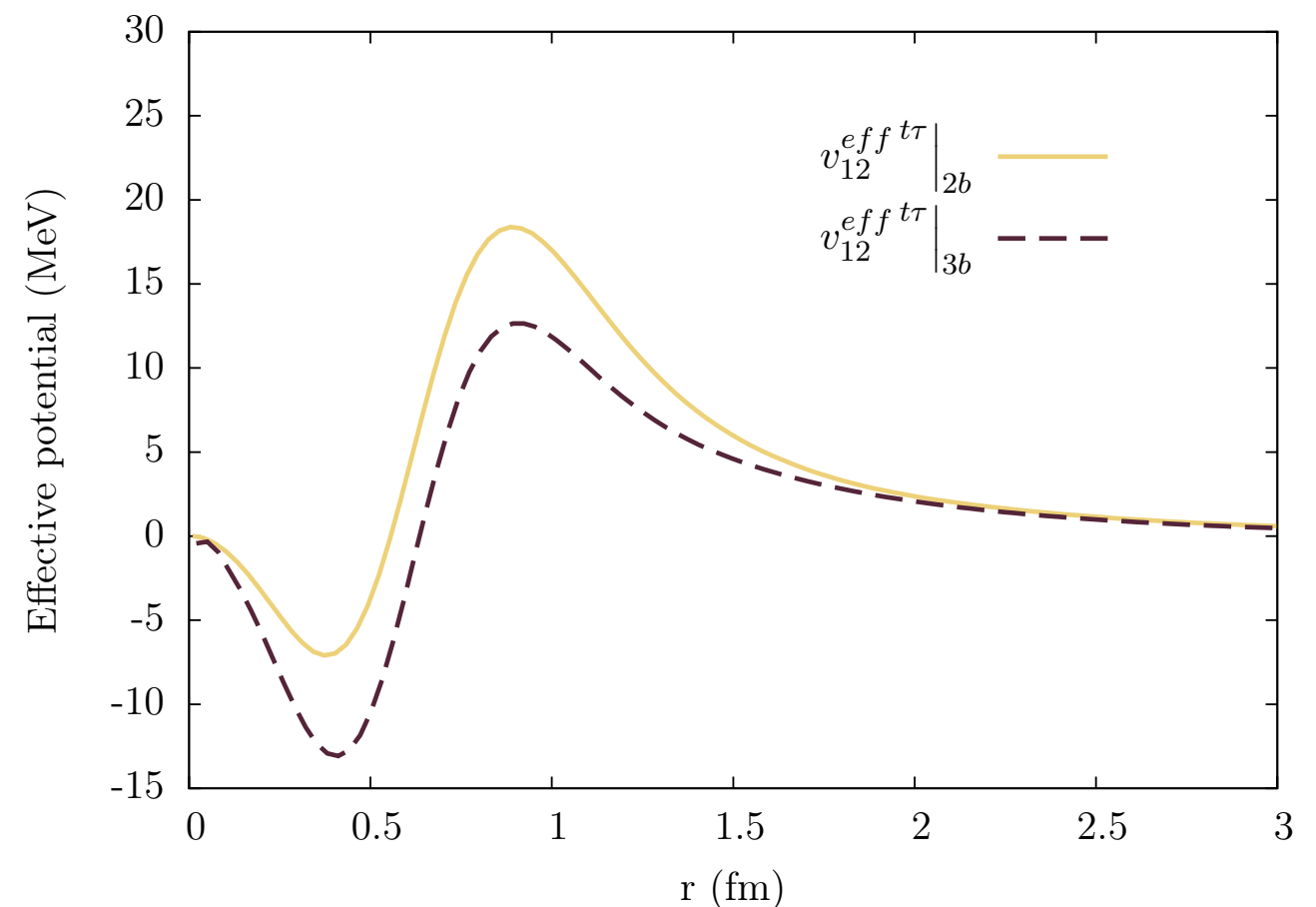
Cluster expansion of the effective
interaction and weak operators

Effective interaction at three-body cluster level



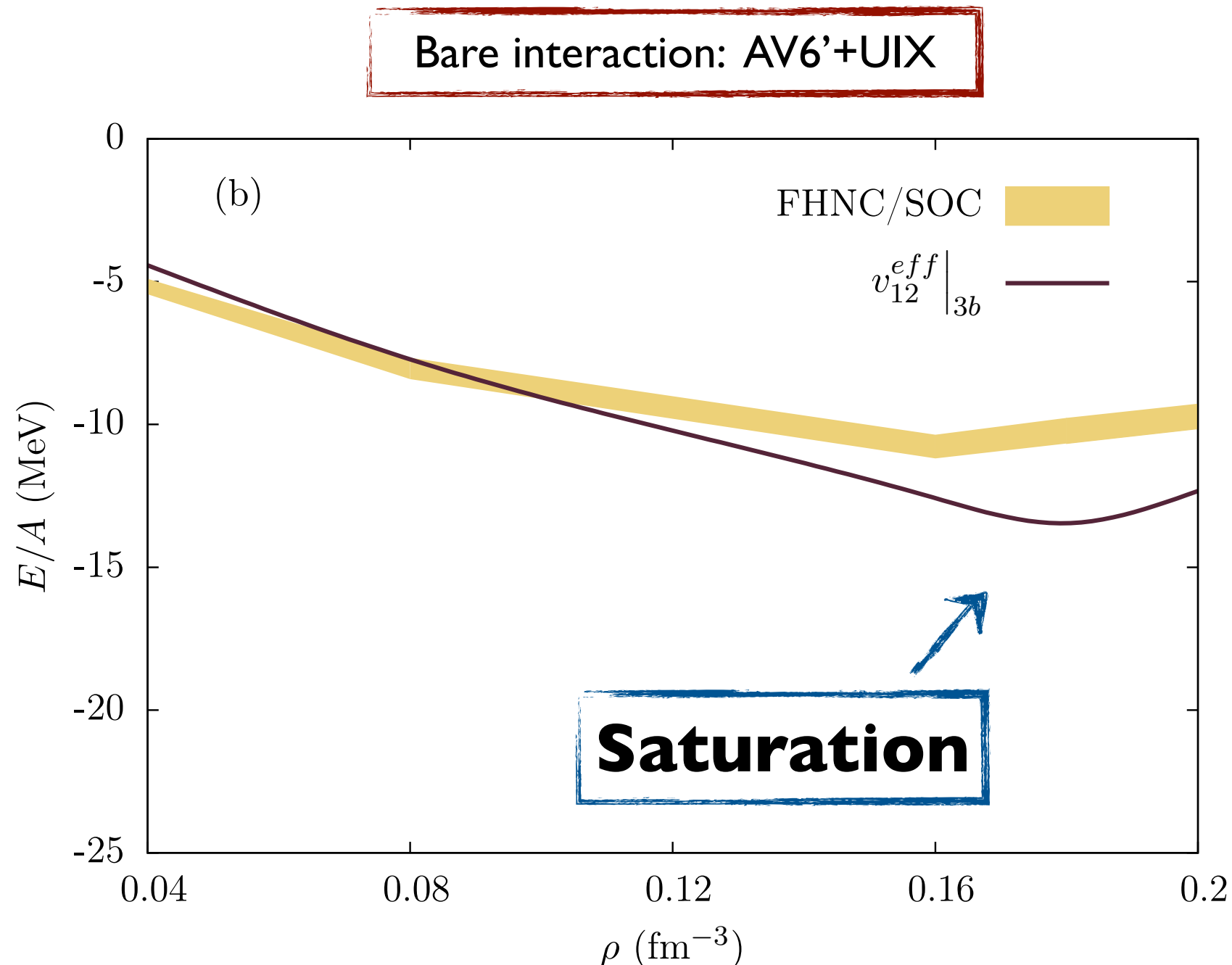
Scalar channel of the effective interaction at two- and three-body cluster level

Tensor tau channel of the effective interaction at two- and three-body cluster level



Effective interaction at three-body cluster level

Including the three body cluster in the effective potential makes the equation of state of SNM much closer to the one obtained with the full FHNC/SOC cluster summation.



Last step: the parameters of the correlations entering \hat{v}_{12}^{eff} are adjusted for the effective interaction to reproduce FHNC/SOC result.

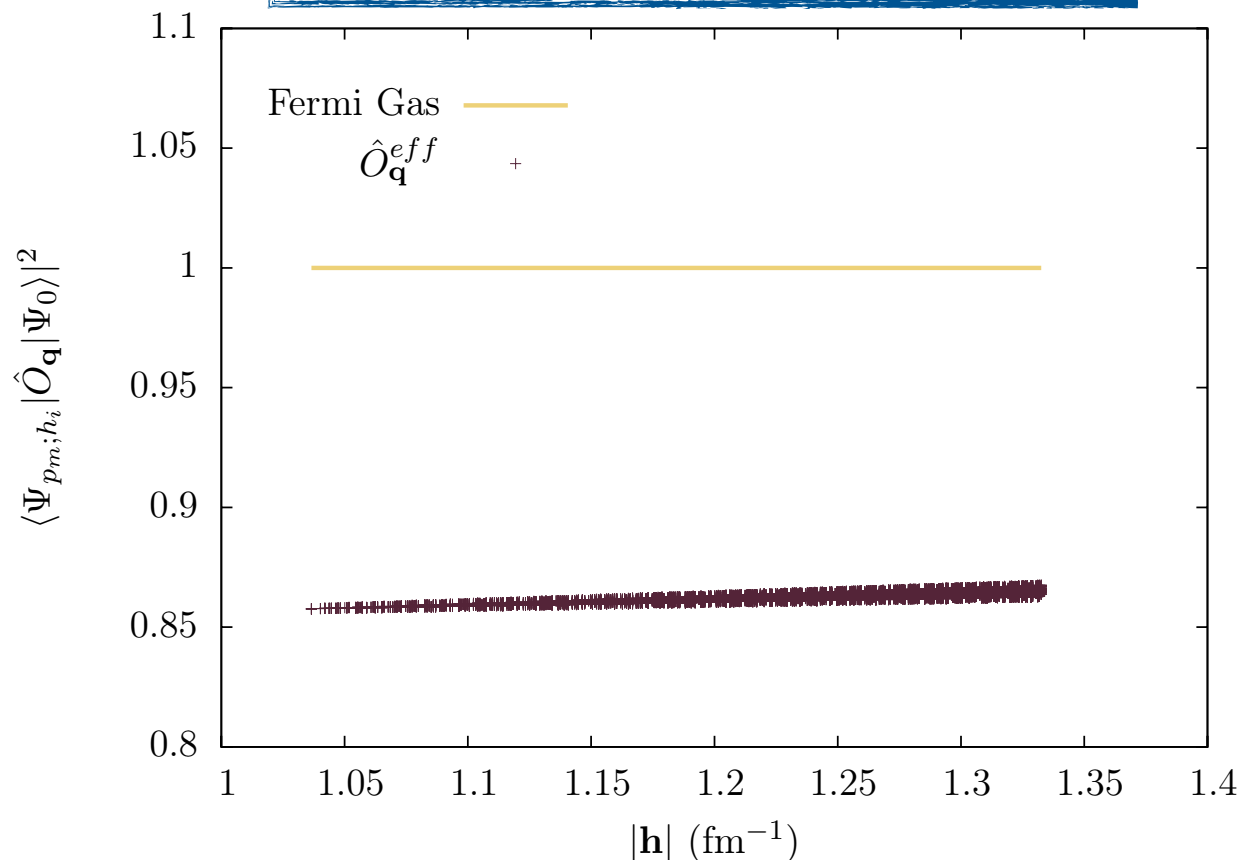
Perturbation theory in Fermi gas basis

Using the effective operators, the response is given by

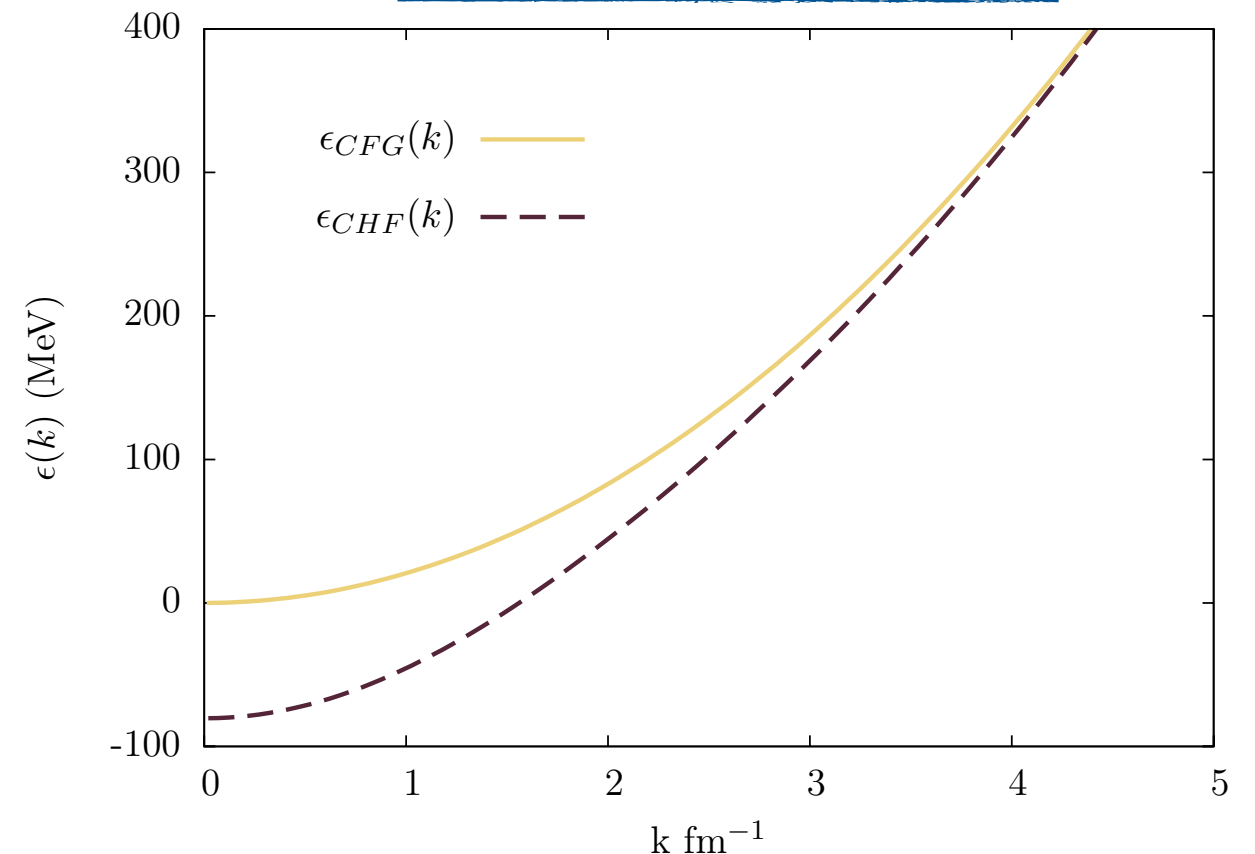
$$S(\mathbf{q}, \omega) = \frac{1}{A} \sum_{p_m h_i} |\langle \Phi_{p_m; h_i} | \hat{O}_{\mathbf{q}}^{eff} | \Phi_0 \rangle|^2 \delta(\omega + \epsilon_{p_m} - \epsilon_{h_i}).$$

- Correlated Fermi Gas (CFG) $\epsilon_{n_i} = \frac{\mathbf{k}_i^2}{2m}.$
- Correlated Hartree Fock (CHF) $\epsilon_{n_i} = \frac{\mathbf{k}_i^2}{2m} + \sum_{n_j=1}^A \int dx_j \phi_{n_i}^*(x_i) \phi_{n_j}^*(x_j) v_{ij}^{eff} \mathcal{A}[\phi_{n_i}(x_i) \phi_{n_j}(x_j)]$

Quenching of weak operators

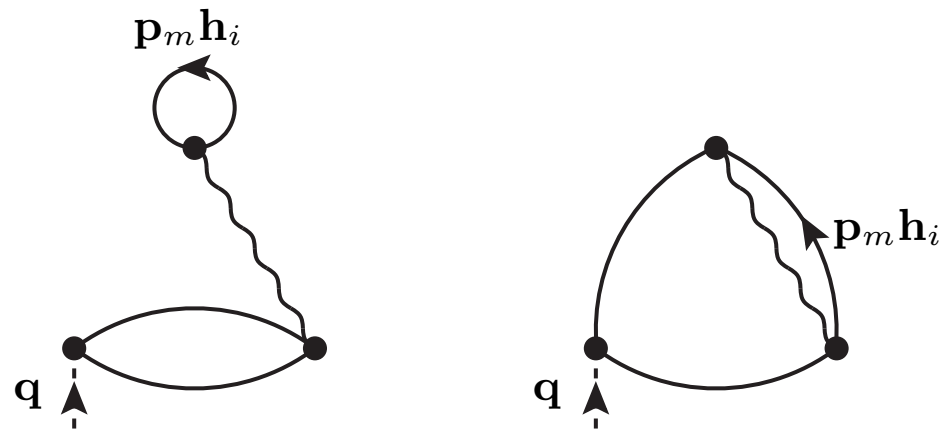


Single particle energies



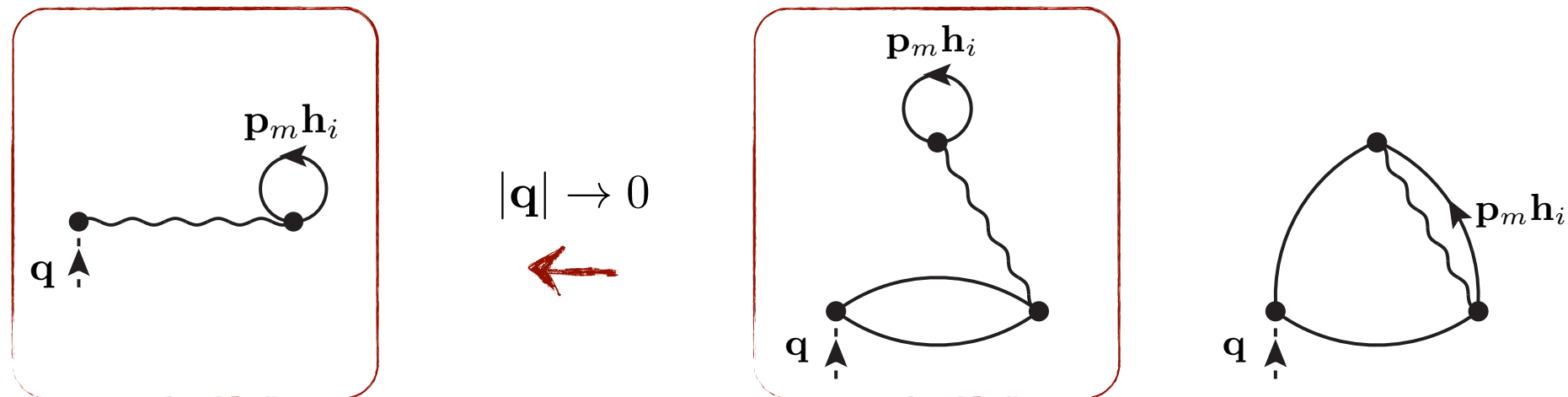
Effective operator at three-body cluster level

For the sake of consistency, the 3b cluster contribution to the effective weak operators have been included in the calculations.



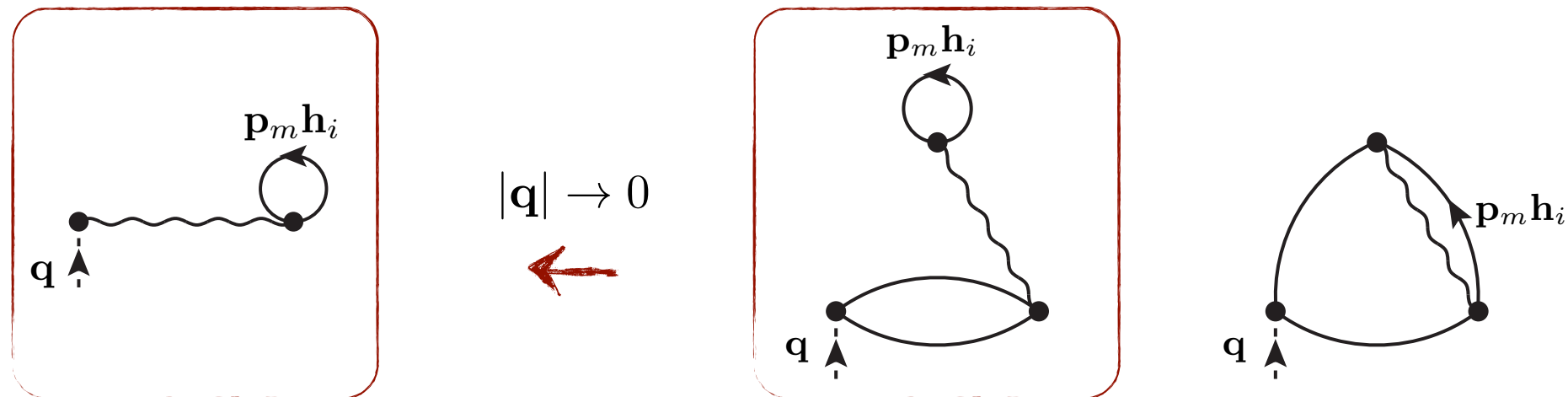
Effective operator at three-body cluster level

For the sake of consistency, the 3b cluster contribution to the effective weak operators have been included in the calculations.

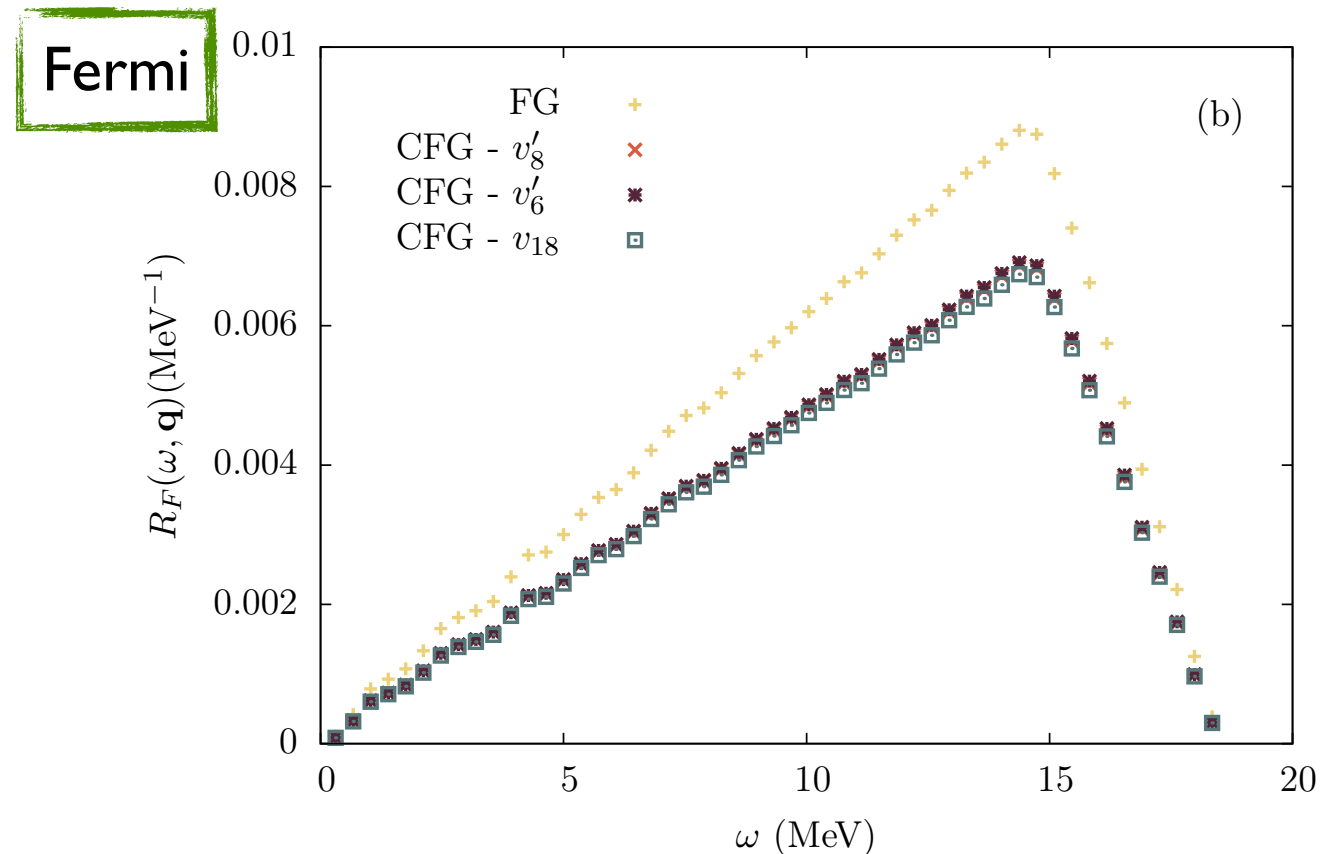
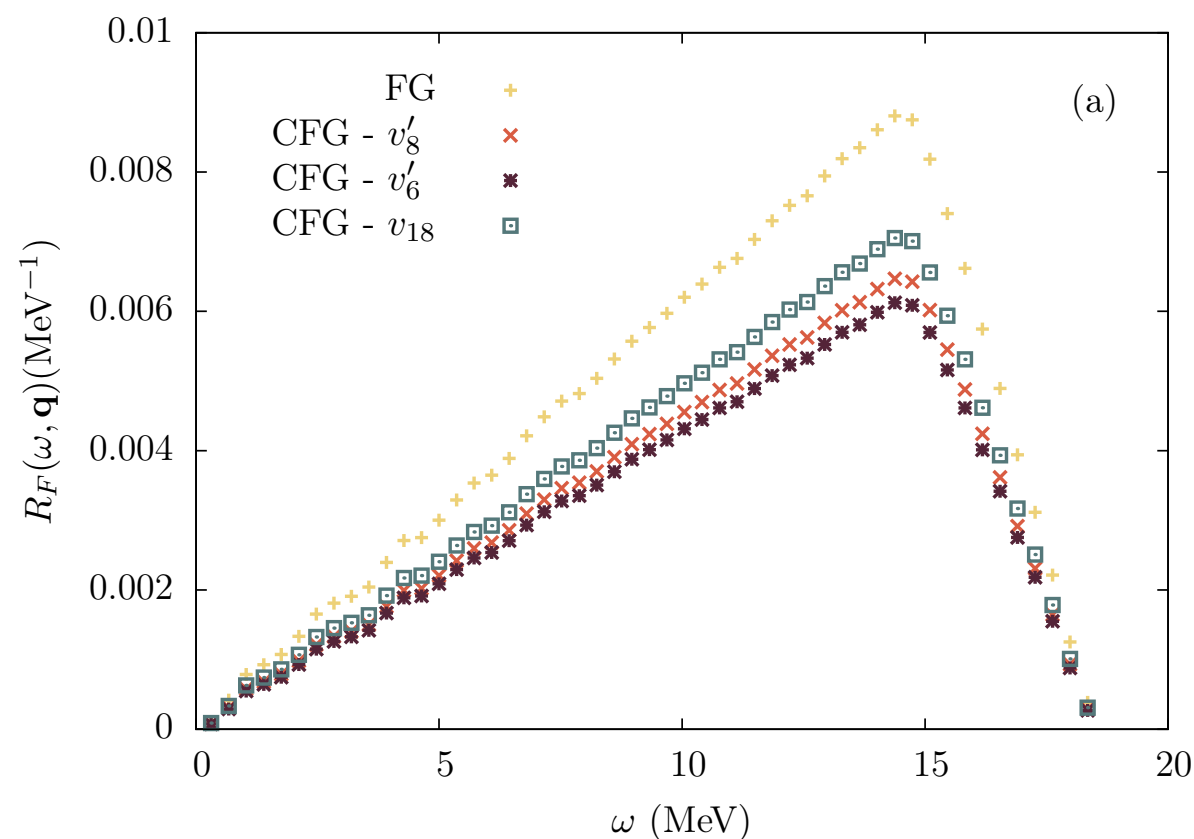


Effective operator at three-body cluster level

For the sake of consistency, the 3b cluster contribution to the effective weak operators have been included in the calculations.

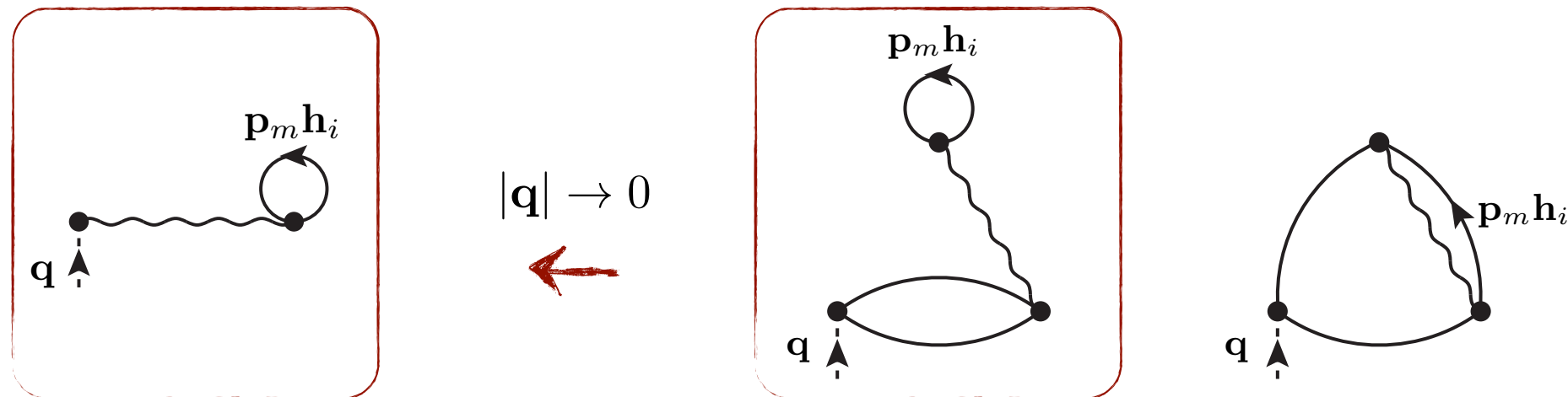


The unphysical strong dependence on the correlation function at small $|q|$ is removed.

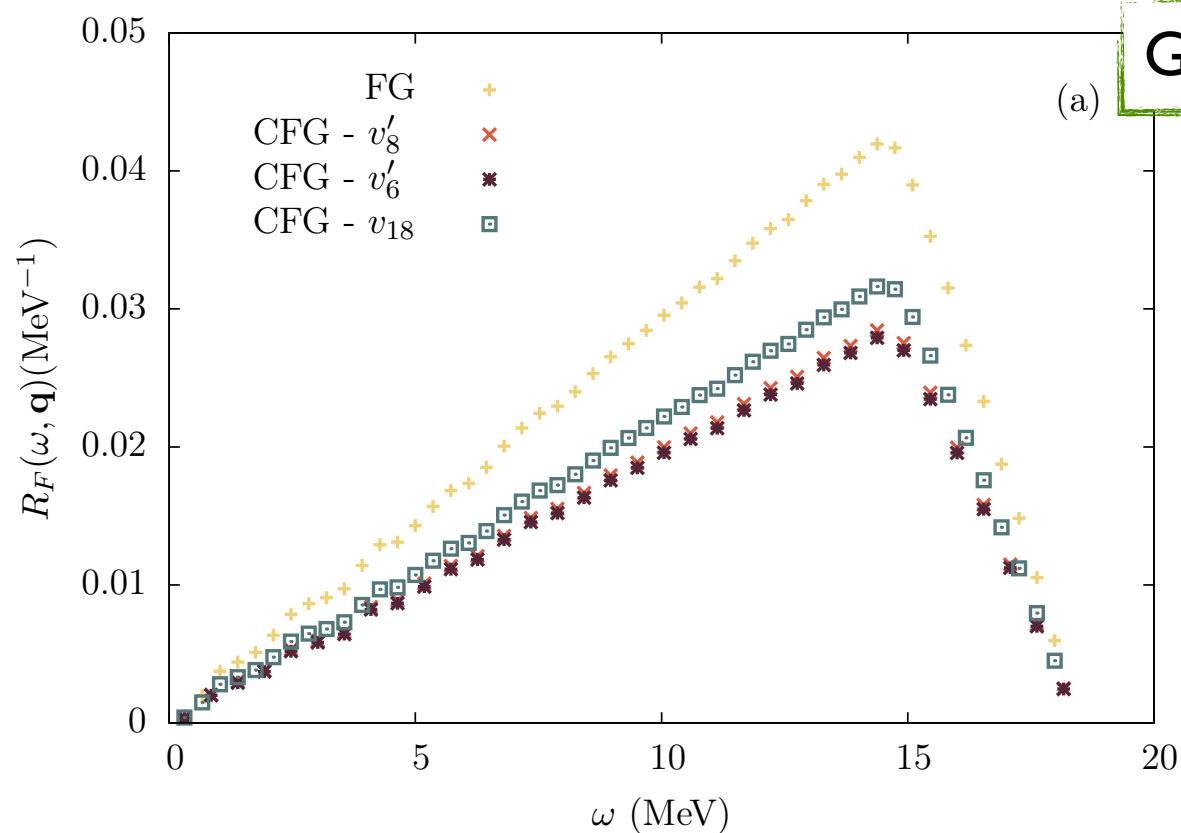


Effective operator at three-body cluster level

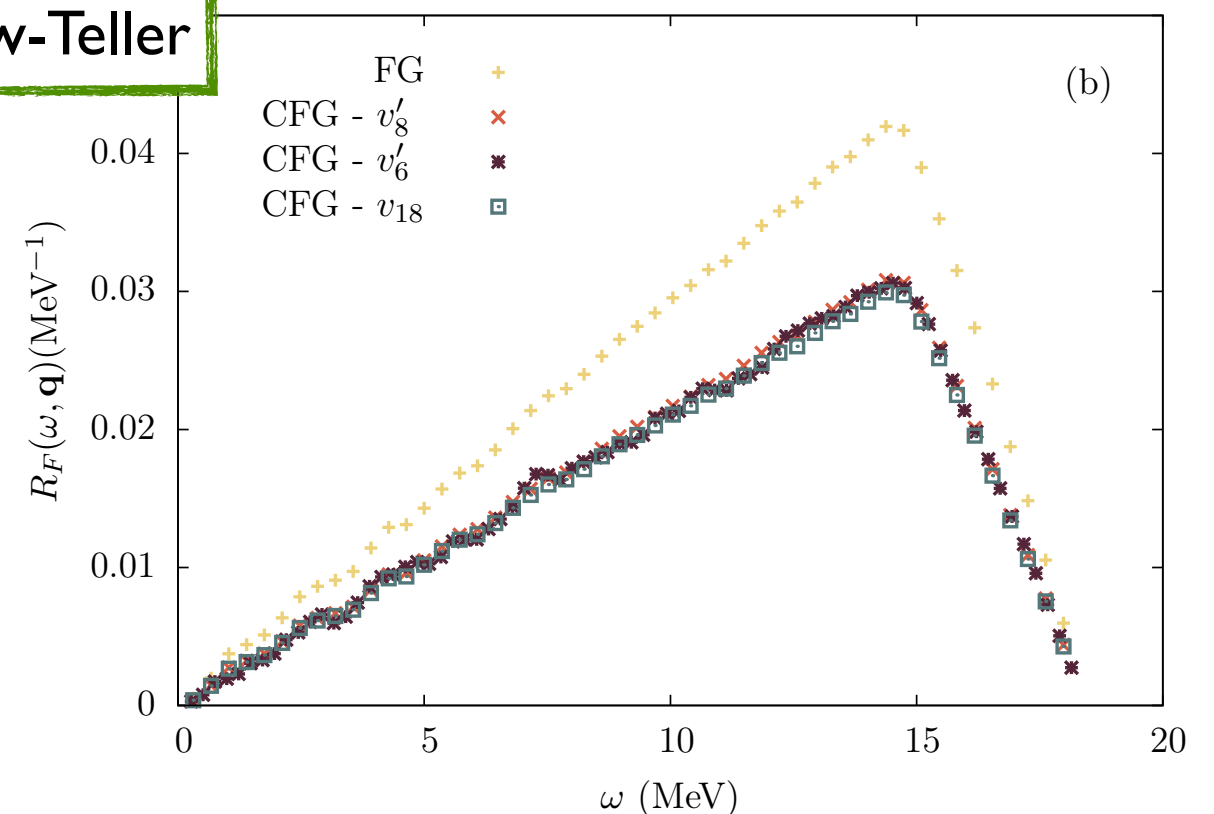
For the sake of consistency, the 3b cluster contribution to the effective weak operators have been included in the calculations.



The unphysical strong dependence on the correlation function at small $|\mathbf{q}|$ is removed.



Gamow-Teller



Long range correlations: Tamm-Dancoff

The effective operators at 3b cluster level can only take into account short-range correlations.

Long-range correlations are included by expanding the final state in the basis of one |p|h states: Tamm-Dancoff approximation

$$|\Phi_n\rangle_S^{CTD} = \sum_{\mathbf{p}_m \mathbf{h}_i S_z} C_{\mathbf{p}_m \mathbf{h}_i}^{n SS_z} |\Phi_{\mathbf{p}_m; \mathbf{h}_i}\rangle_{SS_z}$$

$$\begin{array}{l} \text{Final state} \\ T = 1, T_z = 1 \end{array}$$

The coefficient are found by diagonalizing the effective hamiltonian

$$\hat{H}^{eff} |\Phi_n\rangle_S^{CTD} = \left(\sum_i -\frac{\nabla_i^2}{2m} + \sum_{i < j} \hat{v}_{ij}^{eff} \right) |\Phi_n\rangle_S^{CTD} = (E_0 + \omega_n^S) |\Phi_n\rangle_S^{CTD}$$

The response is given by

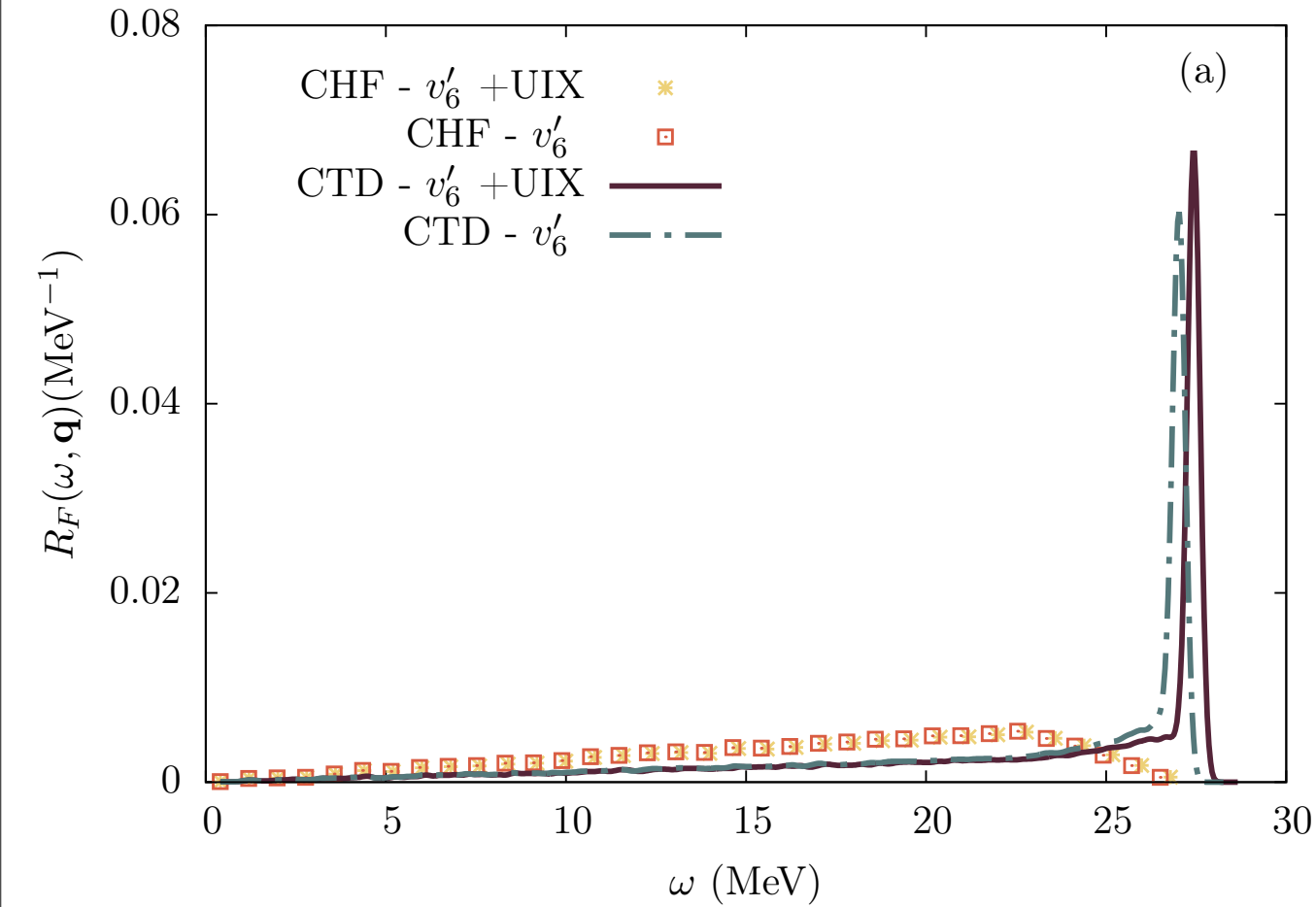
$$S(\mathbf{q}, \omega) = \frac{1}{A} \sum_n \left| \sum_{\mathbf{p}_m \mathbf{h}_i S_z} C_{\mathbf{p}_m \mathbf{h}_i}^{n SS_z} \langle \Phi_{\mathbf{p}_m; \mathbf{h}_i} | \hat{O}_{\mathbf{q}}^{eff} | \Phi_0 \rangle \right|^2 \delta(\omega - \omega_n^S)$$

Short range correlations  Effective operators

Long range correlations  Tamm-Dancoff

**Consistent
Treatment of long
and short range
correlations**

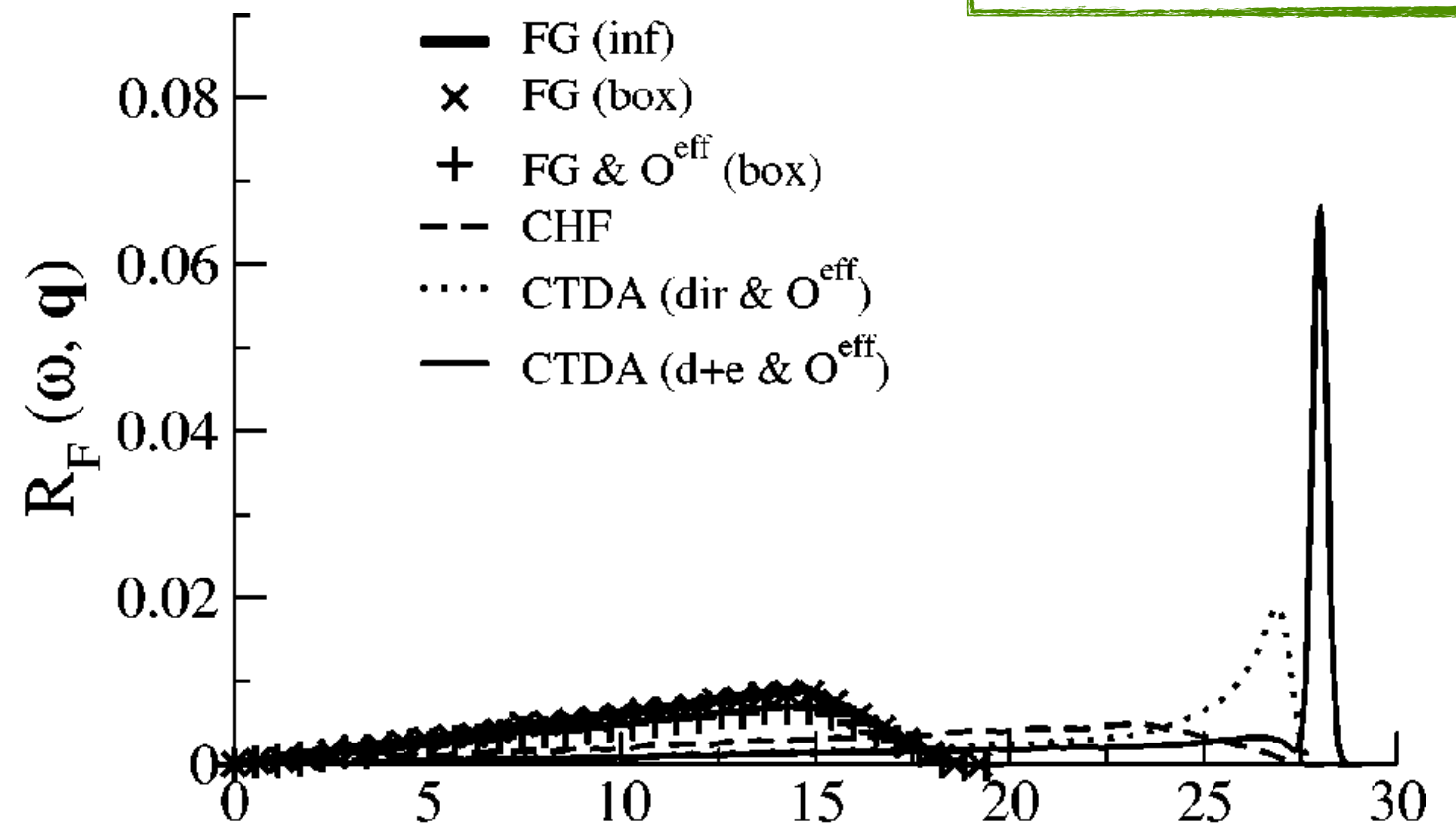
Fermi transition results



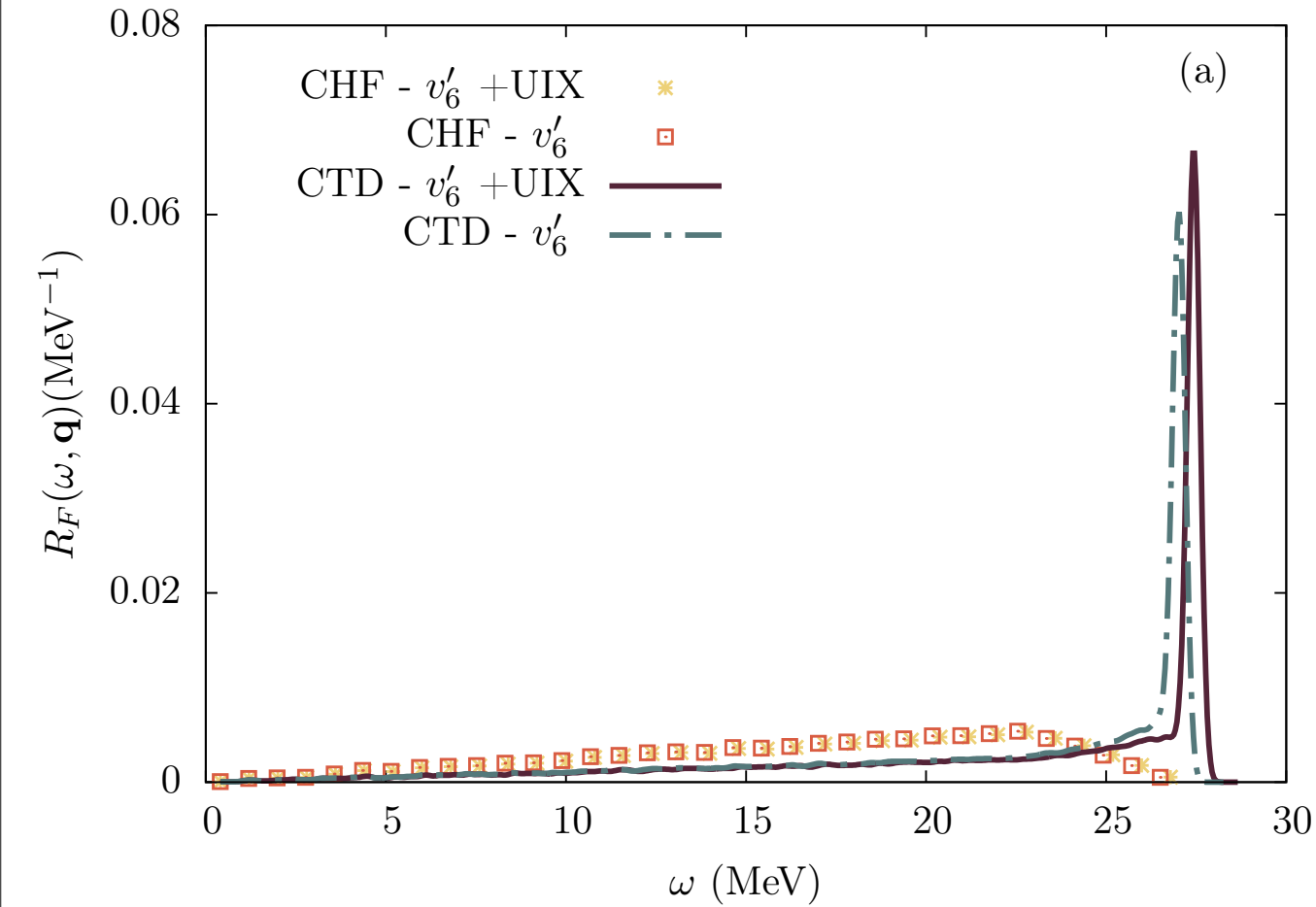
$q = 0.3 \text{ fm}^{-1}$

Cowell et al. (2004)

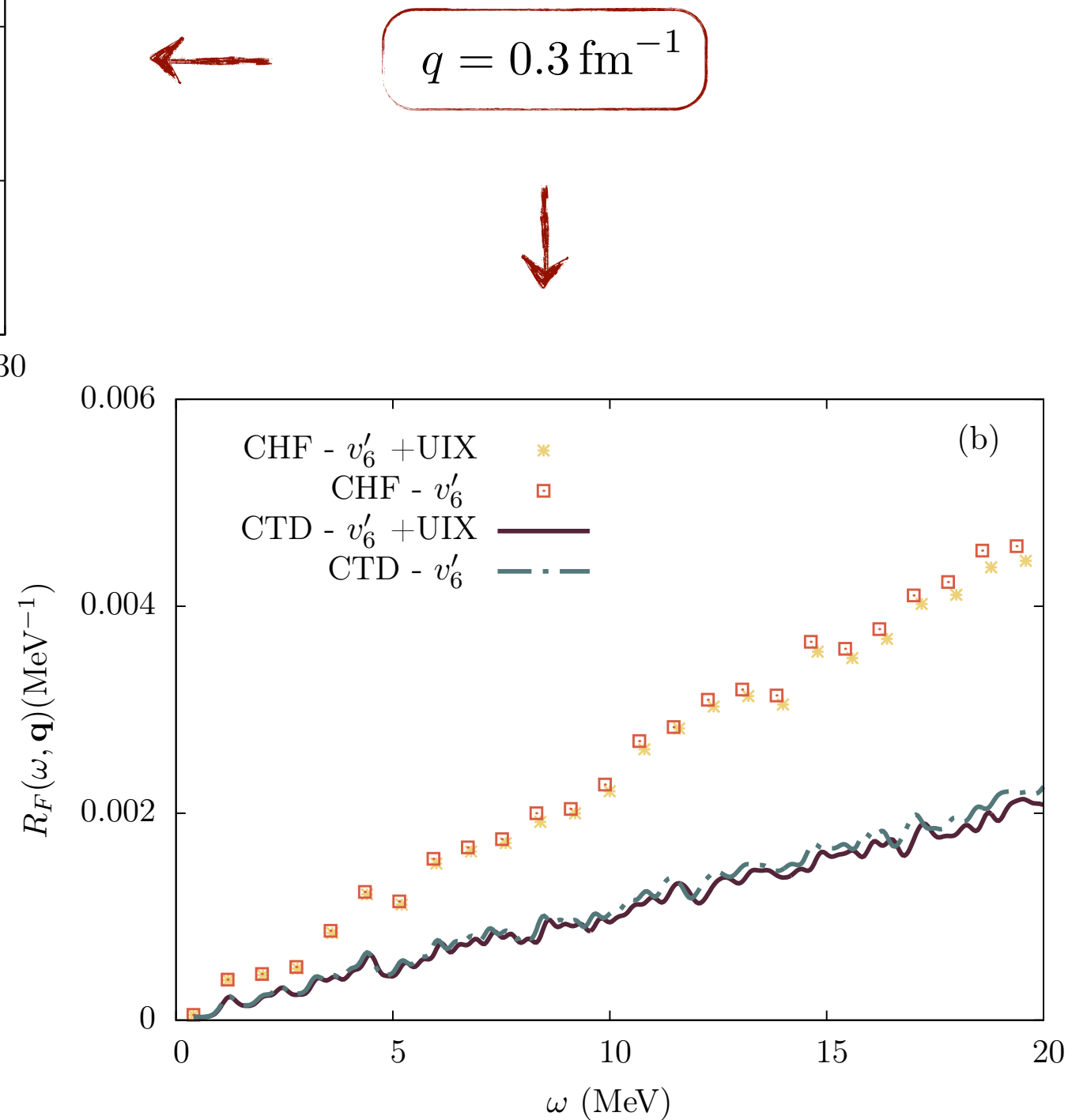
- Collective peak shifted to lower energies
- Small depletion of the peak



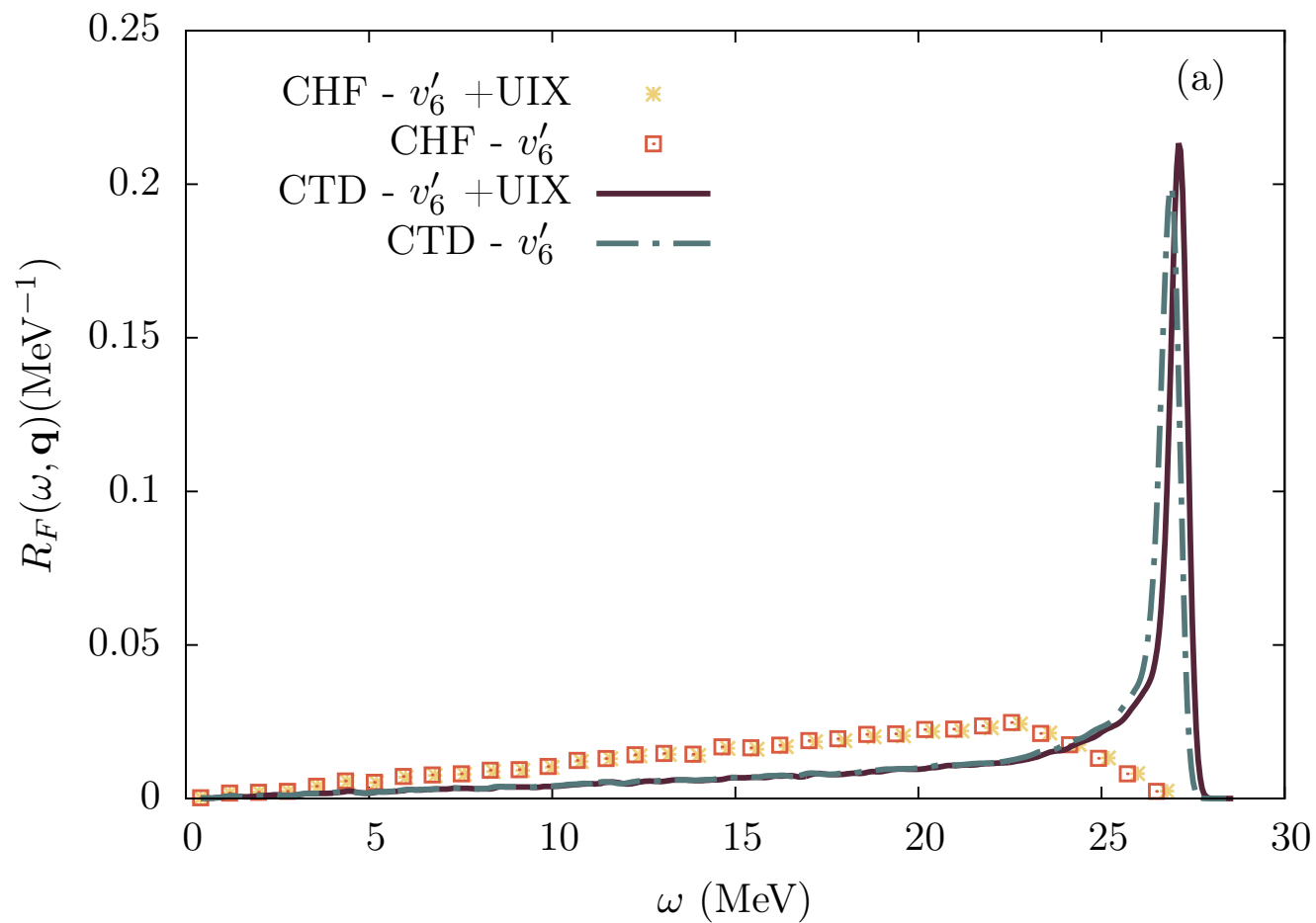
Fermi transition results



- Collective peak shifted to lower energies
- Small depletion of the peak

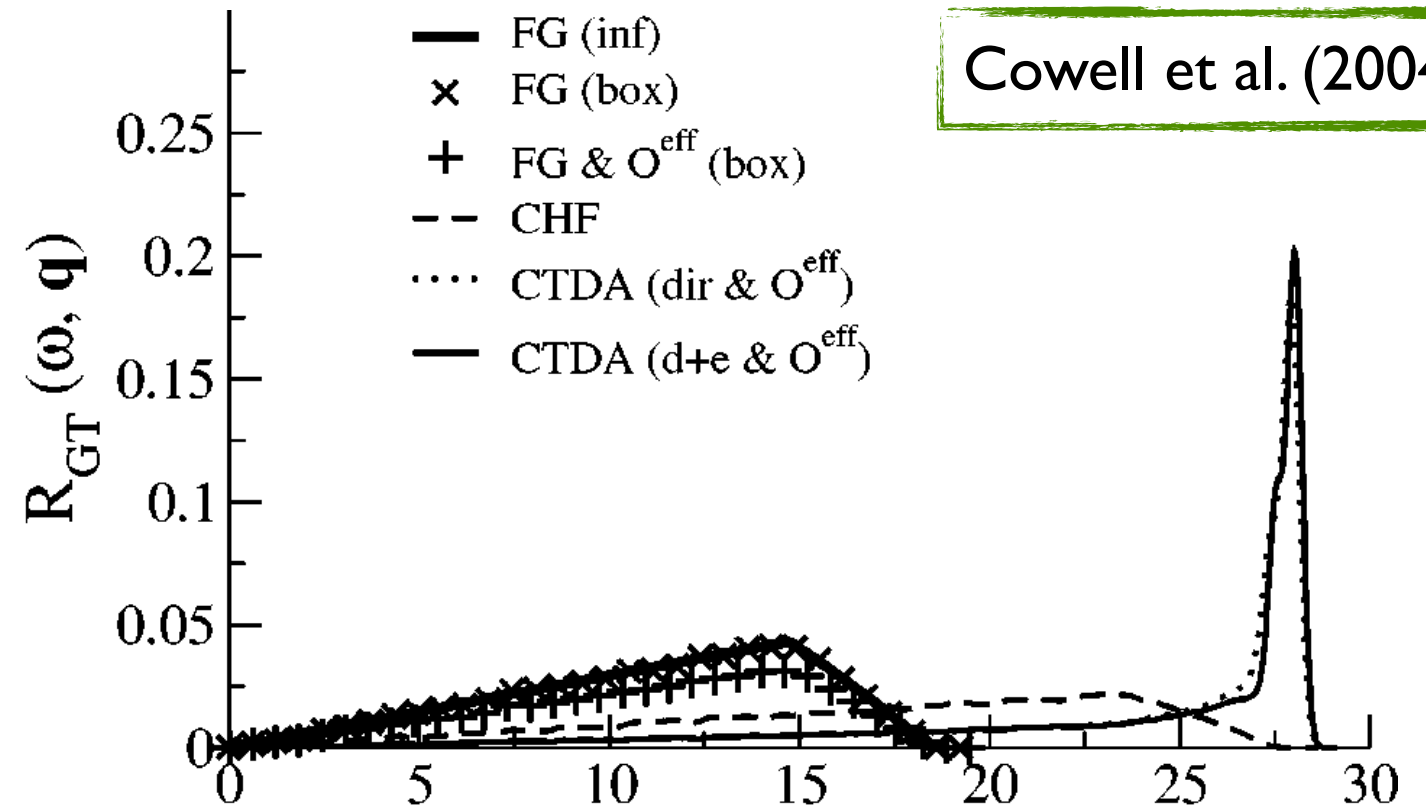


Gamow-Teller transition results

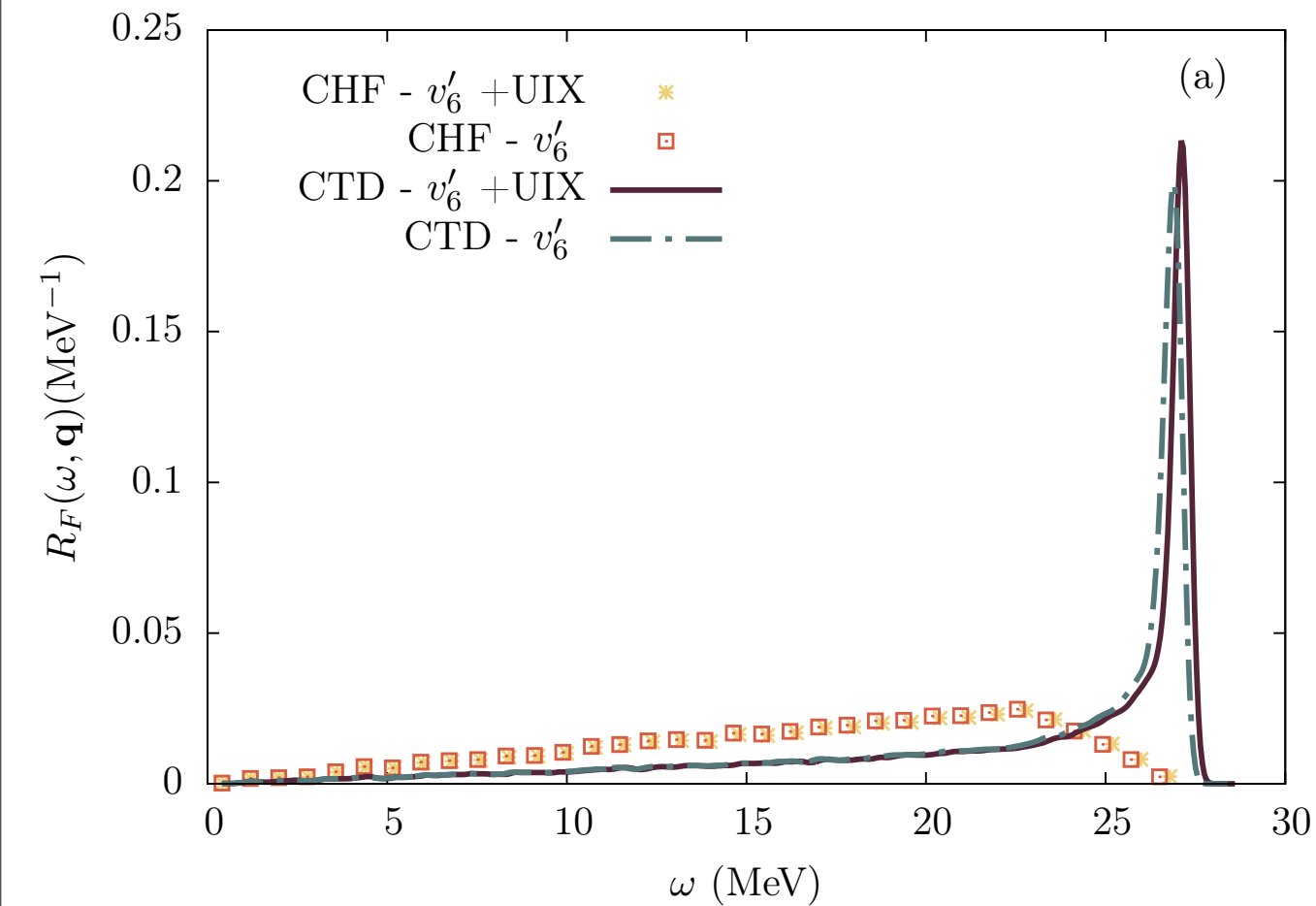


$q = 0.3 \text{ fm}^{-1}$

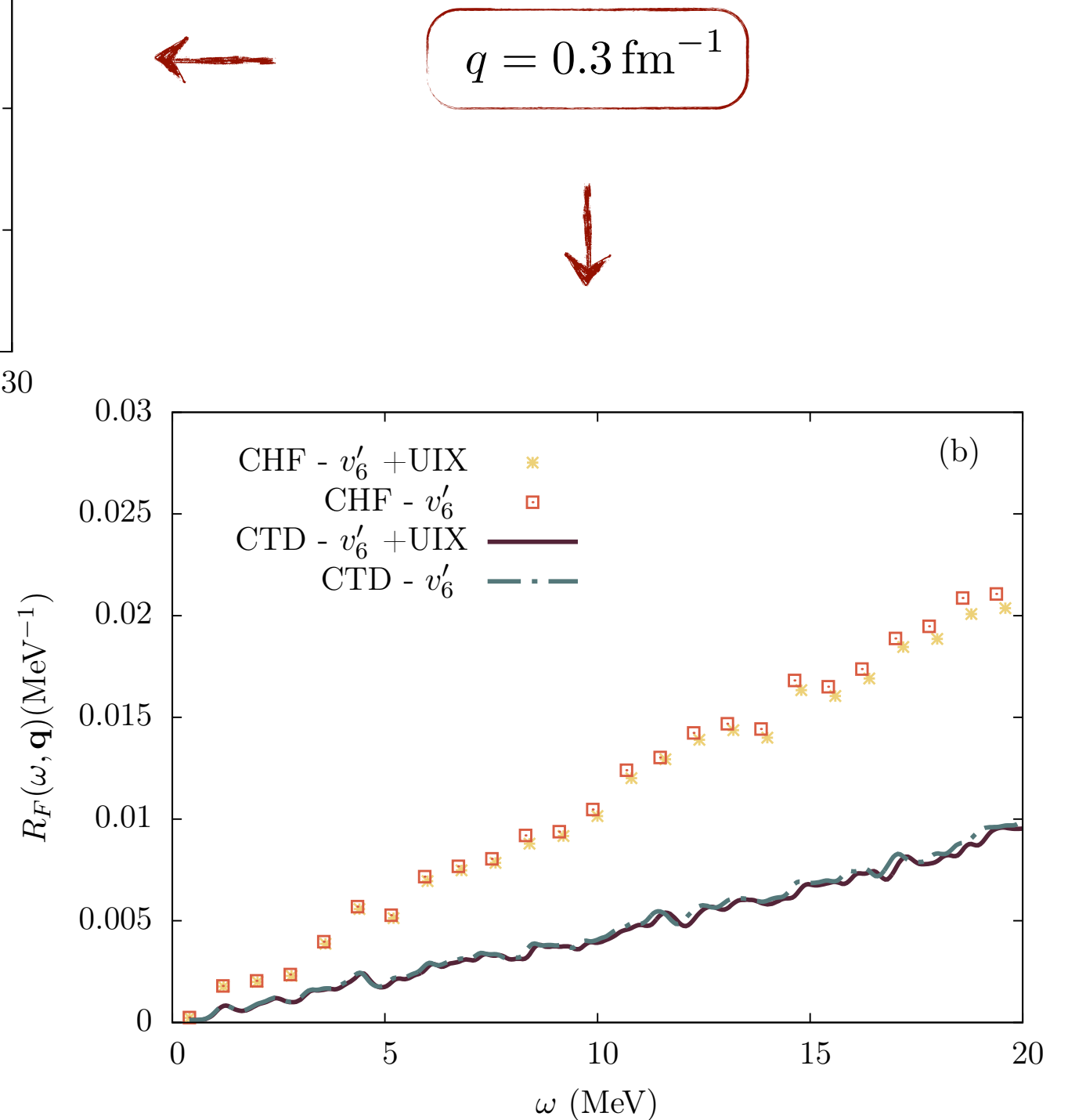
- (Almost) No shift of the collective excitation peak
- No depletion of the peak



Gamow-Teller transition results



- (Almost) No shift of the collective excitation peak
- No depletion of the peak



Sum-rules

The importance of the multiple particle hole excitations can be estimated from the sum rules, obtained by integrating the response

$$\begin{aligned} S(\mathbf{q}) &= \int d\omega S(\mathbf{q}, \omega) \\ &= \frac{1}{A} \int d\omega \sum_n |\langle \Psi_n | \hat{O}_{\mathbf{q}} | \Psi_0 \rangle|^2 \delta(\omega + E_0 - E_n) \\ &= \frac{1}{A} \langle \Psi_0 | \hat{O}_{\mathbf{q}}^\dagger \hat{O}_{\mathbf{q}} | \Psi_0 \rangle . \end{aligned}$$

Sum-rules

The importance of the multiple particle hole excitations can be estimated from the sum rules, obtained by integrating the response

$$\begin{aligned} S(\mathbf{q}) &= \int d\omega S(\mathbf{q}, \omega) \\ &= \frac{1}{A} \int d\omega \sum_n |\langle \Psi_n | \hat{O}_{\mathbf{q}} | \Psi_0 \rangle|^2 \delta(\omega + E_0 - E_n) \\ &= \frac{1}{A} \langle \Psi_0 | \hat{O}_{\mathbf{q}}^\dagger \hat{O}_{\mathbf{q}} | \Psi_0 \rangle. \end{aligned}$$

→ Direct integration of the response

→ Ground-state expectation value

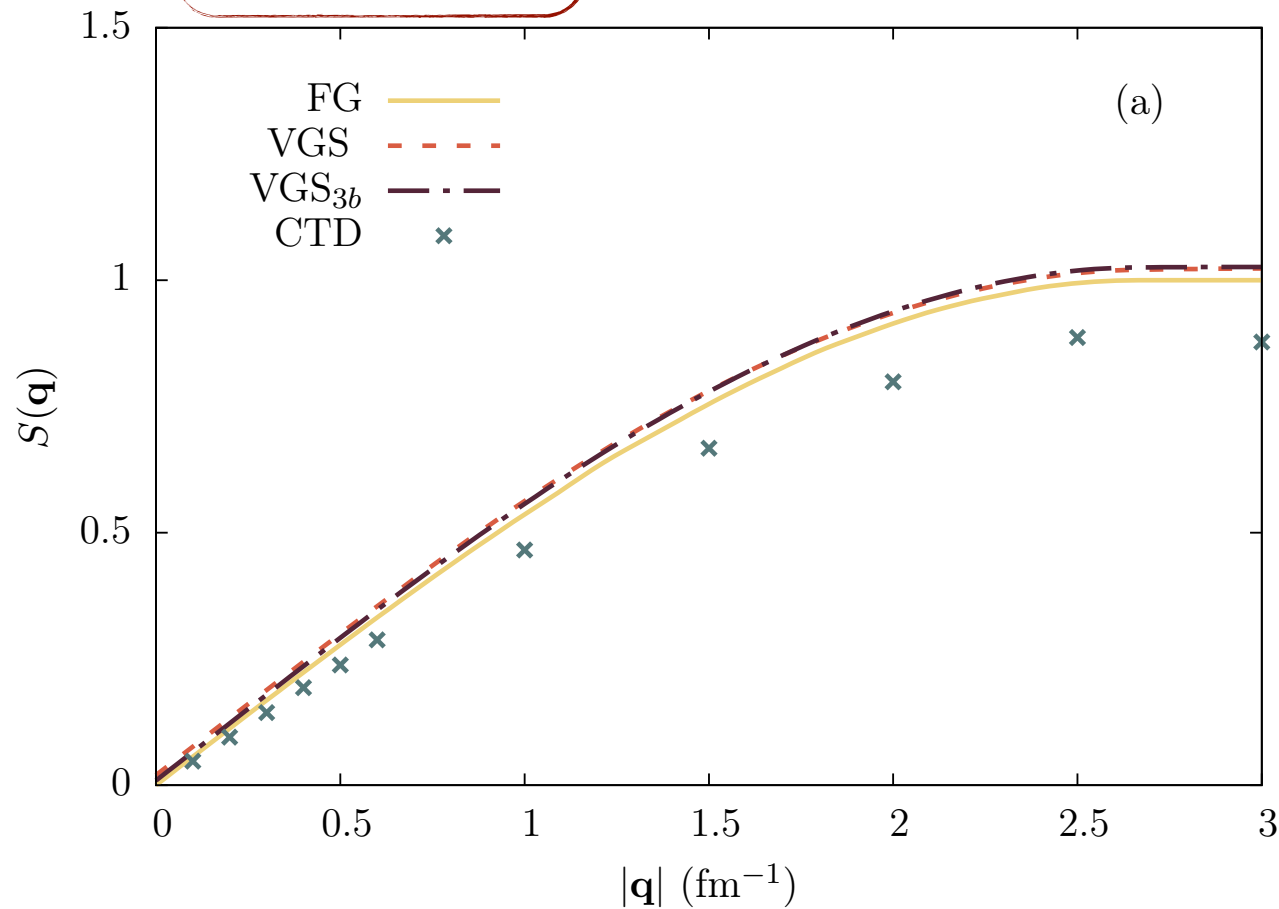
$$S_F(\mathbf{q}) = 1 + \frac{1}{3} \int d\mathbf{r}_{12} g_{12}^\tau(r_{12}) j_0(qr_{12})$$

$$S_T(\mathbf{q}) = 1 + \frac{1}{9} \int d\mathbf{r}_{12} [g_{12}^{\sigma\tau}(r_{12}) j_0(qr_{12}) - g_{12}^{t\tau}(r_{12}) j_2(qr_{12})]$$

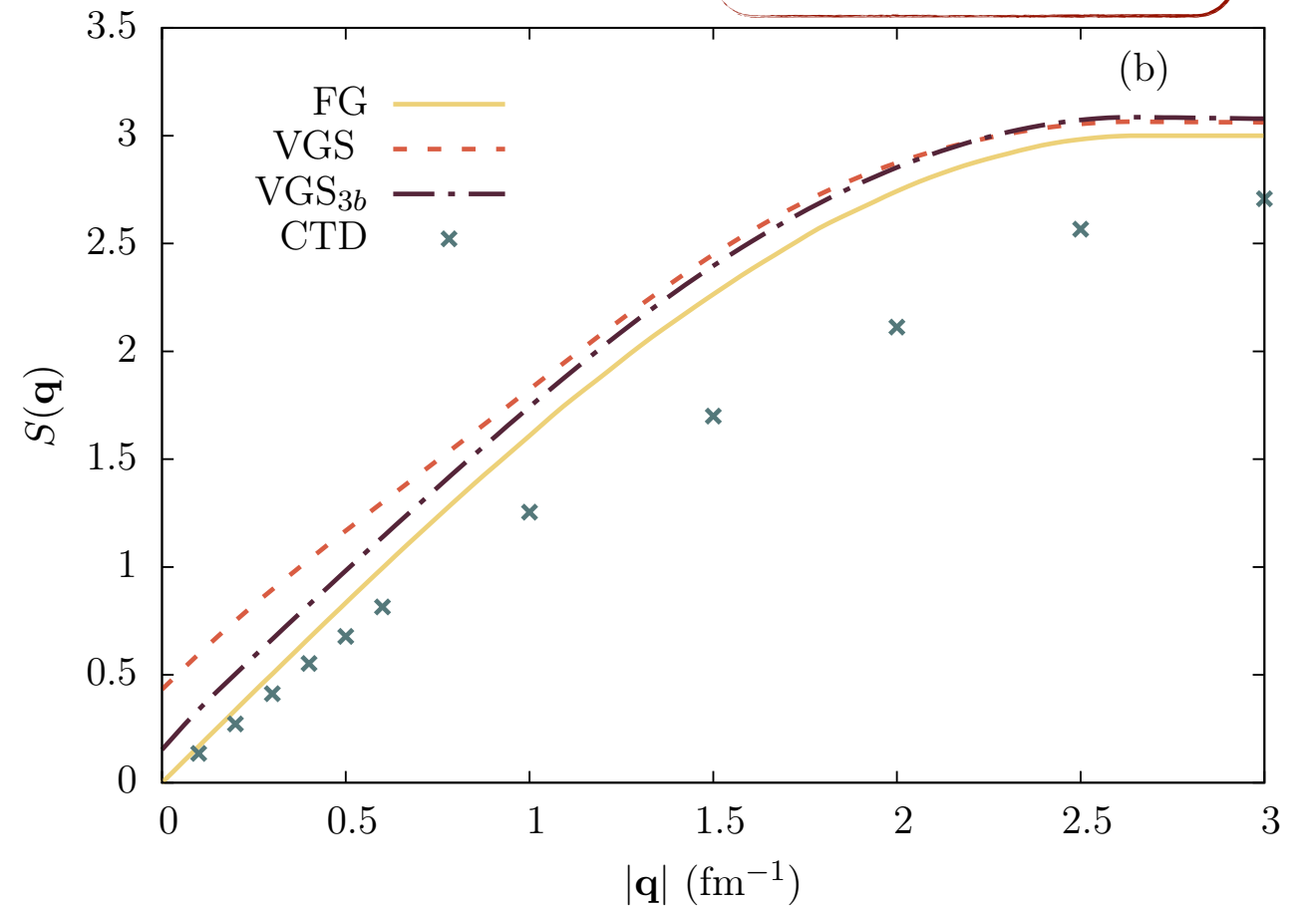
$$S_L(\mathbf{q}) = 1 + \frac{1}{9} \int d\mathbf{r}_{12} [g_{12}^{\sigma\tau}(r_{12}) j_0(qr_{12}) + \frac{1}{2} g_{12}^{t\tau}(r_{12}) j_2(qr_{12})]$$

Sum-rules

Fermi

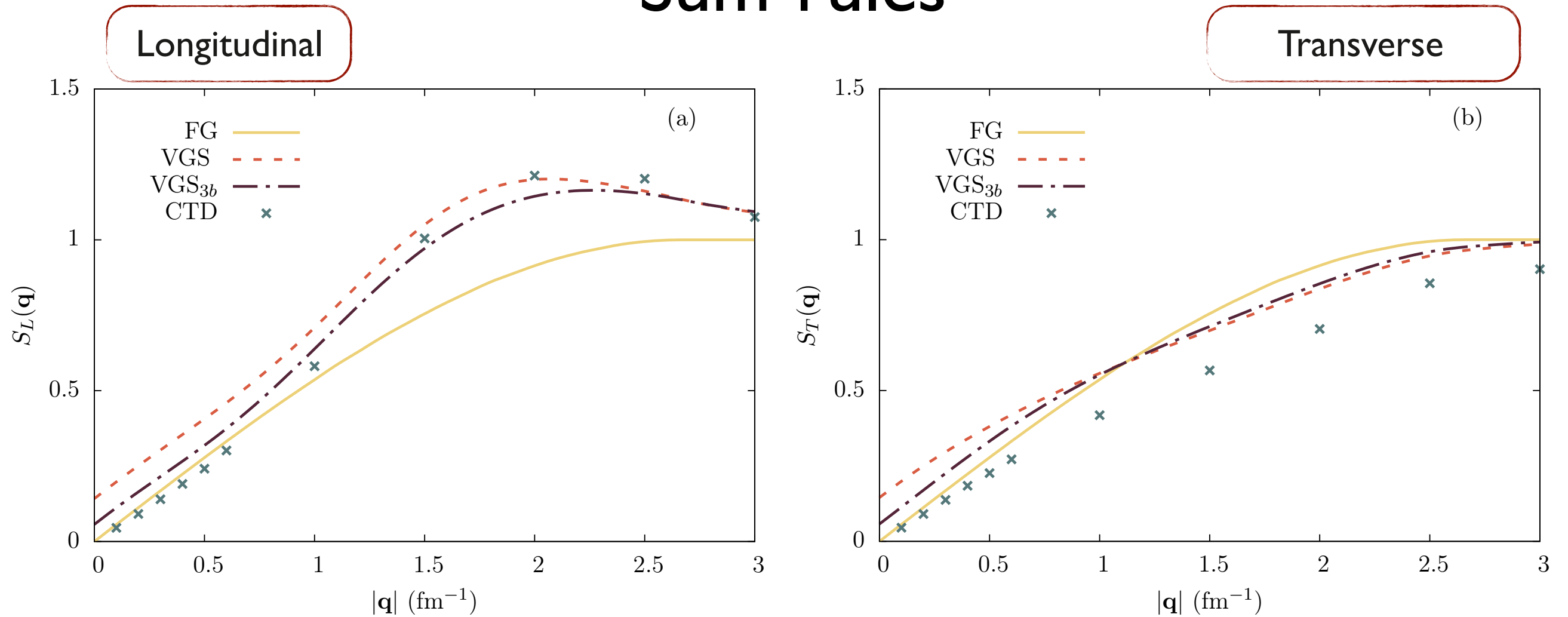


Gamow-Teller



- Because of the the tensor operator in the potential, VGS results for the Gamow Teller transition do not fulfill $S(\mathbf{q} \rightarrow 0) = 0$.
- When the three-body cluster is accounted for, the VGS and CTD curves of the Fermi case come closer to one another. As for Gamow-Teller , the effect is smaller.
- Difference between VGS and CTD curves only due to many particle-hole excitations.

Sum-rules



- The inclusion of the three-body cluster brings the CTD results closer to the VGS at all the values of $|\mathbf{q}|$.
- The positions of the maxima of the CTD and variational results are nearly coincident in the Longitudinal sum rule.
- At small momentum transfer the CTD calculations lie below the the VGS and VGS_{3b} curves.

Conclusions

Conclusions

- We have derived a two-body effective potential from the UIX three body force, within a microscopic approach based on CBF and cluster expansion formalism.
 - The underbinding of SNM appears to be arising from deficiencies of UIX.
- A set of chiral inspired potentials has been implemented in nuclear matter calculations.
 - Although two of them provide reasonable values for the saturation density of SNM, none of them simultaneously explains the binding energy.
 - Need for NNNLO three-body force.
- An effective potential, suitable to be used in FG basis, has been derived at three-body cluster level. The weak response of cold SNM has been computed for both the Fermi and Gamow Teller transitions, including the effect of UIX force.
 - This formalism is ideally suited to carry out consistent calculations of the weak response in the kinematical region relevant to neutron stars' applications.

Conclusion



